

Exploring the potential of using the foot sole pressure  
pattern to control step length in exoskeleton gait.

Anne Hermans (4023307)

May 8, 2019

Supervisor: Prof. Dr. Ir. David Abbink

Mechanical Engineering  
BioMechanical Design  
Bio-inspired Technology  
TU Delft

## Abstract

Semi-autonomous robotic exoskeletons enable paraplegics to walk again. The exoskeleton envelops the paraplegic's waist, legs and feet. When the user gives the command to start walking, the exoskeleton's robotic legs start a cyclic walking motion. The user, aided by crutches, follows this fixed cyclic motion, shifting their weight to the stance leg to allow the other leg to swing. A current challenge in exoskeleton development is to give the user more freedom and autonomy in the interaction with the exoskeleton. This study focuses on allowing the user to control step length in an intuitive manner. It is known from many previous studies found in literature, that during gait the center of pressure in the feet follows a distinctive pattern. Moreover, this pattern correlates with gait parameters such as step length. The goal of the current study is to explore the potential of using this pressure pattern to control step length in exoskeletons for paraplegics. The pressure pattern consists of three temporal parameters: the x- and y-coordinates of the center of pressure (CoP X and CoP Y) and the total force acting perpendicular to the sole ( $F_z$ ). Preliminary experiments were performed, in which three participants traversed a walking track with steps indicated on the floor. Halfway the track step length transitioned from short to long or vice versa. To approximate exoskeleton gait subjects used crutches for balancing while walking. The participants wore sensor shoes that recorded the pressure pattern while they walked. Results indicate that the pressure pattern can be used to distinguish steady state long steps from steady state short steps. This was shown for both an extreme difference in step length, as well as for a moderate difference in step length. Respectively eight and five metrics were identified that showed a likely difference (no overlapping boxes in box plots) between these step groups for all three subjects. Examples of successful metrics include "peak  $F_z$  value" and "CoP X value at 0% of stance phase". Only three of these metrics showed a likely difference between steady state steps and the transition step; i.e. it is harder but possible to gather from the pressure pattern, that a transition in step length is taking place. Results did not, however, indicate any potential in predicting an intended change in step length before the actual transition takes place. This makes the potential of controlling step length by manipulating the pressure pattern questionable but not out of the question. Testing with more participants would likely bring more clarity, as well as studying the capabilities of paraplegic exoskeleton users to manipulate the pressure pattern with upper body movements while walking.



# Contents

<b>I</b>	<b>Introduction</b>	<b>12</b>
<b>1</b>	<b>Background</b>	<b>13</b>
1.1	Semi-autonomous exoskeletons . . . . .	13
1.1.1	Project MARCH . . . . .	13
1.1.2	The paraplegic user . . . . .	13
1.2	Human-exoskeleton interaction . . . . .	15
1.2.1	Exoskeleton control . . . . .	15
1.2.2	A literature overview of existing control methods . . . . .	17
<b>2</b>	<b>Solution space</b>	<b>21</b>
2.1	Research direction . . . . .	21
2.1.1	Considerations for development of exoskeleton control . . . . .	21
2.1.2	CoP as a control signal in literature . . . . .	22
2.2	Human gait . . . . .	25
2.2.1	Terms and definitions . . . . .	25
2.2.2	Paraplegic user in exoskeleton . . . . .	26
2.2.3	Gait cycle . . . . .	26
2.2.4	Crutch usage . . . . .	27
2.2.5	Gait including crutch usage . . . . .	27
<b>3</b>	<b>Research questions</b>	<b>30</b>
3.1	Assumptions . . . . .	30
3.2	Questions . . . . .	30
<b>II</b>	<b>Methods</b>	<b>32</b>
<b>4</b>	<b>Experimental design</b>	<b>33</b>
4.1	Pilot experiments . . . . .	33
4.1.1	Pilot set-up . . . . .	33
4.1.2	Pilot conclusions . . . . .	33
4.1.3	Changes after pilot . . . . .	33
4.2	Hardware . . . . .	34
4.2.1	Soles . . . . .	34
4.2.2	Sensors . . . . .	35
4.2.3	Data acquisition . . . . .	35
4.2.4	Crutches . . . . .	36
4.2.5	Metronome . . . . .	37
4.3	Walking tracks . . . . .	37
4.4	Carrying out the experiments . . . . .	37
4.4.1	Protocol . . . . .	37
4.4.2	Walking rhythm . . . . .	40

4.4.3	Crutch usage . . . . .	40
4.4.4	Subject descriptions . . . . .	40
4.4.5	Sensor failure . . . . .	41
<b>5</b>	<b>Data analysis</b>	<b>42</b>
5.1	Steps and step groups . . . . .	42
5.1.1	Stance and swing phase . . . . .	42
5.1.2	The step groups . . . . .	43
5.2	Comparisons . . . . .	43
5.2.1	Between trial groups . . . . .	43
5.2.2	Between step groups . . . . .	43
5.3	Data processing . . . . .	46
5.3.1	Calibration, zeroing and rotation . . . . .	46
5.3.2	Separating the trials . . . . .	46
5.3.3	Separating the steps . . . . .	47
5.3.4	Calculating CoP X, CoP Y and Fz . . . . .	47
5.3.5	Finding the mean and confidence interval . . . . .	50
5.4	Visualizing the data . . . . .	50
5.4.1	Box plots . . . . .	51
<b>III</b>	<b>Results</b>	<b>53</b>
<b>6</b>	<b>General results</b>	<b>54</b>
6.1	Fz: vertical force component . . . . .	55
6.2	Cop X: the x-coordinate of the center of pressure . . . . .	55
6.3	CoP Y: the y-coordinate of the center of pressure . . . . .	55
<b>7</b>	<b>Comparing the steady states</b>	<b>59</b>
7.1	Fz: vertical force component . . . . .	60
7.1.1	Overlay plots . . . . .	60
7.1.2	Value and timing of the peak Fz . . . . .	61
7.1.3	Box plots . . . . .	62
7.2	CoP X: x-coordinate of the center of pressure . . . . .	63
7.2.1	Overlay plots . . . . .	63
7.2.2	CoP X: peaks indicated . . . . .	64
7.2.3	Box plots . . . . .	66
7.3	CoP Y: y-coordinate of the center of pressure . . . . .	69
7.3.1	Overlay plots . . . . .	69
7.3.2	Box plots . . . . .	70
7.4	Conclusions . . . . .	72
<b>8</b>	<b>Comparing the steady state beginning to the pre-transition step</b>	<b>73</b>
8.1	Fz: vertical force component . . . . .	74
8.1.1	A-trials . . . . .	74
8.1.2	B-trials . . . . .	74
8.2	CoP X: x-coordinate of the center of pressure . . . . .	76
8.2.1	A-trials . . . . .	76
8.2.2	B-trials . . . . .	77
8.3	CoP Y: y-coordinate of the center of pressure . . . . .	79
8.3.1	A-trials . . . . .	79
8.3.2	B-trials . . . . .	79
8.4	Conclusions . . . . .	81

<b>9 Comparing the steady state beginning to the transition step</b>	<b>82</b>
9.1 Fz: vertical force component	83
9.1.1 A-trials	83
9.1.2 B-trials	85
9.2 CoP X: x-coordinate of the center of pressure	86
9.2.1 A-trials	86
9.2.2 B-trials	88
9.3 CoP Y: y-coordinate of the center of pressure	90
9.3.1 A-trials	90
9.3.2 B-trials	92
9.4 Conclusions	94
<b>10 The moderate track: C- and D-trials</b>	<b>95</b>
10.1 Fz: vertical force component	96
10.1.1 Overlay plots	96
10.1.2 Box plots	97
10.2 CoP X: x-coordinate of the center of pressure	98
10.2.1 Overlay plots	98
10.2.2 Box plots	99
10.3 CoP Y: y-coordinate of the center of pressure	101
10.3.1 Overlay plots	101
10.3.2 Box plots	102
10.4 Conclusions	104
<b>11 Comparing the extreme to the moderate track</b>	<b>105</b>
11.1 Comparison 6	106
11.1.1 Comparing the transition steps from A- and C-trials	106
11.1.2 Comparing the transition steps from B- and D-trials	106
11.2 Comparisons 5 and 7	106
11.2.1 Comparing the moderately to extremely long steps	106
11.2.2 Comparing the moderately to extremely short steps	106
11.3 Conclusions	108
<b>IV Concluding</b>	<b>109</b>
<b>12 Conclusions</b>	<b>110</b>
<b>13 Discussion</b>	<b>112</b>
13.1 Assumptions	112
13.2 Experiment evaluation	112
13.2.1 Tethered sensors	113
13.2.2 Rigidity of the foot plates	113
13.2.3 Sensor failure	113
13.3 Limitations	113
13.4 The outcome	114
13.4.1 Relating the results to literature	114
13.4.2 Interpreting the results	114
13.5 Future visions	115
13.6 Future work	115
13.7 Final conclusion	116
<b>Gratitude</b>	<b>117</b>
<b>Appendices</b>	<b>118</b>

<b>A Protocol sheets</b>	<b>119</b>
<b>B Results overview images subjects 1 and 3</b>	<b>122</b>
<b>C Comparisons 5 and 7, subjects 2 and 3</b>	<b>129</b>
<b>References</b>	<b>132</b>

# List of Figures

1.1	ReWalk exoskeleton and MARCH I exoskeleton design . . . . .	14
1.2	Visualisation of the sensorimotor loop of human locomotion after SCI. . . . .	18
1.3	Visualisation of all possible signal routes between human and exoskeleton. . . . .	18
1.4	Visualisation of the complete system of a SCI patient walking in an exoskeleton. . . . .	19
2.1	Future vision . . . . .	23
2.2	Moving the CoP with the ankle, from Winter (1995) . . . . .	26
2.3	Oscillations of the CoM, pelvis and thorax during gait. . . . .	28
2.4	Foot and crutch placement, base of support and lateral movement of the CoM during a gait cycle. . . . .	29
4.1	The basic structure of the sensor shoes. . . . .	35
4.2	The wearable sensor shoe. . . . .	35
4.3	An OptoForce sensor. . . . .	35
4.4	Wearable sensor shoe, crutch and DAQ unit fixture on lower leg. . . . .	36
4.5	Walking track schematic. . . . .	38
4.6	Walking tracks photo. . . . .	39
4.7	Velcro pattern on floor and sole. . . . .	39
5.1	Step phases . . . . .	42
5.2	The walking track, with details. . . . .	44
5.3	Visual representation of comparisons 1, 2 and 3 between step groups. . . . .	46
5.4	All forces recorded during A and B trials, subject 1. . . . .	48
5.5	All torques recorded during A and B trials, subject 1. . . . .	48
5.6	The three parameters selected to present the generated data. . . . .	49
5.7	CoP X and CoP Y plotted in the xy-plane . . . . .	51
5.8	CoP X plotted vs time since last right foot strike . . . . .	52
5.9	Mean and CI of Fz, CoP X and CoP Y . . . . .	52
6.1	Five step groups. . . . .	54
6.2	Fz mean and 95% CI, subject 2 results overview. . . . .	56
6.3	CoP X mean and 95% CI, subject 2 results overview. . . . .	57
6.4	CoP Y mean and 95% CI, subject 2 results overview. . . . .	58
7.1	Comparison 1 . . . . .	59
7.2	Fz - comparison 1, A&B-trials . . . . .	60
7.3	Value vs. timing of maximum Fz - comparison 1 . . . . .	61
7.4	Timing of Fz peak value, comparison 1 . . . . .	62
7.5	Fz peak value, comparison 1. . . . .	62
7.6	CoP X - comparison 1, A&B-trials . . . . .	63
7.7	CoP X including peaks, subject 2, steady state steps . . . . .	64
7.8	CoP X with peaks, short and long steady state steps plotted together . . . . .	65



7.9	Absolute sum of rises explained . . . . .	65
7.10	CoP X Lowest valley to highest peak, comparison 1 . . . . .	66
7.11	CoP X absolute sum of rises, comparison 1 . . . . .	67
7.12	CoP X at foot strike, comparison 1 . . . . .	67
7.13	CoP X rise between first two peaks, comparison 1 . . . . .	68
7.14	CoP X total rise, comparison 1 . . . . .	68
7.15	CoP Y - comparison 1, A&B-trials . . . . .	69
7.16	CoP Y at 0% of stance phase, comparison 1 . . . . .	70
7.17	CoP Y rise from 0% to 20% of stance phase, comparison 1 . . . . .	70
7.18	CoP Y rise from 20% to 80% of stance phase, comparison 1 . . . . .	71
7.19	CoP Y rise from 80% to 100% of stance phase, comparison 1 . . . . .	71
8.1	Comparison 2. . . . .	73
8.2	Fz - comparison 2, A-trials. . . . .	74
8.3	Fz - comparison 2, B-trials . . . . .	75
8.4	Fz - comparison 2, B-trials. . . . .	75
8.5	CoP X, absolute sum of rises, right foot, A-trials, comparison 2 . . . . .	76
8.6	CoP X at foot strike, right foot, A-trials, comparison 2 . . . . .	76
8.7	CoP X, rise between first two peaks, right foot, A-trials, comparison 2 . . . . .	77
8.8	CoP X, absolute sum of rises, right foot, B-trials, comparison 2 . . . . .	77
8.9	CoP X at foot strike, right foot, B-trials, comparison 2 . . . . .	78
8.10	CoP X, rise between first two peaks, right foot, B-trials, comparison 2 . . . . .	78
8.11	CoP Y - comparison 2, A-trials . . . . .	79
8.12	CoP Y - comparison 2, B-trials . . . . .	80
8.13	CoP Y at 0% of stance phase, B-trials, comparison 2 . . . . .	80
9.1	Comparison 3. . . . .	82
9.2	Fz - comparison 3, A-trials. . . . .	83
9.3	Fz peak value, comparison 3, A-trials . . . . .	84
9.4	Timing of Fz peak value, comparison 3, A-trials . . . . .	84
9.5	Fz, comparison 2, B-trials. . . . .	85
9.6	CoP X, absolute sum of rises, A-trials, comparison 3 . . . . .	86
9.7	CoP X at foot strike, A-trials, comparison 3 . . . . .	87
9.8	CoP X, rise between first two peaks, A-trials, comparison 3 . . . . .	87
9.9	CoP X, absolute sum of rises, B-trials, comparison 3 . . . . .	88
9.10	CoP X at foot strike, B-trials, comparison 3 . . . . .	88
9.11	CoP X, rise between first two peaks, B-trials, comparison 3 . . . . .	89
9.12	CoP Y - comparison 3, A-trials . . . . .	90
9.13	CoP Y rise from 20% to 80% of stance phase, comparison 3 . . . . .	91
9.14	CoP Y rise from 80% to 100% of stance phase, comparison 3 . . . . .	91
9.15	CoP Y - comparison 3, B-trials . . . . .	92
9.16	CoP Y at 0% of stance phase, B-trials, comparison 3, left foot . . . . .	92
9.17	CoP Y rise from 20% to 80% of stance phase, B-trials, comparison 3, left foot . . . . .	93
9.18	CoP Y rise from 80% to 100% of stance phase, B-trials, comparison 3, left foot . . . . .	93
10.1	Comparison 4. . . . .	95
10.2	Fz - comparison 4, C&D-trials . . . . .	96
10.3	Timing of Fz peak value, comparison 4, right foot . . . . .	97
10.4	Fz peak value, comparison 4, right foot . . . . .	97
10.5	CoP X - comparison 4, C&D-trials . . . . .	98
10.6	CoP X absolute sum of rises, comparison 4, right foot . . . . .	99
10.7	CoP X at foot strike, comparison 4 . . . . .	99

---

10.8	CoP X rise between first two peaks, comparison 4, right foot . . . . .	100
10.9	CoP Y - comparison 4, C&D-trials . . . . .	101
10.10	CoP Y at 0% of stance phase, comparison 4 . . . . .	102
10.11	CoP Y rise from 20% to 80% of stance phase, comparison 4 . . . . .	102
10.12	CoP Y rise from 80% to 100% of stance phase, comparison 4 . . . . .	103
11.1	Comparisons 5, 6 and 7. . . . .	105
11.2	Fz, CoP X and CoP Y, comparisons 5, 6 and 7, subject 1, left foot. . . . .	107
A.1	Protocol sheet used during experiments. . . . .	120
A.2	Progress sheet used during experiments. . . . .	121
B.1	Fz mean and 95% CI, subject 3 results overview . . . . .	123
B.2	CoP X mean and 95% CI, subject 3 results overview . . . . .	124
B.3	CoP Y mean and 95% CI, subject 3 results overview . . . . .	125
B.4	Fz mean and 95% CI, subject 1 results overview . . . . .	126
B.5	CoP X mean and 95% CI, subject 1 results overview . . . . .	127
B.6	CoP Y mean and 95% CI, subject 1 results overview . . . . .	128
C.1	Fz, CoPX and CoPY, comparisons 5, 6 and 7, subject 2, left foot. . . . .	130
C.2	Fz, CoPX and CoPY, comparisons 5, 6 and 7, subject 3, left foot. . . . .	131

## List of Tables

1.1	Intention estimation levels . . . . .	17
2.1	Control options assessed on definite and theoretic criteria. . . . .	22
2.2	Studies in which body movements were used to control an exoskeleton . . .	24
5.1	Trial details. . . . .	45
5.2	All possible comparisons between step groups within the same trial group. . . . .	46
5.3	The step group comparisons selected for consideration in this study. . . . .	46
5.4	Phase matrix to determine foot floor strike. . . . .	49
5.5	Mean and confidence interval taken per step, across trials. . . . .	50
5.6	The mean and confidence interval are taken per step group, across trials and steps in a step group. . . . .	50
7.1	Summary of the metrics presented in chapter 7. . . . .	72
8.1	Summary of the metrics presented in 8. . . . .	81
9.1	Summary of the metrics presented in chapter 9. . . . .	94
10.1	Summary of the metrics presented in chapter 10. . . . .	104

# Glossary

**A-trial** trial starting with 130cm swings transitioning to 40cm swings..

**ASIA** American Spinal Injury Association.

**B-trial** trial starting with 40cm swings transitioning to 130cm swings..

**BoS** base of support.

**CoP Y** y-coordinate of the center of pressure.

**C-trial** trial starting with 110cm swings transitioning to 60cm swings..

**CI** confidence interval.

**CNS** central nervous system.

**CoG** center of gravity.

**CoM** center of mass.

**CoP** center of pressure.

**CoP X** x-coordinate of the center of pressure.

**D-trial** trial starting with 60cm swings transitioning to 110cm swings..

**fBoS** base of support formed by the feet.

**Fz** replacement force along z-axis.

**IMU** inertial measurement unit.

**LFS** left foot strike.

**LIFC** initial floor contact of the left foot.

**LS** left foot stance phase.

**post** post-transition.

**pre** pre-transition.

**RFS** right foot strike.

**RIFC** initial floor contact of the right foot.

**RS** right foot stance phase.

**SCI** spinal cord injury.

**ssb** steady state beginning.

**sse** steady state end.

**tr** transition.

**Part I**

**Introduction**

# Chapter 1

## Background

### 1.1 Semi-autonomous exoskeletons

A semi-autonomous exoskeleton is a robotic suit that can be worn by a paraplegic user, see figure 1.1. The suit is attached around the waist and runs down the outside of the user's legs, ending in foot plates that cradle the feet from below. The robotic 'legs' are strapped to the user's legs at several places, both on the upper and lower leg. When the proper command is given, the robotic exoskeleton starts making a walking motion, moving the user's legs. With this, semi-autonomous exoskeletons give back the ability to walk to paraplegics.

#### 1.1.1 Project MARCH

The students working on project MARCH ([www.projectmarch.nl](http://www.projectmarch.nl)), a student team from the TU Delft, have devoted themselves to making the best possible exoskeleton for paraplegics. Each year since 2016, a new and improved MARCH exoskeleton has been developed. At the start of this study, the first MARCH exoskeleton was being developed for participation in the first ever "*CYBATHLON Championship for Athletes with Disabilities*" ([www.cyathlon.ethz.ch/en](http://www.cyathlon.ethz.ch/en)) hosted by ETH Zürich in October 2016. It was the intention to add 6 sensors to the MARCH exoskeleton, each sensor measuring in 6 degrees of freedom (DoFs); two in each foot sole, two in each crutch. These would have measured the floor reaction forces and torques in the feet and crutches.

#### 1.1.2 The paraplegic user

Paraplegia due to spinal cord injury (SCI) yearly affects thousands of people world wide. SCI may be caused by trauma, disease or degeneration and can result in loss of sensory function and/or motor control of limbs or the entire body. The higher up the spinal cord the injury occurs, the more extensive the effects are. All motor and sensory information that travels between brain and body has to pass through the spinal cord. A lesion at a certain level disrupts the flow of information below that level, while higher levels remain unaffected. Therefore, SCIs are classified according to the level at which the lesion occurs. Lesions at the thoracic, lumbar or sacral segments of the spinal cord can result in paraplegia; in which the arms are spared but the trunk, legs and pelvic organs may be involved (Maynard Jr. et al., 1997). The degree to which the latter are affected again depends on the level of injury. The ASIA (American Spinal Injury Association) impairment scale is a common scale categorizing severity of the lesion. Grade A denotes a complete lesion; no motor or sensory function remaining below the level of injury, including the sacral segments S4-S5. Grade B constitutes some sensory, but no motor, function remaining below the level of injury, whereas in grades C and D some sensory as well as motor function



Figure 1.1: The photo on the left shows a paraplegic user in the ReWalk exoskeleton (ReWalk Robotics, [www.rewalk.com](http://www.rewalk.com)), the image on the right features a rendering of the MARCH I exoskeleton design.

is preserved. Grade E constitutes normal functioning. This study focuses on paraplegia patients with a low thoracic or lumbar lesion ASIA grade A; patients without any sensory and motor function in their legs, with good control over trunk muscles.

The World Health Organization estimates that every year, world wide, between 250 000 and 500 000 people suffer a spinal cord injury. SCI prevalence varies per country and per year recorded. Several studies (Singh, Tetreault, Kalsi-Ryan, Nouri, & Fehlings, 2014; Wyndaele & Wyndaele, 2006) indicate that it is most prevalent in the USA (906 and 755 patients per million people, respectively), with a reported prevalence in Europe of 252/million (Wyndaele & Wyndaele, 2006). The same review study indicates that incidence is also highest in Northern America (51/million), with European (19.4/million), Asian (23.9/million) and Australian (16.8/million) levels far below that. The Netherlands has a relatively low reported incidence (12.4/million) (Singh et al., 2014). The percentage of males suffering SCI is greater compared to females; roughly a 4:1 ratio (Sadowsky, Volshteyn, Schultz, & McDonald, 2002; Wyndaele & Wyndaele, 2006; Singh et al., 2014) and patients are either relatively young or quite old: the average age at injury is early thirties with the highest frequency occurring between 15 and 30 years old - or over 70 years old (Sadowsky et al., 2002; Singh et al., 2014).

Life expectancy of SCI patients is increasing, with a predicted median survival time of 38 years post injury for patients suffering a SCI at an age between 25 and 34 years old (Wyndaele & Wyndaele, 2006). Ninety percent of the patients suffer from long term motor dysfunctions and “SCI and its complications impose great direct and indirect financial burdens; the annual treatment cost for each patient is estimated to be 26,270 dollars” (Yousefifard et al., 2016), while “estimated lifetime economic burden associated with SCI in Canada ranges from CAD\$1.47 million for a person with incomplete paraplegia to \$3.03 million for one with complete tetraplegia” (Singh et al., 2014). The average lifetime cost of treating an individual with traumatic SCI in the USA is estimated to be

between a half and two million dollars (Sadowsky et al., 2002). Long term complications may include urinary tract infection, bladder and bowel dysfunction, deep vein thrombosis, osteoporosis, pressure sores, respiratory problems and psychological disorders (*World Health Organization Fact sheet no.384*, 2013; Singh et al., 2014; Wyndaele & Wyndaele, 2006).

Treatment options for SCI are limited as “*neurogenesis rarely occurs in central nervous system and self-healing in injured cells is rather limited*” (Yousefifard et al., 2016). As of now, the only technologies that allow paraplegics to get around are wheelchairs and powered exoskeletons, of which the former is by far the most used. A wheelchair, either electric or hand-powered, can give a paraplegic a large part of their mobility back, but many kinds of terrain remain inaccessible to them; stairs, curbs, pebbles, etc. A semi-autonomous exoskeleton could open up such locations and - perhaps even more importantly - could mitigate many of the indirect complications associated with SCI as well. Regularly assuming an upright position alone and making walking motions has health benefits, such as improved bowel function and circulation and higher bone density (if weight is placed on the bones). However, the greatest benefits of powered exoskeletons may be those affecting the psyche of the patient, who otherwise always has to look up to people from a seated position.

## 1.2 Human-exoskeleton interaction

In exoskeletons currently on the market, the user gives the command to start walking and the robotic exoskeleton responds by starting a fixed cyclic walking motion. A literature study I did at the start of this study, investigated how this basic interaction could be further developed to better suit all the intricacies of human gait (rhythm, step size, balance, speed, direction, feedback loops, etc.), and what is already being done in this field. The literature study focused on both interaction directions: human-to-exoskeleton control and exoskeleton-to-human feedback. For the current study a focus on human-to-exoskeleton control was chosen.

### 1.2.1 Exoskeleton control

The user should be able to signal her/his intentions to the exoskeleton. To describe intention estimation methods, several distinctions can be made. User input signals to the controller may be...

- ...explicit or implicit.
- ...intuitive or trained.
- ...gathered using invasive or non-invasive techniques.
- ...able to distinguish between many or few user intentions.
- ...able to classify intention very specifically or non-specifically.
- ...used to distinguish high-level, mid-level or low-level motion intention.

Finally, something can be said about the origin of the user input signals. For example, is the origin...

...neural activity, muscular activity, body (part) posture, manual input, voice, contextual or environmental information, etc.

The operational definition of explicit and implicit walking intention detection as defined by Jang et al. (2010) is used. They state: “*The explicit walking intention is defined*



as a user's action for walking by user-defined rules (e.g., press the control buttons for walking actions such as start walking, or stop walking) and implicit walking intention as user's natural (unaffected) physical activities (e.g., muscle contraction, angle of ankle or knee joint, etc.) is detected by bio/kinesthetic sensors while walking without user's explicit operation." It can be argued that the less use is made of explicit signalling (thus, the more of implicit signalling), the more intuitive a control strategy is. Indeed, it seems logical that a user will not need training when an intention estimator is based on natural physical activities. However, this analogy does not always hold. For example, even though ReWalk stepping is based on 'natural' weight shifts, it takes patients up to 30 hours to master it. Vice versa, the use of some buttons (explicit input) or shifts may be very intuitive and require little training. Fleischer and Hommel (2008) argue that a human-exoskeleton interface should be intuitive in order to minimize the time required for learning and to allow the user to concentrate on the task to be performed itself, instead of on control of the exoskeleton. The exoskeleton described by Strausser and Kazerooni (2010) knows two interaction modes: PT (physical therapist) mode, in which the user's therapist pushes buttons to select the desired action and HMI (human machine interface) mode, in which intended action is derived from natural motions. Results showed that HMI mode produced a more fluid and natural gait than PT mode, which is an argument in favour of intuitive control.

Tucker et al. (2015) describe invasiveness of the information as "*the relative ease (in time, effort, and risk) with which a sensor may be applied and removed. These range from completely noninvasive (e.g. fully embedded within the device) to highly invasive (e.g. surgically implanting electrode arrays in the motor cortex)*". A non-invasive sensor is preferred. This has to be optimized with respect to the richness of the information such a sensor can provide, which is related to "*both the variety of discernible activities and the specificity of motion intention obtainable through a given modality*" (Tucker et al., 2015). As exoskeletons' functionalities start increasing from merely walking in a straight line to, for example, climbing stairs or walking at different speeds, the controller needs to be able to distinguish between a growing number of user intentions; from a binary walking/not walking to an array of options. Still, the controller needs to be able to classify intention specifically; the command 'stop walking' must not be confused with the command 'climb stairs'.

Another distinction that can be made about user input to the controller, is whether it is used to determine intended *modality* such as walking or climbing stairs; intended *step parameters* such as desired foot position, step timing or step length; or intended *joint and limb states* such as torque or limb velocities. I will use the headers *high level*, *mid level* and *low level* intention estimation levels, see table 1.1.

Summarizing, an intention estimation method that is implicit, intuitive and uses rich information gathered with non-invasive sensors is preferable. No demands are made as for the origin of such input. However, there are some correlations that usually hold. For example, neural activity generally requires invasive sensors that can be used to estimate a large range of intentions only if implemented in an explicit, non-intuitive way. Manual input is very explicit, probably not intuitive, but extremely specific and can distinguish many different intentions.

Intention estimation levels are closely correlated with autonomy. If the human can only determine the desired modality, the robot can act relatively autonomous on the corresponding subtasks. If the human on the other hand, can make decisions on joint torques or limb velocities, the robot hardly has any autonomy. Some kinds of user input signals lend themselves better to a certain intention estimation level than to others, as will become apparent in subsequent sections.

Intention estimation level	Estimated intention	Examples
High level	modality	walking; climbing stairs; standing; sitting; walking on tilted path
Mid level	step parameters	step timing, step length, step height
Low level	joint and limb states	joint torques, limb positions, limb velocities

Table 1.1: Intention estimation levels

### 1.2.2 A literature overview of existing control methods

Figure 1.2 demonstrates how the human sensorimotor loop is affected by spinal cord injury (SCI). In healthy humans, the CNS controls the head, upper body and the lower body and receives proprioceptive feedback about their states. This feedback can directly be used in the spine to modify the control signals it sends. Thus two reflex loops are formed: between the spine and the upper body and between the spine and the lower body. Head, upper body and lower body have output states; motion and joint torques. Proprioceptive sensors transfer information about these states to the CNS. The lower body state influences upper body state, which in turn influences head state; this explains the orange arrows splitting off these states and leading back to the respective body parts. The eyes can see the the states of the upper and lower body; hence the visual feedback signal going from upper and lower body state towards the head. This information is processed in the brain. Moreover, the vestibular system gives information about the state of the head directly to the brain. In humans suffering from SCI, the described loop is intersected. Information from the CNS to the lower body and from the lower body to the CNS can no longer be transferred. In theory, these two arrows are the only ones affected. The eyes can still perceive the state of the lower body and lower body state still influences the upper body. However, since motor neurons cannot reach lower body muscles, its state is trivial: there is no motion and no active joint torques. After SCI, all control centres high up in the CNS have been left unaffected; only the spinal cord has been injured. Unfortunately, the spinal cord is the passageway for all control and sensory signals - as well as the origin of gait patterns and reflexes. In short, two kinds of control signals (reflexes and motion patterns) can no longer be produced, while all other control signals can no longer reach the lower limbs.

In figure 1.3 an exoskeleton, exoskeleton controller and walking aid (crutches) have been added to the human sensorimotor loop of locomotion, in order to restore the gait function of the paralyzed legs. In addition, figure 1.3 depicts all possible signal routes that can be employed for communication between human and exoskeleton.

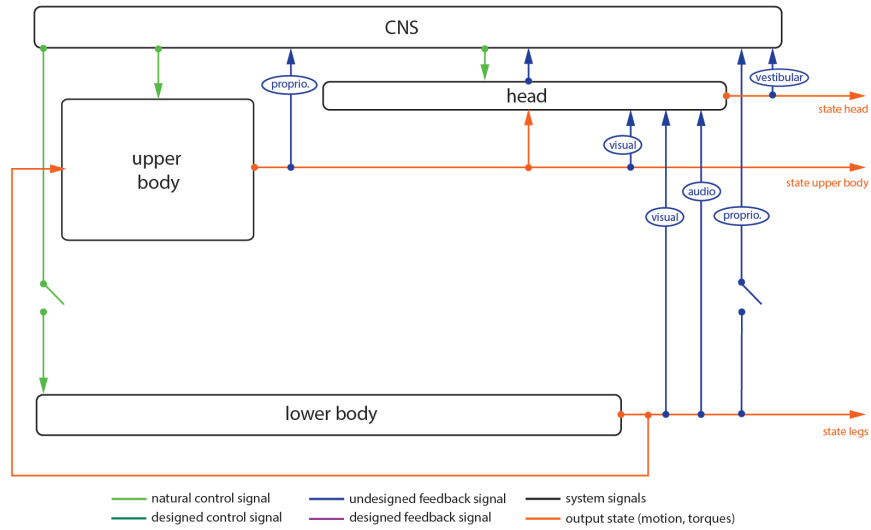


Figure 1.2: Visualisation of the sensorimotor loop of human locomotion after SCI.

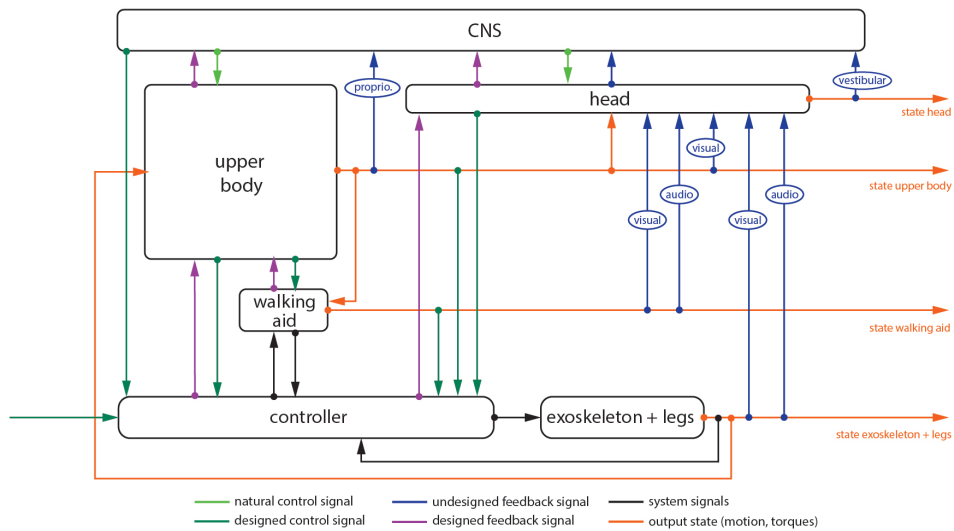


Figure 1.3: Visualisation of all possible signal routes that can be employed for communication between human and exoskeleton.

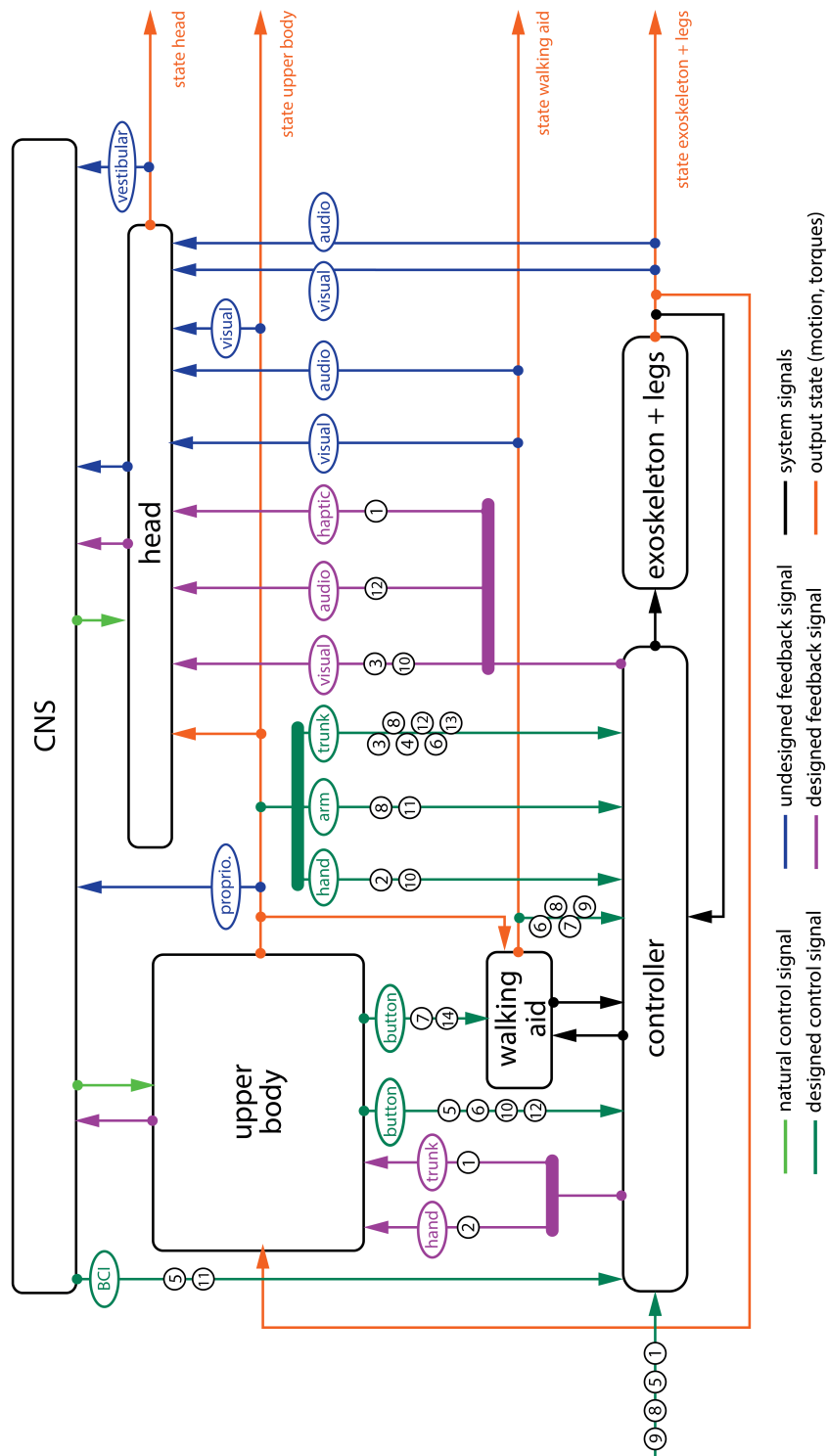


Figure 1.4: Block scheme visualising the complete system of a SCI patient walking in an exoskeleton, showing signal routes employed in literature. The numbers indicate which strategies are employed by various authors.

Figure 1.4 shows what signal routes, for both feedback and control, have been employed in literature by various authors. Sometimes, several studies describe different aspects of the same design, or small iterations of the same design. In such cases those studies have been clustered under one number. The numbers in the figure correspond to the following:

- ① Raj, Neuhaus, Moucheboeuf, Noorden, and Lecoutre (2011) (Mina)
- ② Hasegawa, Jang, and Sankai (2009); Hasegawa, Sasaki, and Tsukahara (2012); Hasegawa and Nakayama (2014); Hasegawa and Ozawa (2014) (tested independently from any exoskeleton)
- ③ Tsukahara, Kawanishi, Hasegawa, and Sankai (2010) (HAL)
- ④ Suzuki et al. (2005) (HAL)
- ⑤ Contreras-Vidal and Grossman (2013); Kilicarslan, Prasad, Grossman, and Contreras-Vidal (2013) (Rex)
- ⑥ Jang et al. (2010) (tested independently from any exoskeleton)
- ⑦ Acosta-Marquez and Bradley (2005) (digital and physical scale model of conceptual exoskeleton)
- ⑧ Strausser and Kazerooni (2010) (eLEGS, now called EKSO)
- ⑨ Kolakowsky-Hayner (2013) (EKSO)
- ⑩ Johnson, Repperger, and Thompson (1996) (MAPAS)
- ⑪ Gancet et al. (2012); Cheron et al. (2012) (Mindwalker)
- ⑫ Esquenazi, Talaty, Packel, and Saulino (2012) (ReWalk)
- ⑬ H. A. Quintero, Farris, and Goldfarb (2012); H. A. Quintero, Farris, Hartigan, Clesson, and Goldfarb (2011) (Indego, formerly Vanderbilt exoskeleton)
- ⑭ Arazpour et al. (2012) (IRGO)

## Chapter 2

# Solution space

### 2.1 Research direction

#### 2.1.1 Considerations for development of exoskeleton control

Currently, the human user can communicate intention only on the highest level, see table 1.1. After observing and interviewing a paraplegic walking in the ReWalk exoskeleton it seems that autonomy leans heavily towards the side of the robot. Depriving the user of "mid-level control" gives rise to a number of problems. Due to the step length being fixed, the user cannot reach a desired endpoint, but ends up either too far away or too close. Nor can the user take a longer step to step across a threshold or another obstacle; instead an unfortunate step on top of such a small obstacle may cause instability. Similar difficulties may arise due to fixed step height, while the fixed step frequency forces the user to adjust to the robot's rhythm. This requires training and high focus. If the user does not follow the robot's rhythm accurately (i.e. does not shift weight to stance leg in time) gait is interrupted and instability may follow.

In addition to the user having no influence over these parameters, the resulting robot action is also unpredictable to the user. It takes time and training to get adjusted to robot step rhythm. Uncertainty about which leg will do what makes balancing hard. Constantly anticipating and adjusting to robot action demands high cognitive effort of user. All of this gives the user an insecure feeling.

The insights described so far were included in the design process, looking for the appropriate solution space. In figure 1.3 the dark green arrows represent the possible control signal routes from user to exoskeleton. From left to right in figure 1.3 they are: external control e.g. by therapist; a brain computer interface; hand controls such as buttons; hand control integrated in crutch; control by state of the crutch (position, orientation, velocity, force); control by state of the upper body (trunk, arm and hand position, orientation, velocity); control by state of the head (head orientation). In section 1.2.1 it was determined that it is desirable that the control method should be implicit, intuitive, information-rich and non-invasive. It is difficult to establish beforehand whether a proposed control method will be intuitive and rich, but the implicitness and invasiveness can be ascertained without testing. Figure 2.1 shows the control options from figure 1.3 assessed on these criteria. Only crutch state and upper body state are potentially both implicit and non-invasive. They might very well also be rich in information and intuitive, but this will have to be validated by experiments. For the current study the potential of using the upper body state expressed as the foot sole pressure pattern was chosen, for several reasons. Firstly, since scientists are already endeavoring to make exoskeletons self-balancing (e.g. Ugurlu, Doppmann, Hamaya, Forni, and Teramae (2016), Contreras-

Vidal and Grossman (2013)) and therefore render crutches obsolete, it is illogical to study and develop new control methods relying on crutch usage. Secondly, with self-balancing prospects in mind, Project MARCH was planning to incorporate pressure sensors in the foot soles of their exoskeleton. Thus it made sense to investigate other applications of such sensors. (Unfortunately, these sensors did not end up in the first MARCH exoskeletons). Thirdly, by using pressure sensors in the foot soles, information about the upper body can be gathered, without the need to equip the upper body with sensors. Donning an exoskeleton is something of an inconvenience in itself already, so it is preferable that no additional sensors should be put on. Fourthly, it is known (e.g. Chiu, Wu, and Chang (2013), Fuchioka et al. (2015), Verkerke, Hof, Zijlstra, Ament, and Rakhorst (2005)) that in natural walking, there is a certain pressure pattern in the foot soles that depends on step parameters. It might therefore well be an intuitive control method. And finally, for this study highly sensitive force/moment sensors (from OptoForce) were available, likely able to provide rich information.

Thus it was decided to investigate the potential of *using force and moment data from the foot soles as a control signal for the user to convey mid-level intention to the exoskeleton*. From the three step parameters, step length was chosen to focus on in this study. The future vision for this concept is that a paraplegic walking in an exoskeleton can control step length by manipulating the pressure pattern measured by sensors in the foot soles. To minimize cognitive effort for the user, it is desirable that such control be implicit and intuitive. Ideally the user should not even explicitly have to decide to alter their step length - just as during normal walking one does not consciously think about their step length. The image in figure 2.1 illustrates this future vision and how this vision is currently only a 'dot on the horizon'. Section 2.1.2 will discuss relevant knowledge from literature as well as knowledge gaps that will have to be investigated in order to make this dot on the horizon a reality.

	implicit	non-invasive	rich?	intuitive?
external BCI				
hand (console)				
hand (crutch)				
crutch state				
upper body state				
head state				

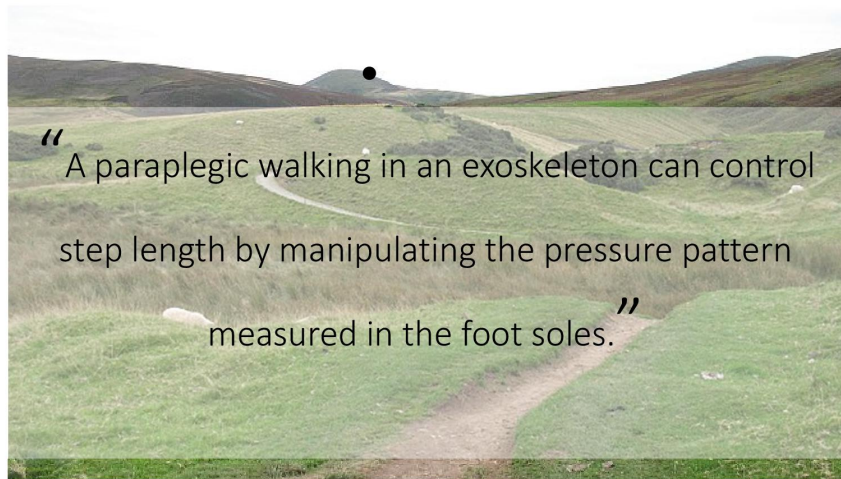
Table 2.1: Control options assessed on definite and theoretic criteria.

## 2.1.2 CoP as a control signal in literature

Figure 1.4 showed what control (dark green arrows) methods have already been described in literature. Table 2.1.2 lists the studies that have made use specifically of body movements, to control an exoskeleton. These studies correspond to the numbers on the green arrows labeled 'arm' and 'trunk' in figure 1.4. There is only one study (Strausser & Kazerooni, 2010) in which a step parameter, step length, can be controlled by the user. In this case, the control signal was arm angle. Apparently, CoP has never been used to influence step parameters.

Several studies have been found that have succeeded in deriving gait parameters from sensor data during gait. For example, Alvarez, Gonzalez, Lopez, and Alvarez (2006) were able to derive step length from data produced by an accelerometer on the lower back, while Zijlstra and Hof (2003) were able to do the same with step frequency as well. Verkerke et al. (2005) used a FRF-measuring treadmill to derive the CoP, from which step frequency and step length could be derived. It is, however, unknown how it affects

## DOT ON THE HORIZON



*Figure 2.1: The dot on the horizon: is this a viable vision for the future of exoskeletons?*

gait including crutches, according to the strategy described in section 2.2.4. It is also unknown, if there is a specific pressure pattern that can be associated with transitioning between step lengths, and if this pattern could be predictive of step length. Also, it is still unknown how such research as Verkerke et al. (2005) would hold up with in-sole sensors instead of a floor-reaction-forces measuring treadmill. It is unknowns such as these that inspired the research questions listed in the next chapter.



Table 2.2: Studies in which body movements were used to control an exoskeleton

Reference	Device	Sensors	Strategy
(Jang et al., 2010)	exoskeleton	glove with fsr in palm gyro sensor on back	Leaning on crutches and tilting forward means <i>start walking</i> . Lifting crutches and leaning left or right <i>selects a step</i> .
(Tsukahara et al., 2010)	exoskeleton	torso tilt frf's on feet CoP in sagittal plane	<i>Standing up</i> is initiated when thresholds for those sensors are exceeded
(H. a. Quintero, Farris, & Members, 2012; H. A. Quintero et al., 2011)	exoskeleton	joint encoders accelerometer on thigh	Moving CoP forward means <i>stand up</i> . Leaning forward and left means start walking with a right step, leaning forward and right vice versa. Leaning forward means continue walking. Not leaning forward means stop walking. Leaning backwards means sit down.
(Suzuki et al., 2005)	exoskeleton	three rate gyros on back	When torso tilt exceeds 0.05 rad on either left or right, step with contralateral leg is initiated.
(Strausser & Kazerooni, 2010)	exoskeleton	arm angle	arm angle (swinging the arm) initiates steps and determines step length
(Kolakowsky-Hayner, 2013)	exoskeleton	pressure sensors in foot soles instrumented crutches	weight transfer to one foot combined with certain crutch position triggers contralateral step
(Hassan, Kadone, Suzuki, & Sankai, 2014)	single-leg exoskeleton	IMUs measure cane angle and hip and knee angle of unaffected leg frf on heel and forefoot of affected leg and tip of cane	Affected leg is controlled using information about motion of unaffected leg and ground contact of affected leg.
(Esquenazi et al., 2012)	exoskeleton	tilt sensor for trunk angle	Leaning forward triggers start walking

## 2.2 Human gait

### 2.2.1 Terms and definitions

If we want to use the pressure distribution in the foot soles as a control input, it is important to know a little bit about this pressure distribution during gait in general, about the terms used in this context and how they relate to each other.

The base of support (BoS) can be defined as *“the possible range of the centre of pressure (CoP), the origin of the ground reaction vector.”* In static walking, where static equilibrium is always fulfilled, *“the vertical projection of the body centre of mass (CoM) should be within the base of support”* (Hof, Gazendam, & Sinke, 2005). However, in dynamical walking, the velocity of the center of mass (CoM) has to be taken into account as well. *“Even if the CoM is above the BoS, balance may be impossible if CoM velocity is directed outward. The reverse is also possible: even if the CoM is outside the BoS, but its velocity directed towards it, balance can be achieved,”* say Hof et al. (2005), who therefore propose that for a dynamic balance, not the CoM should be directly above the BoS, but the ‘extrapolated center of mass’ (XcoM), which is the quantity  $\mathbf{r} + \frac{\mathbf{v}}{w_0}$ ; consisting of the position of the CoM on the horizontal plane and its velocity divided by the natural frequency of the inverted pendulum that represents the body.

There is a constant interaction between the CoP and the CoG (the vertical projection of the CoM on the floor), which is especially apparent during quiet standing. The ankle plays a large part in influencing the position of the CoP. By pushing the toes away (plantar flexion of the ankle), the CoP is moved forward, while by pulling the toes upwards (dorsiflexion of the ankle), the CoP is moved backwards. Ankle inversion moves the CoP laterally, while ankle eversion moves the CoP medially.

Winter (1995) uses an example to illustrate the difference between the CoP and the CoG and how they interact, see figure 2.2. The body is modelled as an inverted pendulum. Both the body weight as well as the vertical reaction force cause a moment, with arms  $g$  and  $p$ , respectively. If  $Wg > Rp$ , a clockwise angular acceleration will occur. The central nervous system registers this and will send a ‘plantar flexion’ signal to the ankle. This will move the CoP forward, beyond the CoG, resulting in a counter clockwise angular acceleration. As long as the CoP can be moved beyond the XcoM, balance can be maintained using this ‘ankle strategy’. When the XcoM moves further forward, this does not necessarily mean that a fall will occur. Once the XcoM moves out of the possible area of the CoP (the current BoS), another strategy is required: now, the BoS may be changed. In this case, a foot may be placed further forward.

Thus is illustrated how the body, under control of the central nervous system, manipulates the position of the CoP in order to maintain a dynamic balance. The same principles are at work during walking, but extra factors enter the story. Now, the BoS is constantly changing. During single support phase, while the CoP stays within the BoS, the XcoM and even the CoM regularly move outside of the BoS; a fall is initiated, but stopped as soon as the swing foot is put down. During the double support phase, both the CoG and the CoP remain within the BoS (Lugade, Lin, & Chou, 2011).

Concluding, the CoP and CoG are not the same thing and even in quiet standing they are not always in the same place. However, they are clearly related: the position of the CoP is constantly adjusted in order to keep the CoM above the BoS, or bring it back above the BoS.

Besides CoP, CoM, CoG and BoS, the following two terms are used:

**Gait pattern** - The manner of walking, including speed, step frequency, step length and crutch placement.

**Pressure pattern** - The resulting pressure distribution in the foot soles through time. In addition to the CoP, it also consists of the force that acts perpendicular to the foot sole ( $F_z$ ), in the CoP.

### 2.2.2 Paraplegic user in exoskeleton

A paraplegic, even wearing a semi-autonomous exoskeleton, cannot use ankle plantar/dorsiflexion or in-/eversion. Therefore, the position of the CoP in the BoS formed by the feet cannot directly be controlled. However, for now and most likely for quite some time to come, paraplegic exoskeleton users employ crutches. These can serve 1) to enlarge the BoS, 2) to enhance CoM position control and 3) to manipulate the CoP. The BoS is enlarged because now there are four instead of two support areas that make up the BoS: two feet, two crutches. This creates a much more stable balance. The paraplegic has control over upper body movements, so he/she can influence the position of the CoM. Having the crutches as extra contact points between upper body and the floor, allows for more control over this. Thirdly, the paraplegic can control how much weight is on each crutch and feels this as well, allowing for CoP manipulation.

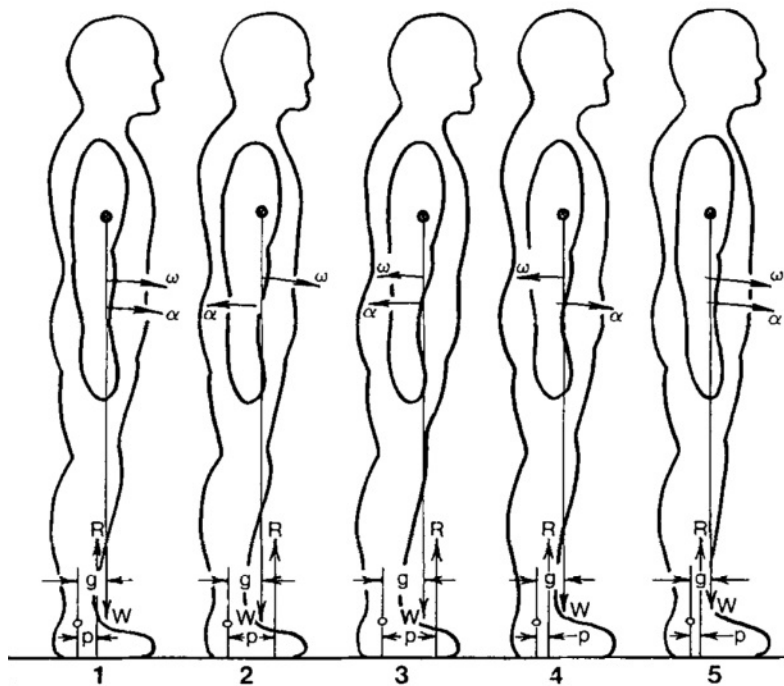


Figure 2.2: From Winter (1995).  $g$  and  $p$  are the positions of CoG and CoP, respectively.  $\alpha$  and  $\omega$  are the angular accelerations and velocities, respectively.  $W$  is body weight and  $R$  is the vertical reaction force.

### 2.2.3 Gait cycle

Figure 2.3 shows the translations of the CoM during one gait cycle, as presented in several different sources. All three sources show a very similar pattern. "The fore-aft oscillation is typical for a normal subject. The change from minimum to maximum, mostly during

*the double support, takes less time than the change from maximum to minimum, during the single stance. This tends to slightly distort the sinewave to a sawtooth form”* (Crowe, Schiereck, De Boer, & Keessen, 1995). This indicates that after heel strike, the weight is shifted towards the new stance foot fast during double support. When the swing leg is swung forward, the CoM lags behind a bit, staying above the stance leg. The maximum lateral amplitude occurs in the middle of the single support phase. This amplitude is such that the CoM is above the stance leg when it's at its maximum.

#### 2.2.4 Crutch usage

The way in which users walk in an exoskeleton was carefully observed. One user was observed directly as well as on video; videos of other users were found on the web. This was done primarily to analyse the way in which the crutches are employed during exoskeleton gait. The manner in which the crutches are employed, the ‘crutch strategy’, influences the gait pattern and the pressure pattern. A physical therapist who trains paraplegics to walk in the ReWalk exoskeleton, confirmed that the observed crutch strategy is the one taught to and employed by all ReWalk users. It consists of the following:

- Both crutches are lifted simultaneously.
- Both crutches are put down simultaneously.
- Crutches are lifted during mid-swing or terminal swing phase.
- Crutches are put down simultaneously or shortly after the swing foot.
- Crutches are placed far apart in the lateral direction (approximately 1.4m apart).
- Crutch placement in the frontal plane is roughly symmetric with respect to the sagittal plane.
- In the sagittal plane, crutches are placed roughly in the same place.
- In the sagittal plane, crutches are put down in an area ranging from the toe of the forward foot to roughly one footlength in front of the forward foot.

#### 2.2.5 Gait including crutch usage

Figure 2.4 shows a schematic overview of a gait cycle including crutches. Each square block can be interpreted as a ‘snap shot’ of the moment in time indicated on the left, as percentage of the gait cycle. The purple lines indicate CoM movements. Since gait speed is relatively slow and because the crutch usage makes the gait more static than normal (dynamic) gait, it is expected that the CoP will not differ very much from the CoM and image 2.4 has been constructed using the graphs in figure 2.3, to give a sense of what we can expect to find in this study.

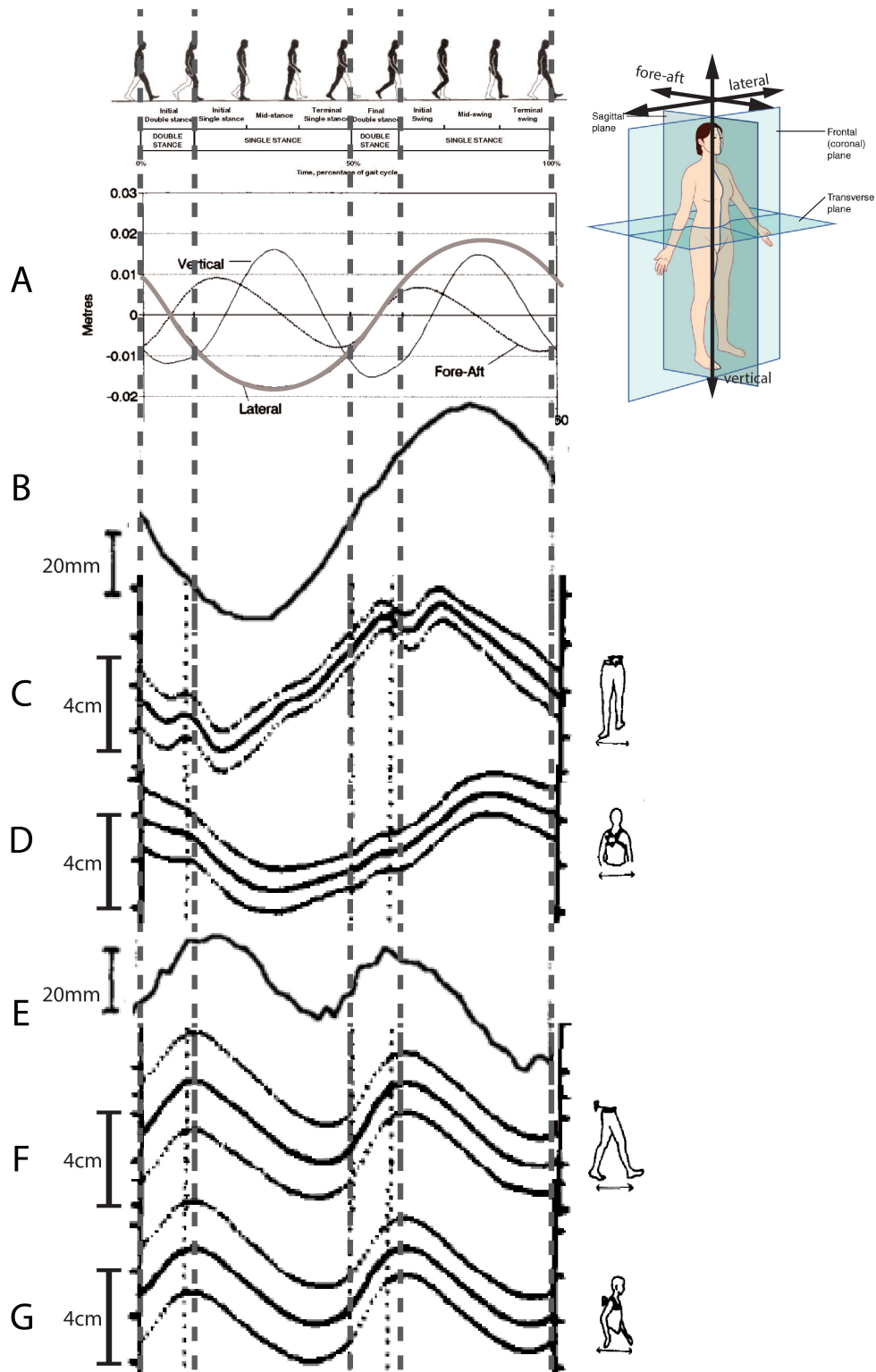


Figure 2.3: Anterior-posterior and medio-lateral translations of the CoM, pelvis and thorax during gait. A shows translations averaged over 12 trials, subject was an 11-year-old boy. B and E show data from a single trial of an adult male subject, where B shows medio-lateral and E anterior-posterior oscillations. C, D, F and G show data recorded from a single adult subject, average of 6 trials, C and F showing pelvic translations, D and G thorax translations. Source material from: Gait cycle: (Martin-Felez et al., 2011), anterior-posterior translations, from top to bottom adapted from: (Crowe et al., 1995; Zijlstra & a.L. Hof, 1997; Stokes et al., 1989), human anatomical planes adapted from: <http://oerpub.github.io/epubjs-demo-book/content/m45990.xhtml>.

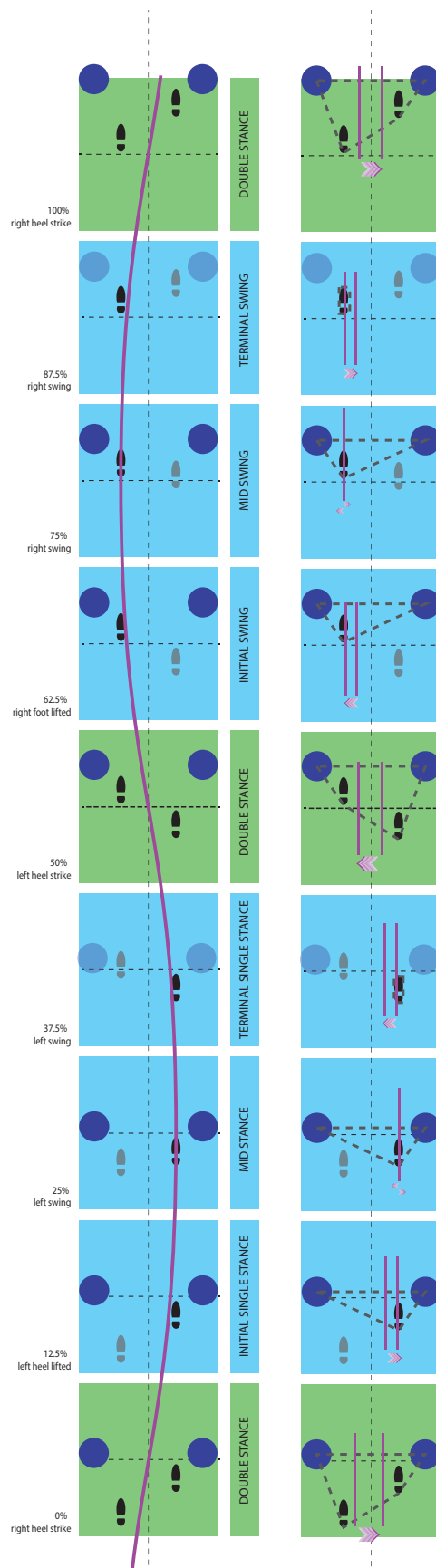


Figure 2.4: Lateral movement of the CoM during a gait cycle with crutches. Black feet are on the ground, grey feet are lifted. The dark blue circles indicate the areas where crutches may be put down; light blue areas indicate lifted crutches. On the left side, the purple line indicates the motion path of the CoM. On the right, the lateral motion of the CoM during that 'snapshot' is indicated by the arrows between the two lines. The grey dotted lines indicate the BoS.

## Chapter 3

# Research questions

We want to know if it might be feasible for the human user to control the exoskeleton's gait pattern by manipulating the pressure pattern. We want the user to be able to do this intuitively. Therefore we want to base it on healthy gait. In healthy walking, the pressure pattern and the gait pattern interact and influence each other. A paraplegic in an exoskeleton cannot directly influence the gait pattern, but they can supposedly influence the pressure pattern (see section 3.1 for some elaboration on assumptions such as this one). A comparable strategy has been experimented with by Vallery and Buss (2006) and Vallery, Van Asseldonk, Buss, and van der Kooij (2009), where healthy limb motion was used to estimate paralysed limp motion.

### 3.1 Assumptions

In order to assess the validity of the proposed step length control strategy, a lot of questions have to be answered. To limit the scope of this study, a number of assumptions will be made. Making these assumptions allows us to focus on the research questions below. In the discussion (chapter 13) we will come back to these assumptions.

- A paraplegic walking in an exoskeleton can manipulate the pressure pattern with torso, arm and crutch movements while walking, without actually changing step size (since only the exoskeleton can do this).
- If pressure pattern variations occur when step length varies during healthy gait, this means that manipulating the pressure pattern to control step length in exoskeleton gait, is an intuitive control method.
- Changing the pressure pattern remains an intuitive manipulation, even if a person cannot use their leg muscles to change the pressure pattern, and therefore has to rely on upper body muscles, arm muscles and crutches to do this.

### 3.2 Questions

Ultimately, the main question that needs answering is:

**Main question.** *Is there potential in using the pressure pattern to intuitively control step length in semi-autonomous exoskeletons?*

In order to answer the main research question, a number of other questions have to be addressed. First of all, if the observed pressure pattern does not differ between extremely long and extremely short steps, it is not much use exploring this research direction further:

**Question 1.** *Can the pressure pattern possibly be used to distinguish extreme steady state long from extreme steady state short steps?*

- ⇒ What metrics show a likely difference between steady state long and steady state short steps?
- ⇒ Do these metrics show a likely difference between long and short steps, for both feet?
- ⇒ Do these metrics show a likely difference between long and short steps, for all three subjects?

In section 7.1.3 we define 'likely difference'. Only if the answer to this question is yes, it makes sense to ask the next question:

**Question 2.** *Can the pressure pattern possibly be used to identify a change in step length before it happens?*

- ⇒ What metrics identified in answering question 1, show a likely difference between the steady state beginning and pre-transition step group?
- ⇒ Do these metrics show a likely difference in this comparison, for both feet?
- ⇒ Do these metrics show a likely difference in this comparison, for all three subjects?

If this question can be answered with yes, there is definitely potential in controlling exoskeleton step length with the pressure pattern. It would mean that the pressure pattern changes before the BoS changes: this would make it a more likely intention conveyor. If the answer is no, it may still be valuable to look at the transition in step lengths itself:

**Question 3.** *Can the pressure pattern possibly be used to identify a change in step length while it is happening?*

- ⇒ What metrics identified in answering question 1, show a likely difference between the steady state beginning and transition step group?
- ⇒ Do these metrics show a likely difference in this comparison, for both feet?
- ⇒ Do these metrics show a likely difference in this comparison, for all three subjects?

Depending on the answers found to these questions (especially question 1), it may or may not be useful to look at a more moderate difference in step lengths:

**Question 4.** *Can the pressure pattern possibly be used to distinguish between steady state long and steady state short steps, when the difference in step length is less extreme?*

- ⇒ What metrics identified in answering question 1, show a likely difference between moderate steady state long and moderate steady state short steps?
- ⇒ Do these metrics show a likely difference in this comparison, for both feet?
- ⇒ Do these metrics show a likely difference in this comparison, for all three subjects?

Finally, if question 3 can be answered with 'yes', it is interesting to know if the pressure pattern in the transition step differs from the previous steps simply because in the transition step the BoS is different, or *because* it is a transition step:

**Question 5.** *Does the pressure pattern of the transition step depend on the length of the steps before/after it?*

- ⇒ Is there a difference in pressure pattern between transition steps from extremely long to extremely short steps, and moderately long to moderately short steps?
- ⇒ Is there a difference in pressure pattern between transition steps from extremely short to extremely long steps, and moderately short to moderately long steps?
- ⇒ Is there a difference in pressure pattern between extreme/moderate long steps?
- ⇒ Is there a difference in pressure pattern between extreme/moderate short steps?



**Part II**  
**Methods**

# Chapter 4

## Experimental design

### 4.1 Pilot experiments

Several small pilot experiments were performed to test hardware and to explore the best ways in which to perform the study. In these small tests the researcher acted as subject. Before detailing final experimental design, some notes will be made on what these pilot experiments meant for the study as a whole.

#### 4.1.1 Pilot set-up

In the pilot experiments the same sensor shoes were used as in the actual study; see section 4.2. In addition to this, similar force/torque sensors were installed in the crutches. With coloured tape markings were made on the floor: six lines 65cm apart followed by six lines 20cm apart. This allowed for two full long steps and two full short steps with a transition step in between. The researcher traversed this track a number of times wearing the sensor shoes and using the sensor crutches, recording data.

#### 4.1.2 Pilot conclusions

- Steps of the same length produce very similar data over different trials; repeatability is good.
- Even looking roughly over the data, clear differences can be noted between long and short steps.
- After some experimenting with the resulting data it was decided to use three parameters to express the data: the total force perpendicular to the sole ( $F_z$ ), the center of pressure along the anterior/posterior sole axis (CoP Y) and the center of pressure along the medio-lateral sole axis (CoP X). See figure 5.6 and section 5.3.4 for more information.

#### 4.1.3 Changes after pilot

**Crutch sensors** The sensors in the crutches generated a lot of seemingly very interesting data during the pilot trials. However, it was unclear what to do with all this information, especially since the position and orientation of the crutches is unknown. In deliberation with prof.dr.ing. Heike Vallery it was decided to narrow down the focus of the study by eliminating the crutch force/torque sensors from the study altogether, instead of widening the scope and focus by adding more sensors and data to the crutches.

**Ski shoes** It was soon noted that at the end of a step, before toe-off, there is a large push-off force. It was hypothesized that this force is produced by ankle muscles. Since exoskeletons at the time did not feature actuated ankle joints it seemed desirable to eliminate such forces from the study. To try to achieve this some data was recorded while the subject wore ski shoes. Ski shoes obstruct movement in the ankle. Contrary to expectation, the toe push-off forces became higher when the ski shoes were used; apparently it not (just) the ankle joint that produces them. The ski shoes were dismissed from the study.

**Track length** It was decided to add extra steps at the start and end of the tracks, to remove the transient effects of participant's starting and stopping walking.

**Velcro floor markings** In the pilot trials there was no way to know if foot placement was correct. Incorrect foot placement would lead to undesirable unknowns. Variation in  $y$ -direction would cause variation in step length other than the prescribed research parameter step length. Variation in  $x$ -direction would lead to varying BoS; any found effects in the pressure pattern might consequently be the result of this variation in  $x$ -direction instead of the prescribed variation in  $y$ -direction. As a solution to this problem, it was decided to indicate the steps on the floor with Velcro tape and to equip the soles with corresponding Velcro patches. See section 4.3 for more explanation on this solution.

**Metronome** In order to restrict unwanted variation in gait as much as possible, it was decided to prescribe the same walking rhythm to each subject. In the pilot trials several metronome patterns were experimented with. Firstly, it was found that it was difficult to maintain the exact same rhythm across the step length transition. Therefore it was decided to turn off the metronome sound one step before the transition; subjects were instructed to keep on walking in a rhythm that felt natural after that. Secondly, it was found that if every step was indicated by only one sound, this produced a stilted gait. Therefore it was decided to indicate each step with one main sound and two minor clicks to indicate step cadence. See section 4.2.5 for more information.

The experience gathered from the pilot experiments was used in subsequent trials. The rest of this chapter is dedicated to describing the methods used in the main experiments of this study.

## 4.2 Hardware

Most insole pressure sensors are not suitable for this study, because the generated data can only be evaluated in their own dedicated software. Moreover, the MARCH exoskeleton was going to feature OptoForce sensors in the soles. To make the results of the current study of value for Project MARCH, it was therefore decided to use these robust and sensitive sensors in this study as well. Matching hardware was produced to accommodate these sensors.

### 4.2.1 Soles

The soles are a rigid construction. A single rigid aluminum top plate is connected to two separate aluminum bottom plates by a sensor each. Thus, all forces are transferred from the floor to the foot through one of the sensors. In theory a single sensor would be sufficient. However, this would cause very large moments around the  $x$ - and  $z$ -axes which would overload the sensor. Therefore a two-sensor construction was chosen. Since the bottom plates are not connected, the sensors measure forces and moments individually. See figure 4.1 for an image of this basic structure. The image also shows the six cylindrical

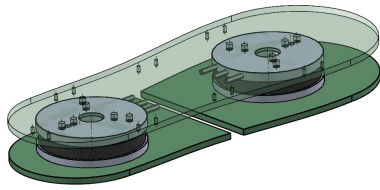


Figure 4.1: The basic structure of the sensor shoes. The plates shown in green are made of aluminum. The top plate is made transparent for clarity. The sensors - the cylindrical disks - connect the top plate to the two bottom plates.



Figure 4.2: The wearable sensor shoe can be easily put on and adjusted using the black Velcro straps.



Figure 4.3: One of the 6 axis force sensors used in this study. Brand: OptoForce. Model: HEX-70-CE-2000N, interface type USB. On the right is the sensor, left is the data acquisition unit with micro USB exit port.

holes where each sensor is screwed to the top plate. They are attached to the bottom plates in exactly the same manner. The plates were fabricated using highly accurate CNC water jet cutting, so that the screw holes are in exactly the same place as in the sensors, avoiding internal tensions.

#### 4.2.2 Sensors

See figure 4.3 for a photo of one of the sensors produced by OptoForce. The sensors measure force and torque in all three directions (6 axis force sensor). Nominal capacity:  $F_x$  and  $F_y \pm 300\text{N}$ ,  $F_z$  (compression)  $2000\text{N}$ ,  $F_z$  (tension)  $800\text{N}$ ,  $T_x$  and  $T_y \pm 15\text{Nm}$ ,  $T_z \pm 10\text{Nm}$ . When one of the sensor in the front of the sole failed, the front sensors were replaced by a model with higher capacity:  $F_x$  and  $F_y \pm 800\text{N}$ ,  $F_z$  (compression)  $4000\text{N}$ ,  $F_z$  (tension)  $1000\text{N}$ ,  $T_x$  and  $T_y \pm 35\text{Nm}$ ,  $T_z \pm 30\text{Nm}$ .

#### 4.2.3 Data acquisition

The sensors are connected to a data acquisition (DAQ) unit (one per sensor) by cable, see figure 4.3. From the two sensors installed in one sole, one DAQ unit is incorporated in the sole. Since there is not enough space in the sole to house both DAQ units, the other one is strapped to the lower leg with a small fixture made especially for this purpose, as seen



*Figure 4.4: Wearable sensor shoe, crutch and DAQ unit fixture on lower leg. The straps to strap the wearable sensor shoe to the foot had not been made when this photo was taken.*

in figure 4.4. The DAQ units are connected to a laptop computer by a microUSB-to-USB cable. These cables are led along the subject's leg, gather at the waist and from there run to the laptop. During experiments, the researcher has to manage this bundle of cables and make sure that it is not in the way of the subject.

A C++ program (adapted from code supplied by the sensor manufacturer to fit this study's requirements) was used to read and store the data while an experiment was running. Data was read at a frequency of 100-500Hz and stored as a text document with 25 columns: 1 time vector, 24 (4 sensors  $\times$  6 axes) columns with data points.

#### 4.2.4 Crutches

When designing this study, it was the plan to include sensors in the crutches, as can be seen in figure 4.4. Special attachment pieces to incorporate the OptoForce sensor cylinders in the crutches were hand-made. In initial tests, the structure proved adept at measuring forces and torques in the crutches. However, it was later decided to omit these sensors because the extra data from the crutches confused rather than illuminated matters. It turned out to be not very useful to have force/torque information on the crutches, without knowing the position and orientation of the crutches themselves, see

section 4.1.3 for more information regarding this decision. The study was continued with normal crutches, without crutch sensors.

### 4.2.5 Metronome

A digital metronome was used to indicate step rhythm. A slightly different sound indicated a right (R) or left step (L). Between these sounds, two smaller clicks were heard to indicate step cadence (x-x). So the metronome sound can be represented by: R-x-x-L-x-x-R-x-x-L-x-x-etc. Participants were instructed to start walking with a right step after hearing one [R-x-x-L-x-x]-sequence to prepare them. The metronome automatically turned off after the pre-transition step.

## 4.3 Walking tracks

Figure 4.5 shows a schematic visual of one of the walking tracks employed in the experiments. The track consists of nine steps and is traversed in both directions.

There are two tracks displayed on the floor; one has crosses 65cm and 20cm apart, whilst the other has crosses 55cm and 30cm apart. The first track is defined as the *extreme* track and the second as the *moderate* track. In the extreme track, the difference between long and short swings is 90cm (130cm minus 40cm), while in the moderate track this difference is only 50cm (110cm minus 60cm). However, in both tracks the transition step is 85cm.

The black crosses on the floor are made with Velcro tape (hooks side). The sensor soles feature little patches of Velcro as well; the loops side. When the feet are placed correctly in reference to the crosses on the floor, the Velcro hooks and loops do not touch, see figure 4.7, leftmost image. However, if the foot is placed incorrectly with reference to the black cross, the patches of Velcro will touch; see the middle and right image in figure 4.7. When the subject subsequently lifts this foot, he/she will feel the resistance created by the Velcro. Also, subject and researcher will hear the ripping sound of the Velcro patches being pulled apart. By these signs, the researcher will know that the foot has not been placed accurately and the trial should be dismissed. This strategy ensures that foot placement is accurate.

Both tracks can be traversed in both directions: either starting with long steps or starting with short steps. This gives the following four options:

In **A trials** subjects traverse the extreme track starting with long steps.

In **B trials** subjects traverse the extreme track starting with short steps.

In **C trials** subjects traverse the moderate track starting with long steps.

In **D trials** subjects traverse the moderate track starting with short steps.

## 4.4 Carrying out the experiments

### 4.4.1 Protocol

1. Explain procedure to subject:

You will traverse these tracks back and forth four times.

While walking you will use crutches and wear sensor shoes that you can strap onto your own shoes.

A metronome will indicate the walking tempo.

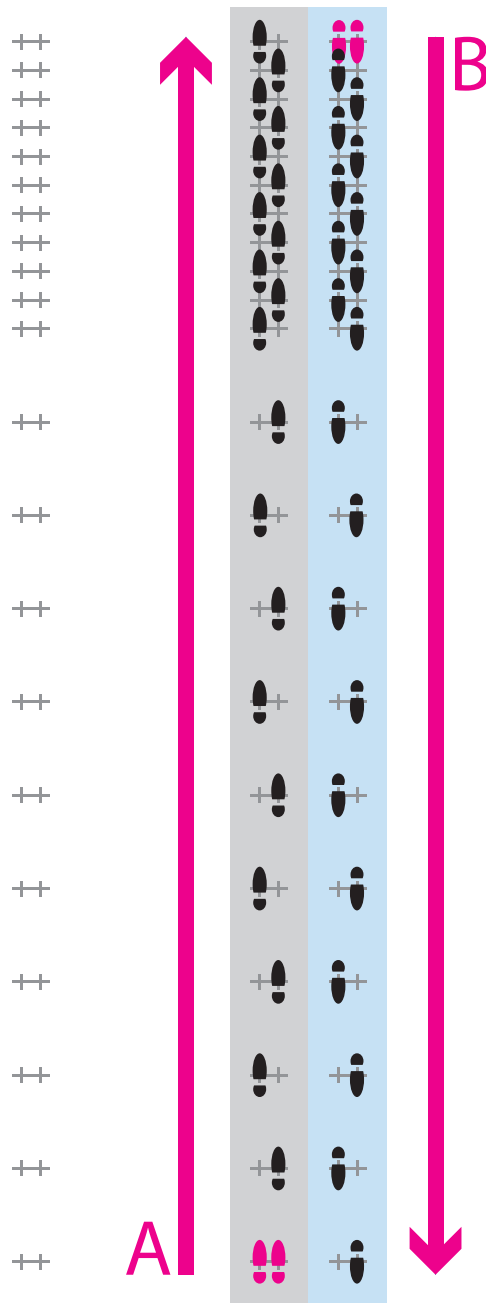


Figure 4.5: Walking track schematic. The crosses on the left represent the actual markings shown on the floor of the track. In the grey shaded area, it is shown how a subject will traverse the track during an A trial (and C trials): first long steps, followed by short steps. During B trials (and D trials), the same floor markings are used; only this time, the subject starts at the other end, so that the short steps will come first. Subjects always start walking with their right foot. Pink foot prints represent the position of the feet before the subject starts walking.



Figure 4.6: A photo of the walking tracks as they were displayed on the floor. The crosses are made of black Velcro band. On the right is the extreme track, on the left the moderate track.

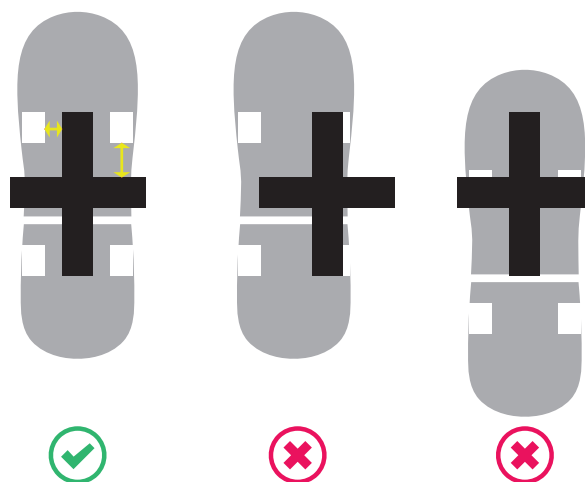


Figure 4.7: The white rectangles represent patches of Velcro - the loops side - attached to the sole. The black cross represents the Velcro crosses attached to the floor - the hooks side. The yellow arrows in the leftmost image indicate the error margins allowed for foot placement. The middle and right image show how the Velcro will touch when the foot is not placed correctly.



The black crosses on the floor show you where to place your feet.

If you misstep, the Velcro on your sole will touch the Velcro on the floor. If you feel/hear this, please let the researcher know. We will do an extra trial.

2. Set crutches to right length.
3. Demonstrate how to use the crutches.
4. Give subject a moment to get used to using the crutches in this way.
5. Strap on the soles.
6. Make sure all cables are properly tucked away.
7. Let subject walk back and forth on each of the 2 tracks a few times.
8. Add metronome to practice.
9. Explain how to indicate the start of a new trial (lift left foot for 2s, lift right foot for 2s)
10. When subject is comfortable with the procedure, continue.
11. Ask subject to walk 10m at comfortable step length with crutches. Count number of steps to calculate comfortable step length.
12. Let subjects start with track AB or track CD at random.
  - Condition A: 65cm-20cm
  - Condition B: 20cm-65cm
  - Rest for 5 minutes.
  - Condition C: 55m-30cm
  - Condition D: 30cm-55cm

See Appendix A for the protocol sheets that were used by the researcher to keep track of the experiment while conducting it.

#### 4.4.2 Walking rhythm

For the first two subjects, the imposed step rhythm differed per trial. In A and C trials a beat of 57BPM was played, in B and D trials a beat of 60BPM. The rationale behind this difference, was that the longer steps demanded a lower step rhythm. It was found, however, that the difference was not noticeable. Therefore, after the first two subjects, a single step rhythm of 55BPM was decided upon.

The metronome stopped automatically when subjects reached the pre-transition step, so that they could go through step length transition in a tempo that felt comfortable to them. Subjects were instructed however, to keep walking in a similar tempo as they had been.

#### 4.4.3 Crutch usage

The crutch usage strategy described in 2.2.4 is demonstrated to the subjects and they are given time to familiarize themselves with this motion.

#### 4.4.4 Subject descriptions

Subjects were three females aged 25-27 years. Length: 1.70m to 1.80m. Weight: 58kg to 85 kg. Comfortable step length ranged from 0.5m to 0.55m.

#### **4.4.5 Sensor failure**

Due to sensor failure, experiments could not be continued after testing with these three subjects. See section 13.2.3 for more elaboration.

# Chapter 5

## Data analysis

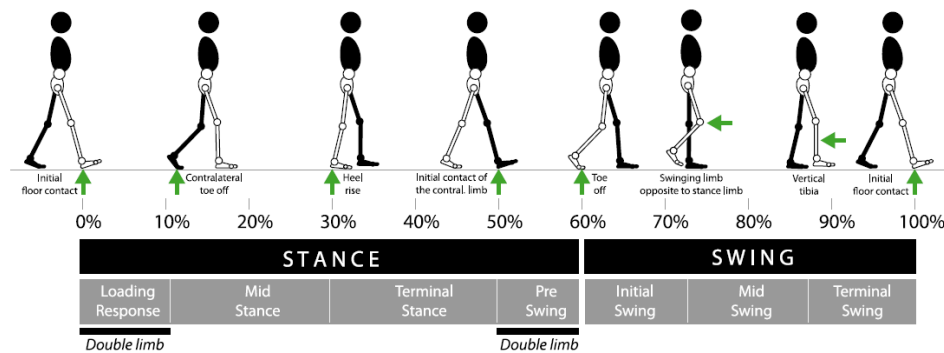


Figure 5.1: Step phases, from (Torricelli et al., 2016)

### 5.1 Steps and step groups

#### 5.1.1 Stance and swing phase

As shown in figure 5.1, each step consists of a stance and a swing phase. During stance of the right foot, swing of the left foot takes place, and vice versa. During every step there are two double limb phases, when both feet are on the floor. The arcs in figure 5.2 represent the swings taken by the left foot (solid) and the right foot (dashed). The colored blocks in figure 5.2 represent the stance phases. It can be seen in this figure as well, that each stance phase overlaps with the previous as well as the following stance phase of the other foot. The arcs show how the length of each swing (step length) changes throughout the track. It can be seen that the fifth swing of the right foot is of a length between the long and short swings: this is where the actual transition from long to short steps takes place. The colored blocks - the stance phases - represent what is actually measured during these experiments: when the foot is on the floor, the pressure pattern is recorded. From this visualization we can also derive how the steps are numbered in this study: according to stance phase. Right foot stance phase RS starts at initial floor contact of the right foot (RIFC) and ends when the right foot is completely lifted from the floor. In figure 5.2: the colored blocks containing the right foot print. Left foot stance phase LS starts at initial floor contact of the left foot (LIFC) and ends when the left foot is completely lifted from the floor. In figure 5.2: the colored blocks containing the left foot print. Whenever full steps are counted/referred to, a combination of a right and left step is meant: starting at

initial floor contact of the right foot (RIFC) and ending at the following RIFC (see figure 5.1).

### 5.1.2 The step groups

Five step groups are identified:

- steady state beginning (ssb)
- pre-transition step (pre)
- transition step (tr)
- post-transition step (post)
- steady state end (sse)

These five step groups are also indicated in figure 5.2, with corresponding colors. These colors will be used throughout this report. Please note that in A and C trials, ssb consists of long steps and sse of short steps; in B and D trials this is the other way around.

## 5.2 Comparisons

### 5.2.1 Between trial groups

Comparisons will be made *within* the following groups: A-trials, B-trials, C-trials, D-trials (A, B, C and D in short). Within each of these groups, right (R) and left (L) will be considered separately. This results in 8 groups: RA, LA, RB, LB, RC, LC, RD and LD.

The largest effects are expected to be found in the A- and B-trials; the trials executed on the extreme tracks. In these trials the difference between big and small steps is the greatest. It is hypothesized, that in the C and D groups, the same effects, but less intense, will be found as in the A and B groups, respectively. Therefore, after initial comparison within the aforementioned eight groups, RA, LA, RB, LB will be compared to RC, LC, RD and LD, respectively.

### 5.2.2 Between step groups

Theoretically, each of these five stepgroups could be compared to the other four, resulting in ten comparisons (see table 1.1, left). However, not all ten of these comparisons are equally valuable. Below the three most interesting comparisons (see table 1.1, right) will be briefly discussed. Figure 5.3 shows these comparisons 1 to 3 and their interrelations.

**1 steady state beginning - steady state end:** this is the basic comparison between long and short steps. If notable differences between these step groups are found in this comparison, it can be concluded that it is promising to use the pressure pattern on the foot soles as an indicator for desired step size. If no differences can be found, it is not worthwhile to continue investigation of comparisons 2 and 3.

**2 steady state beginning - pre-transition:** this is the most important comparison of all. If effects can be found here, that means that the intention to change step length can be predicted a step in advance. Most importantly, it means that with intended step length adjustments, the pressure pattern changes *before* and therefore at that moment *without* an actual change in foot placement and base of support. This is crucial, since paraplegics walking in an exoskeleton cannot change their fBoS.

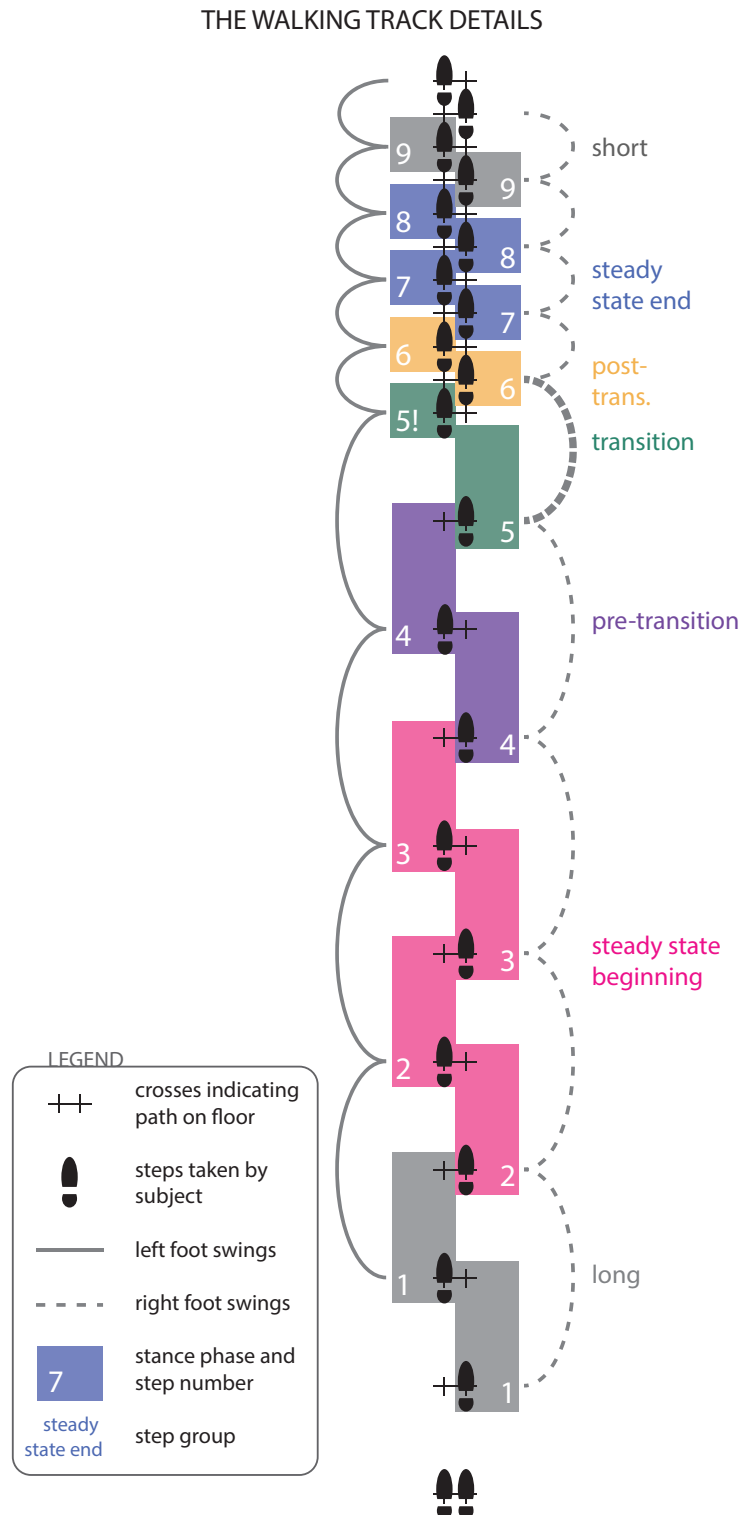


Figure 5.2: The numbered arcs represent the swings taken by the left foot (solid line) and the right foot (dashed line). Colored blocks represent the period that the foot is on the floor, the stance phase. Steps are numbered according to stance phases. Steps are gathered in groups as shown by the different colours and group names. Black crosses represent the Velcro markings on the floor. In step 5, when the left foot is on the floor (indicated by 5!, with exclamation mark), the right foot makes the swing that is the actual transition from long to short steps (indicated by extra thick dashed line).

A trials					C trials				
STEP	Foot on floor	Swing foot	length of swing	group	STEP	Foot on floor	Swing foot	length of swing	group
1	R	L	130 cm		1	R	L	110 cm	
1	L	R	130 cm		1	L	R	110 cm	
2	R	L	130 cm	ssb	2	R	L	110 cm	ssb
2	L	R	130 cm						
3	R	L	130 cm						
3	L	R	130 cm						
4	R	L	130 cm	pre	4	R	L	110 cm	pre
4	L	R	130 cm						
5	R	L	130 cm	tr	5	R	L	110 cm	tr
5	L	R	85 cm						
6	R	L	40 cm	post	6	R	L	60 cm	post
6	L	R	40 cm						
7	R	L	40 cm	sse	7	R	L	60 cm	sse
7	L	R	40 cm						
8	R	L	40 cm						
8	L	R	40 cm						
9	R	L	40 cm		9	R	L	60 cm	
9	L	R	40 cm		9	L	R	60 cm	

B trials					D trials				
STEP	Foot on floor	Swing foot	length of swing	group	STEP	Foot on floor	Swing foot	length of swing	group
1	R	L	40 cm		1	R	L	60 cm	
1	L	R	40 cm		1	L	R	60 cm	
2	R	L	40 cm	ssb	2	R	L	60 cm	ssb
2	L	R	40 cm						
3	R	L	40 cm						
3	L	R	40 cm						
4	R	L	40 cm	pre	4	R	L	60 cm	pre
4	L	R	40 cm						
5	R	L	40 cm	tr	5	R	L	60 cm	tr
5	L	R	85 cm						
6	R	L	130 cm	post	6	R	L	110 cm	post
6	L	R	130 cm						
7	R	L	130 cm	sse	7	R	L	110 cm	sse
7	L	R	130 cm						
8	R	L	130 cm						
8	L	R	130 cm						
9	R	L	130 cm		9	R	L	110 cm	
9	L	R	130 cm		9	L	R	110 cm	

Table 5.1: Details for trials A, B, C and D. Colours correspond to the step groups defined in section 5.1.2. Steps 1 and 9 are discarded to eliminate transient effects.

	ssb	pre	tr	post	sse
ssb		x	x	x	x
pre			x	x	x
tr				x	x
post					x
sse					

Table 5.2: All possible comparisons between step groups within the same trial group.

	ssb	pre	tr	post	sse
ssb		x	x		x
pre					
tr					
post					
sse					

Table 5.3: The step group comparisons selected for consideration in this study.

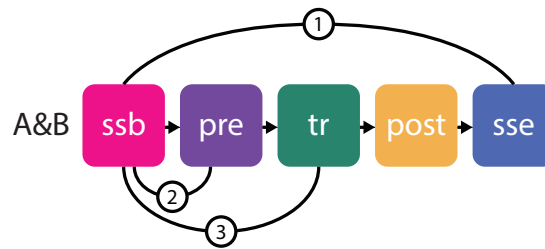


Figure 5.3: Visual representation of comparisons 1, 2 and 3 between step groups. From left to right, the step groups are: steady state beginning, pre-transition, transition, post-transition and steady state end. The colors correspond to colors used throughout this report for these five step groups.

**3 steady state beginning - transition:** if effects are found here, changing step length can be read from the pressure pattern on the foot soles during the change, which is also very valuable information. The actual transition takes place during the second half of the step, when the left foot is on the floor. Therefore, effects perceived in the first half of the transition step (when the right foot is on the floor) are also predictive of the transition.

## 5.3 Data processing

### 5.3.1 Calibration, zeroing and rotation

Data is recorded in two batches: as the subject walks back and forth on the extreme track (which results in one long sequence of data in which A- and B-trials alternate), and as the subject walks back and forth on the moderate track (which results in one long sequence of data in which C- and D-trials alternate). After loading the raw data into Matlab, a few simple processing steps have to be conducted in order to make the data readable at all. First of all, the sensor data has to be calibrated. This is done using the calibration data provided by the sensor producer. Next, the user is shown the start of recorded Fz data plotted in a graph. In this graph, the user indicates which intervals can be used for zeroing the data. These are the intervals where the subjects were asked to alternately raise their feet from the ground for 10 seconds. After calibrating and zeroing, the sensor data is mathematically rotated so that the x- and y-axes from the different sensors become aligned. Figures 5.4 and 5.5 show all force and torque data acquired during the A- and B-trials of subject 1, at this stage in the process of data processing.

### 5.3.2 Separating the trials

After these processing steps, the user is shown the Fz data of all four sensors plotted in four graphs in one column. Since the subjects were asked to alternately lift their right and left foot from the floor before starting each trial, it is easy for the researcher to visually

recognize the start of each new trial in these Fz plots. The researcher indicates the start and end of each trial by pointing and clicking with the mouse pointer in the plot window. These data points will later be used to cut the data and put it in different matrices; one data matrix per trial. First, however, the data is filtered using a 2nd order Butterworth filter.

Next, the filtered data is divided into the different trials and each trial is given its own data matrix. For each trial, the researcher is shown a plot of the Fz data of all four sensors. This is basically a zoomed-in version of the plots the researcher was given before, in which to indicate the start and end of each trial. Now, the researcher is asked to crop the trials more accurately. The first step of a trial is very recognizable: after the right and left leg have been off the floor (giving a  $Fz \approx 0$  result) alternately, the first right heel strike is clearly recognizable as the first instance of a short period of time where Fz of the right heel is zero, followed by a significant rise of the curve. The trial ends at the tenth right heel strike; so the researcher can easily count ten of these bumps in the graph and in that way crop each trial to a consistent ten right heel strikes. After cropping, the researcher is again presented with graphs presenting the Fz values. Using these graphs, the researcher can check if the data was cropped correctly, making adjustments if necessary.

### 5.3.3 Separating the steps

Now that the data is chopped up into different trials, these trials have to subsequently be divided into separate steps. A full step is defined as follows: "the period of time between two subsequent right foot strikes". A right foot strike, or RFS, is defined as follows: "the moment when any part of the right foot makes contact with the floor, when this moment was preceded by a period of time when the right foot was off the floor and followed by a period of time when the right foot is on the floor". The same goes for a left foot strike (LFS). The cutoff value to distinguish between foot on floor and foot off floor, is defined as:

$$cutoff = 0.05 * \bar{Fz}_{max} \quad (5.1)$$

Where the maximum Fz is calculated for every sensor in every trial and 5% of the mean of these values is taken as the cutoff value. Using this cutoff value a phase vector is constructed for every sensor, for each trial. The phase vector has the same length as the data matrix for that trial and contains a 1 or 0 for every data point, denoting if the sensor in question is on (1) or off (0) the floor at that moment. Using these four phase vectors (right front, right rear, left front, left rear) a phase transition vector is constructed, using the strategy denoted in table 5.4. From these phase transition matrices (one for each foot), the foot strikes and foot lifts can be extracted: values of 1, 10 or 11 in the phase transition matrix represent a foot strike at that moment in time. Values of -2, -20 or -22 represent a foot lift at that moment in time. In this way, the trials are cut up in the separate steps.

### 5.3.4 Calculating CoP X, CoP Y and Fz

Figure 5.6 shows the three parameters that are used to summarize the data: the force perpendicular to the sole plates  $F_z$  and the two in-plane coordinates of the center of pressure (CoP):  $CoP_X$  and  $CoP_Y$ .  $F_z$  is as the vertical replacement force, summing up all forces along the x-axis working on the sole, acting in the center of pressure. These three parameters are calculated for each foot separately. Fz is easily calculated by adding the Fz-values of the two sensors in each sensor shoe.  $CoP_X$  and  $CoP_Y$  are calculated as follows:

$$CoP_X = \frac{M_y + (F_x * r_z)}{F_z} \quad (5.2)$$



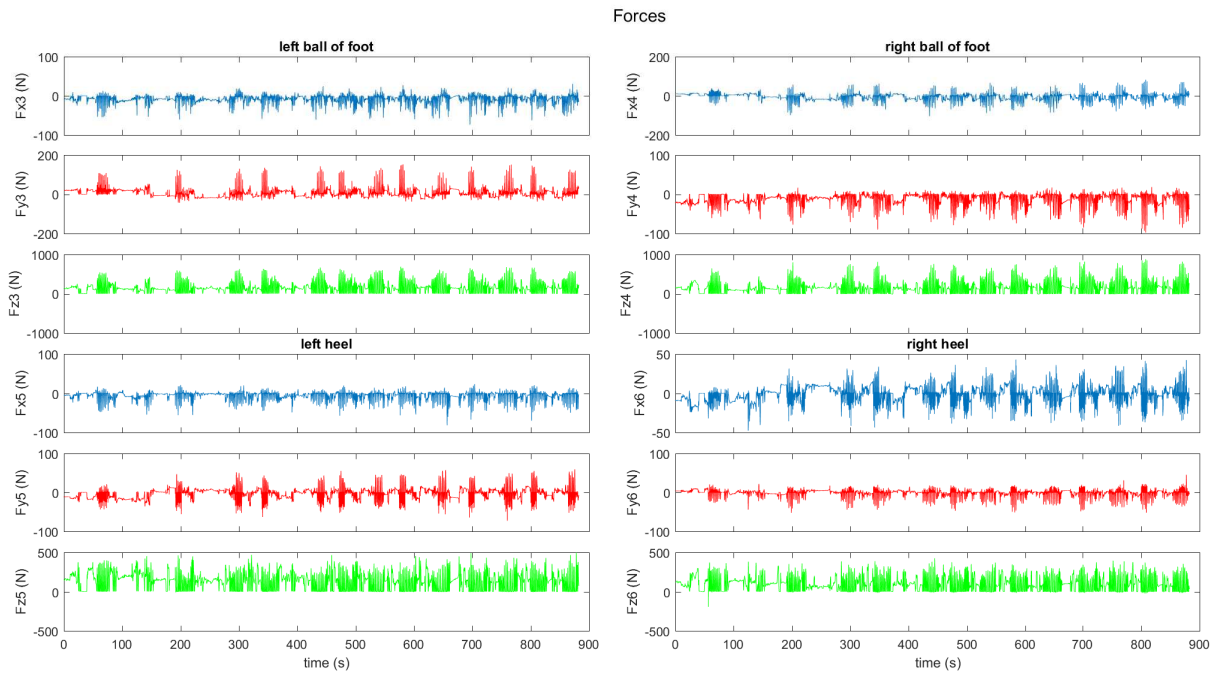


Figure 5.4: All forces recorded during A and B trials, subject 1.

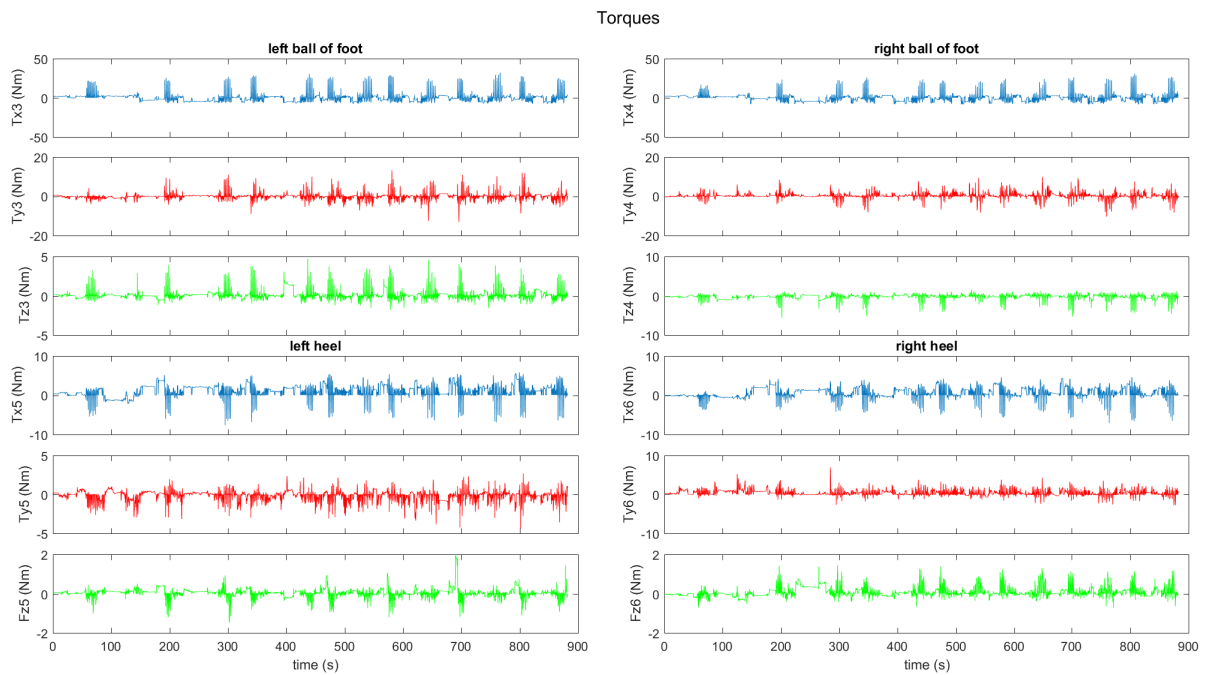


Figure 5.5: All torques recorded during A and B trials, subject 1.




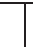


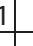
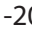
i-1 \ i	 0	 1	 10	 11
 0	0	1	10	11
 1	-2	-1	8	9
 10	-20	-19	-10	-9
 11	-22	-21	-12	-11

Table 5.4: Phase matrix to determine foot floor strike. Each state of foot on/off floor is given a code. Front foot on floor = 1, rear foot on floor = 10. Addition of these two states gives: entire foot off floor = 0, entire foot on floor = 11. In this manner, each data point ( $i$ ) is given a number 0, 1, 10 or 11. The previous data point ( $i-1$ ) is coded in the same manner. Subtraction  $i-2(i-1)$  gives this phase matrix.

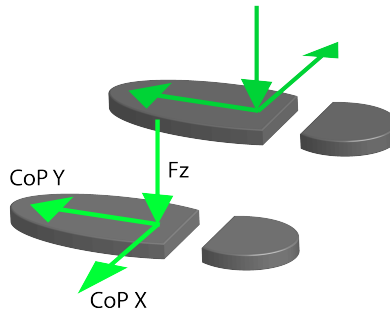


Figure 5.6: The three parameters selected to present the generated data: the x- and y-coordinates of the center of pressure ( $CoP_X$  and  $CoP_Y$ ) and the total force acting perpendicular to the sole  $F_z$ .

$$CoP_Y = \frac{M_x + (F_y * r_z)}{F_z} \quad (5.3)$$

Where  $M_x$  is the moment around the x-axis,  $F_y$  is the force along the y-axis,  $F_z$  is the force along the z-axis and  $r_z$  is the moment arm for  $F_x$  and  $F_y$ ; the thickness of the sensor shoe. Using equations 5.3 and 5.2  $CoP_X$  and  $CoP_Y$  are calculated for each of the four sensors. Next, the front and rear sensor values are combined using equations, resulting in one  $CoP_X$  and  $CoP_Y$  per foot.

$$CoP_{Xf} = CoP_{Xf} \quad (5.4)$$

$$CoP_{Yf} = CoP_{Yf} + d \quad (5.5)$$

$$CoP_{Xr} = CoP_{Xr} \quad (5.6)$$

$$CoP_{Yr} = CoP_{Yr} - d \quad (5.7)$$

Where  $d$  is the distance between the midpoint (in  $xy$ -plane) of the sensor shoe and the center of each sensor,  $CoP_{Xf}$  is the front  $CoP_X$ ,  $CoP_{Xr}$  is the rear  $CoP_X$ ,  $CoP_{Yf}$  is the front  $CoP_Y$  and  $CoP_{Yr}$  is the rear  $CoP_Y$ .

$$CoP_X = \frac{CoP_{Xf} * F_{zf} + CoP_{Xr} * F_{zr}}{F_z} \quad (5.8)$$

$$CoPY = \frac{CoPY_f * F_{zf} + CoPY_r * F_{zr}}{F_z} \quad (5.9)$$

Where CoP X is the CoP X of the entire foot, CoP Y is the CoP Y of the entire foot, Fz is the Fz of the entire foot,  $F_{zf}$  is the Fz of the front sensor and  $F_{zr}$  is the Fz of the rear sensor.

### 5.3.5 Finding the mean and confidence interval

We want to calculate the mean and confidence interval (CI) per step across the four trials. In order to be able to do this, we first need to make the data vector for each step the same length. The lengths of the data vectors for each step differ slightly. We take the longest length ( $l_{max}$ ) and make a query points vector ( $x_q$ ) of that length, but running from 0 to 100 in steps of  $100/l_{max}$ , where 0 corresponds to foot strike (0% of stance phase) and 100 to foot lift (100% of stance phase). Using the Matlab function `interp1` the data points from the original data vectors are mapped onto  $x_q$ . Now, all step data vectors have the same length and a corresponding time vector that runs from 0-100%,  $x_q$ .

Now, it is straightforward to calculate the mean and 95% confidence interval, using Matlab's functions `mean` and `prctile`. We do this both per step, across all trials (see table 5.5) and per step group across all trials (see table 5.6).

steps:	1	2	3	4	5	6	7	8	9
trial 1	step 1	step 2	step 3	step 4	step 5	step 6	step 7	step 8	step 9
trial 2									
trial 3									
trial 4									

Table 5.5: Mean and confidence interval taken per step, across trials.

steps:	1	2	3	4	5	6	7	8	9
trial 1									
trial 2		ssb	pre	tr	post	sse			
trial 3									
trial 4									

Table 5.6: The mean and confidence interval are taken per step group, across trials and steps in a step group.

## 5.4 Visualizing the data

Different ways of presenting the processed data, show different aspects of the results. See, for example, figure 5.7. It shows for all separate steps, the path traversed by the CoP throughout a full step. Some observations can already be made from this image, such as how after step 5, the CoP Y does not go as far backward as before step 5. Interestingly, we can also see that in the left foot, the CoP sometimes moves outside of the sole plate. This only happens at the end of a step. This is likely because at this moment, the back of the foot is already lifting off the floor, rotating around the front edge of the sole. This adds an angular acceleration to the equation, apparently increasing the moment  $M_x$ , apparently increasing  $CoPY$ . This rotation around the front edge of the sensor shoe, is likely also what causes the sensor overload described previously.

Though already some things can be read from such a plot, time is missing in this representation. To solve this, we might use plots such as figure 5.8. As we will see later, in chapter 7, plots like that will actually be used to study the CoP X, since a lot of details are lost in averaging the x-coordinate of the CoP. However, for Fz and CoP Y it is far more convenient to use plots presenting the mean and confidence intervals, such as in figure 5.9, which is an example of averaging the data according to table 5.5. The final step in visualizing the data, is by averaging according to table 5.6. Having done this, it immediately became clear that the ssb in A- and C-trials, shows the same CoP patterns as the sse in B- and D-trials, respectively. In other words; the steady states of long and short steps, really are steady states: it does not matter where in a trial they occur. Therefore, ssb A and sse B; sse A and ssb B; ssb C and sse D; and sse C and ssb D will be combined and analyzed as single groups from now on.

### 5.4.1 Box plots

Since the sample size is too small to perform statistical analyses, box plots will be used to make statements about differences between step groups. The box plots always contain two boxes representing two step groups that are compared to each other. In the presented box plots each box contains the data for the metric in question for all steps in the respective step group. It is decided that *if the boxes do not overlap, there is a likely difference for this metric between these two step groups for this subject* and this specific comparison is labeled **likely different**. If the boxes do overlap, there is no such likely difference and the comparison is labeled **likely similar**. These labels help us evaluate each metric's value in lieu of statistic analysis.

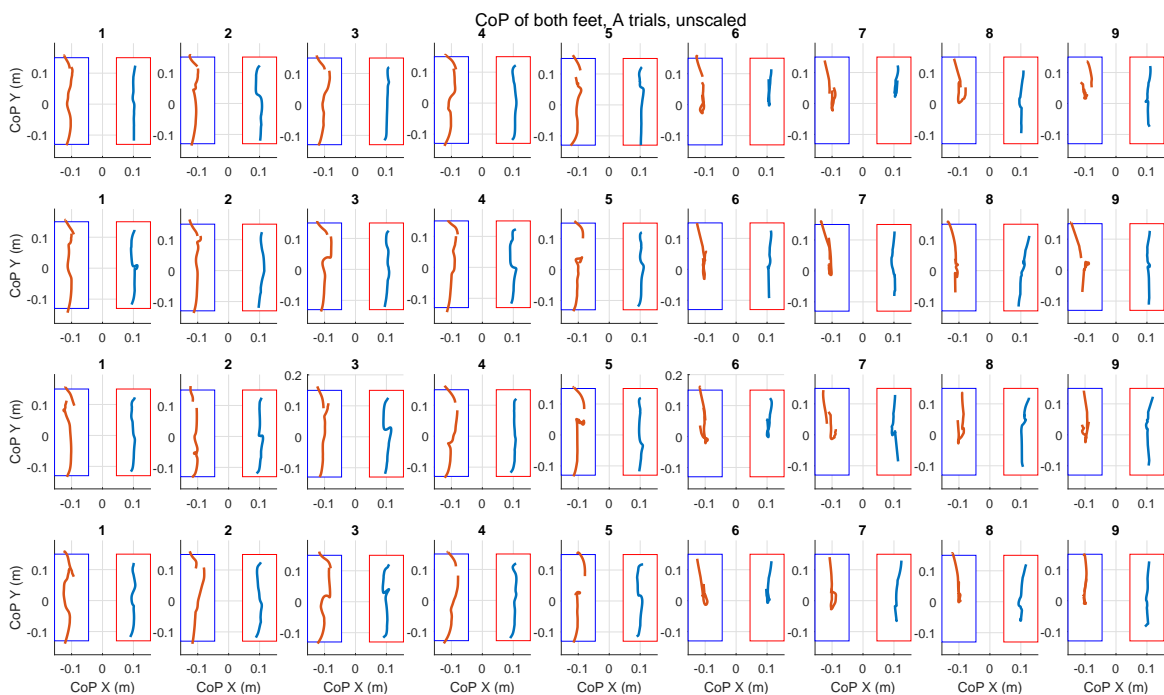


Figure 5.7: CoP X and CoP Y plotted in the xy-plane, for subject 1, A trials. Unscaled (not mapped onto  $x_q$ ) data has been used. Plotted lines represent the CoP trajectory during a full step, starting and ending at right foot strike. Red = left foot, blue = right foot. The boxes are a crude representation of the soles. Red lines show gaps because the steps are cut off according to right foot strike and lift.

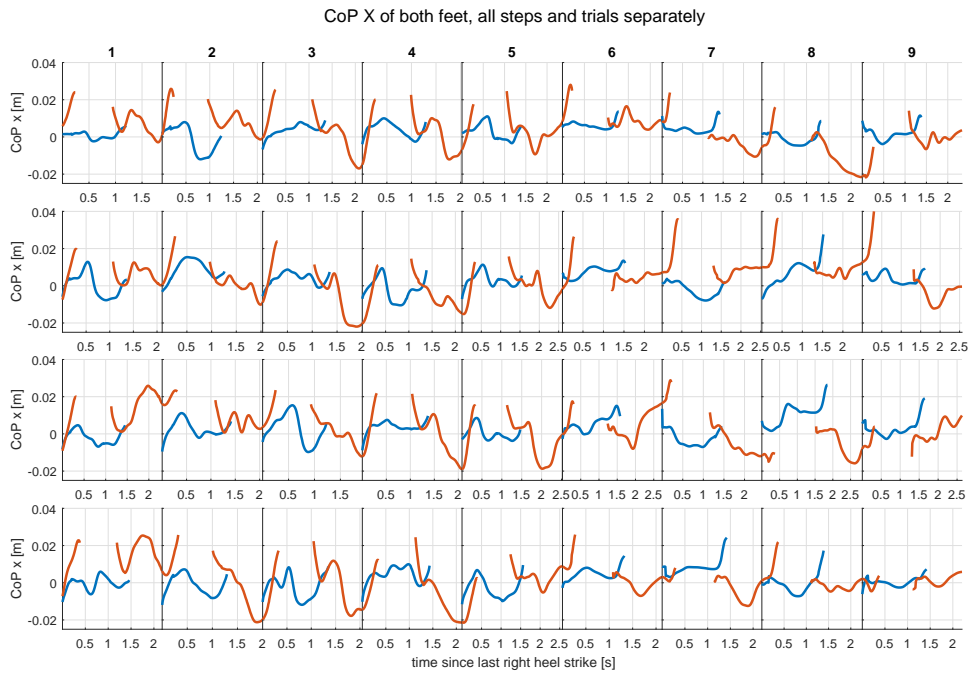


Figure 5.8: CoP X plotted vs time since last right foot strike, for subject 1, A trials. Unscaled (not mapped onto  $x_q$ ) data has been used. Plotted lines represent the path the  $x$ -coordinate of the center of pressure makes during a full step, starting and ending at right foot strike. Red = left foot, blue = right foot.

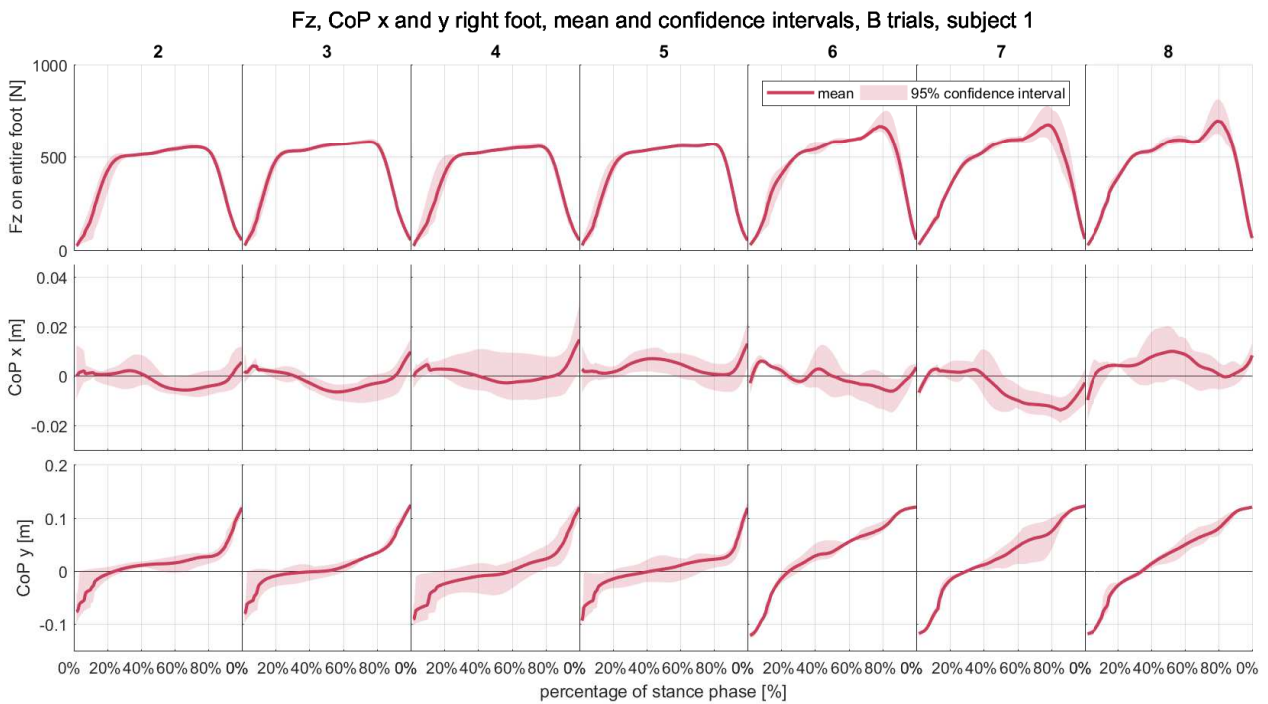


Figure 5.9: Mean and CI of Fz, CoP X and CoP Y, B trials, subject 1, right foot. Steps 1 and 9 have been omitted.

# **Part III**

# **Results**

## Chapter 6

# General results

In figures 6.2 (Fz), 6.3 (CoP X) and 6.4 (CoP Y) on the following pages, an overview is presented of the results for subject 2's A- and B-trials. Each figure shows one of the three parameters Fz, CoP X or CoP Y. Similar figures for subjects 1 and 3 can be found in Appendix B. These figures give a general overview of the results, while the following five chapters will analyze specific comparisons between step groups in a more in-depth manner. The comparisons in chapters 7 (comparison 1), 8 (comparison 2), 9 (comparison 3), 10 (comparison 4), and 11 (comparisons 5, 6 and 7) are studied in order to answer research questions 1 to 5, respectively.



*Figure 6.1: This chapter presents a brief overview of the general results for all five step groups. Subsequent chapters will focus on specific comparisons between these five step groups.*

## 6.1 Fz: vertical force component

Looking at figure 6.2 we notice that the 95% CI is quite narrow and the mean shows a similar pattern even across step groups. Apparently repeatability between steps is great for this parameter. Fz starts rising at 0% of stance phase; in some step groups a plateau is reached that stays relatively stable until Fz starts declining again around 75% of stance phase, until a value of zero is reached at 100% of stance phase, when the foot is lifted. In some other step groups, no such stable plateau is reached and the Fz rises before it drops as the foot is lifted. This 'bump' occurs around 75% of the stance phase and can be interpreted as a push-off force to propel the body forward. This bump is hardly noticeable in the left foot, but very clear in the right foot, especially in the long steps and the transition group in A trials. A possible explanation for this larger bump in the right foot than in the left foot, might have to do with leg dominance. We will pay attention to this bump in subsequent chapters.

## 6.2 Cop X: the x-coordinate of the center of pressure

For this parameter, see figure 6.3, we see a much broader CI, especially in the middle of stance phase. In fact, the CIs are so broad that a lot of data is lost when we study it in this way. When looking more in-depth at the comparisons between step groups we will therefore not make use of mean values. Some observations based on the images in figure 6.3 are: the CoP X profile seems flatter in short steps, and has more of a W-shape in long steps. Again, there is big difference between left and right feet: in the left foot the CoP X moves far more outward at the end of steps, than in the right foot, where the CoP X hovers around zero at 100% of stance phase.

## 6.3 CoP Y: the y-coordinate of the center of pressure

This parameter shows much more narrow CIs than CoP X, and also more recognizable patterns across step groups. In general, the CoP Y makes a forward movement during a step; starting at or below zero and moving to the front limit of the sensor shoe of 15cm. This corresponds to the subject putting down her heel first, and shifting weight forward to place the other foot in front of the first, during stance phase. Already from figure 6.4 we can see that the details of this trajectory differ between step groups, as will be elaborated on in the following chapters. For subject 1 and subject 2, left foot, the CI is very broad at 0% of stance phase: in some steps (from the same step group), the CoP Y starts positive and moves backward before moving forward again, while in other steps the CoP Y starts negative and moves forward throughout the step. This variety in initial CoP Y causes the wide CI at the beginning of a step.



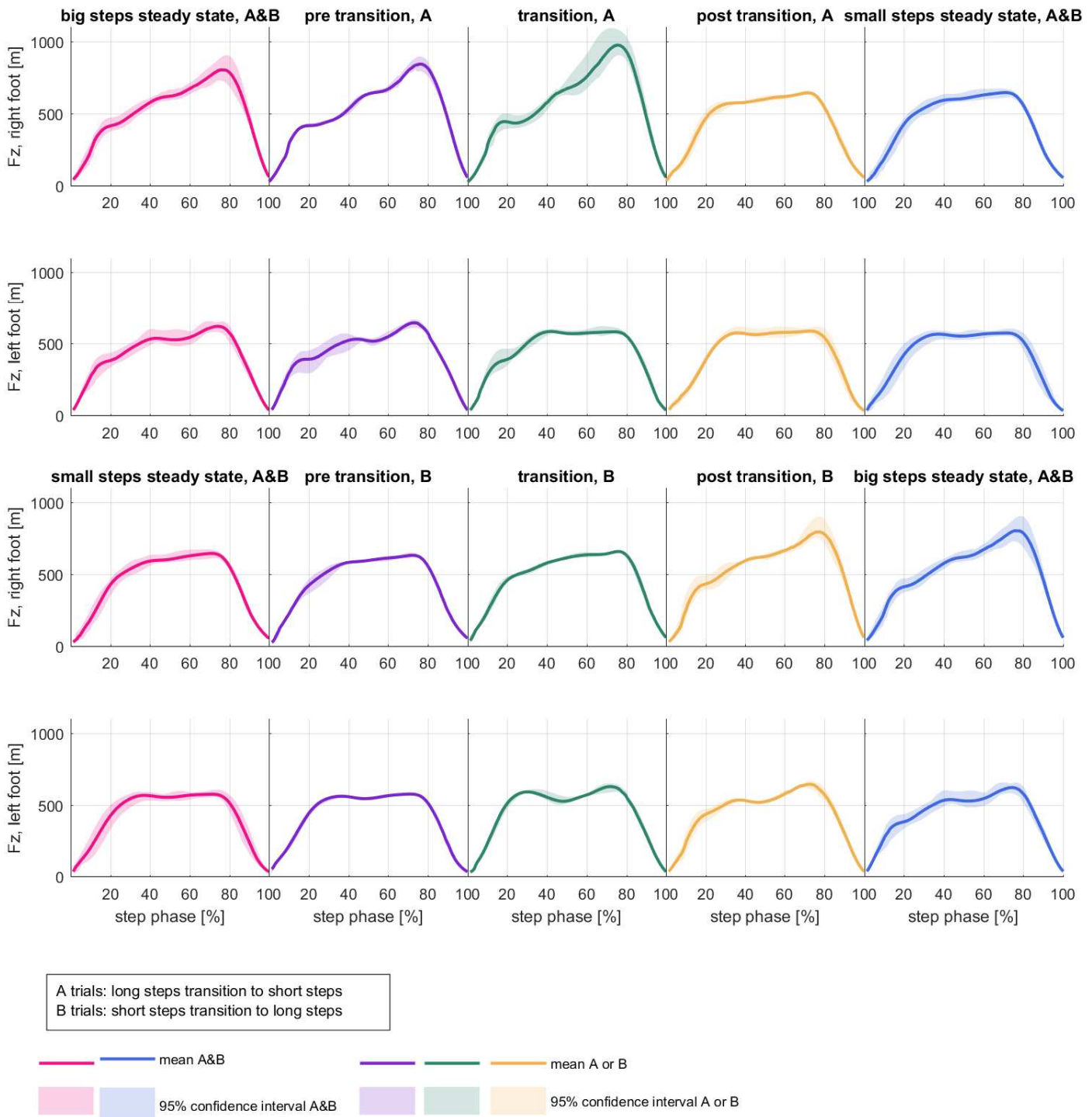


Figure 6.2:  $F_z$  mean and 95% confidence interval per step group across four trials for subject 2. Different colors refer to the five step groups. Top two rows from left to right: steady state long steps (A&B), pre transition (A), transition (A), post transition (A) and steady state short steps (A&B). Bottom two rows from left to right: steady state short steps (A&B), pre transition (B), transition (B), post transition (B) and steady state long steps (A&B). First and third row from the top show left foot data, second and fourth row from the top show right foot data. X-axes show the time, expressed as percentage of stance phase. Y-axes show force in Newton.

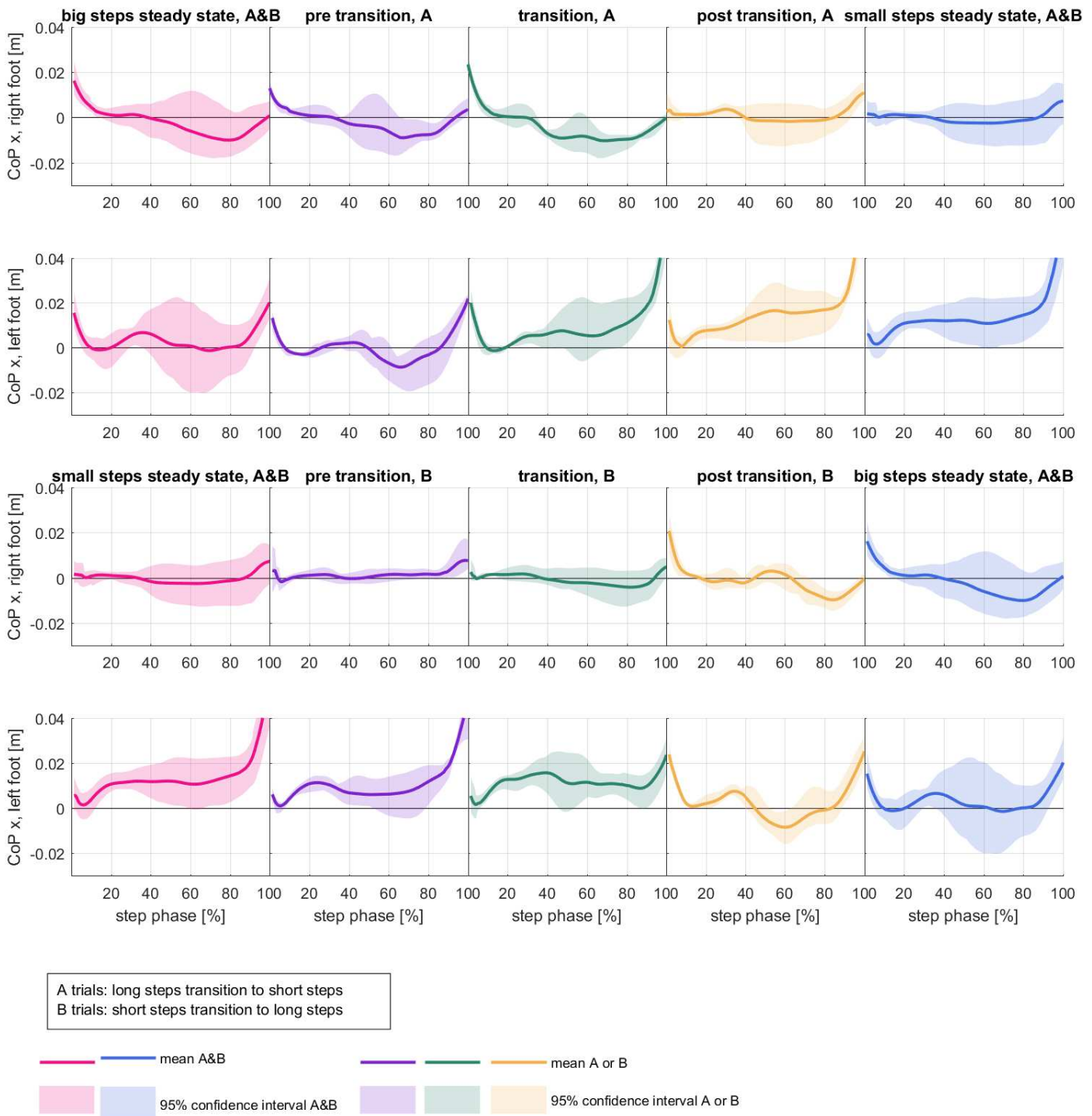


Figure 6.3: CoP X mean and 95% confidence interval per step group across four trials for subject 2. Different colors refer to the five step groups. Top two rows from left to right: steady state long steps (A&B), pre transition (A), transition (A), post transition (A) and steady state short steps (A&B). Bottom two rows from left to right: steady state short steps (A&B), pre transition (B), transition (B), post transition (B) and steady state long steps (A&B). First and third row from the top show left foot data, second and fourth row from the top show right foot data. X-axes show the time, expressed as percentage of stance phase. Y-axes show distance from the center of the foot along the x-axis, in meters.

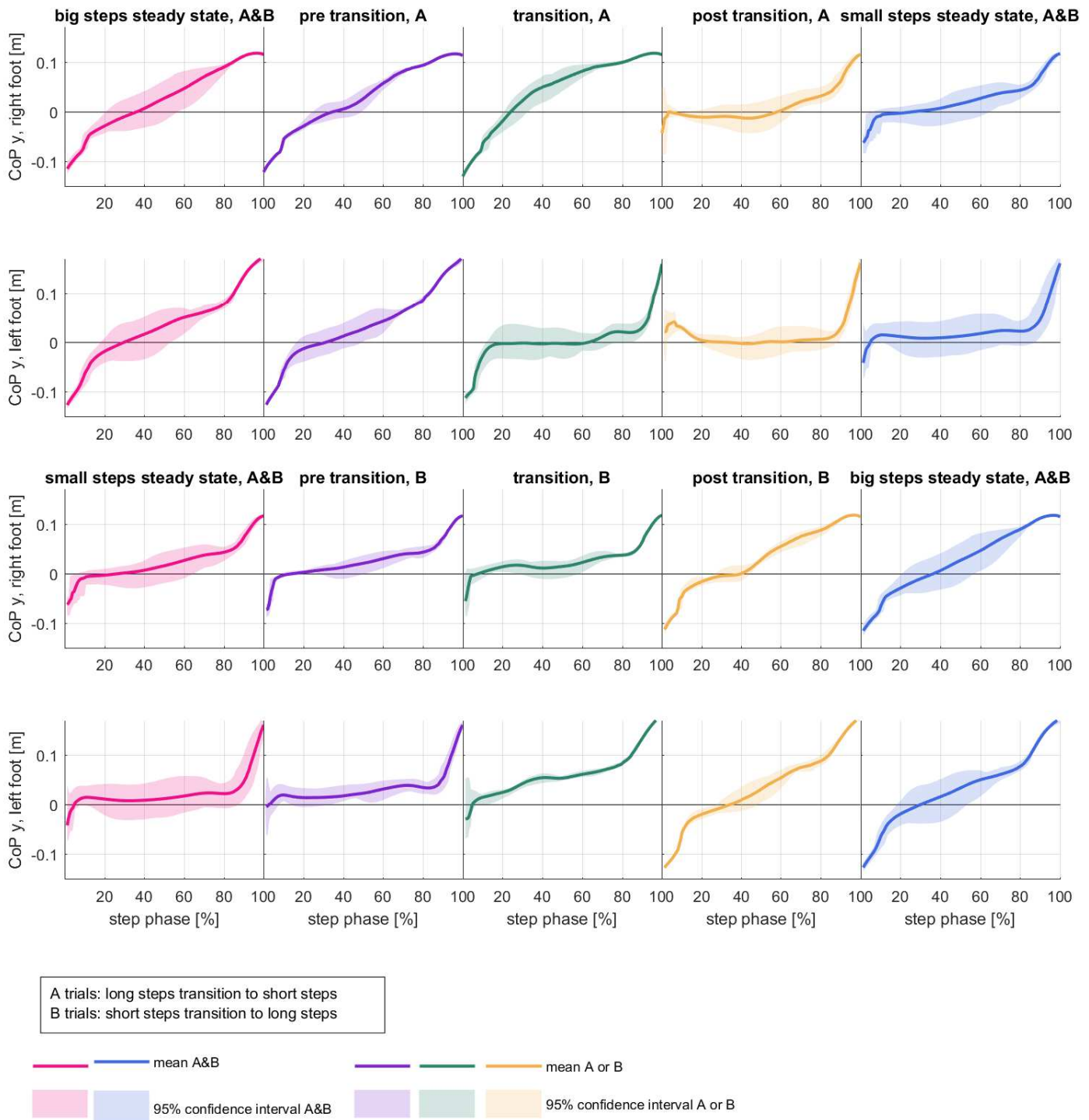


Figure 6.4: CoP Y mean and 95% confidence interval per step group across four trials for subject 2. Different colors refer to the five step groups. Top two rows from left to right: steady state long steps (A&B), pre transition (A), transition (A), post transition (A) and steady state short steps (A&B). Bottom two rows from left to right: steady state short steps (A&B), pre transition (B), transition (B), post transition (B) and steady state long steps (A&B). First and third row from the top show left foot data, second and fourth row from the top show right foot data. X-axes show the time, expressed as percentage of stance phase. Y-axes show distance from the center of the foot along the y-axis, in meters.

## Chapter 7

# Comparing the steady states

**Question 1.** *Can the pressure pattern possibly be used to distinguish extreme steady state long from extreme steady state short steps?*

⇒ What metrics show a likely difference between steady state long and steady state short steps?

⇒ Do these metrics show a likely difference between long and short steps, for both feet?

⇒ Do these metrics show a likely difference between long and short steps, for all three subjects?

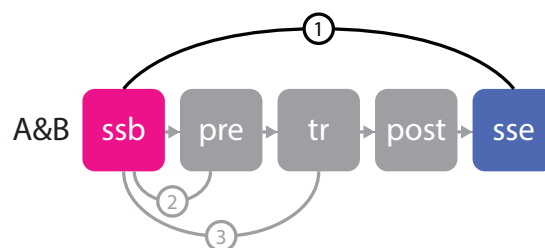


Figure 7.1: Comparison 1 compares the steady state beginning step group (long steps) to the steady state end step group (short steps).

## 7.1 Fz: vertical force component

### 7.1.1 Overlay plots

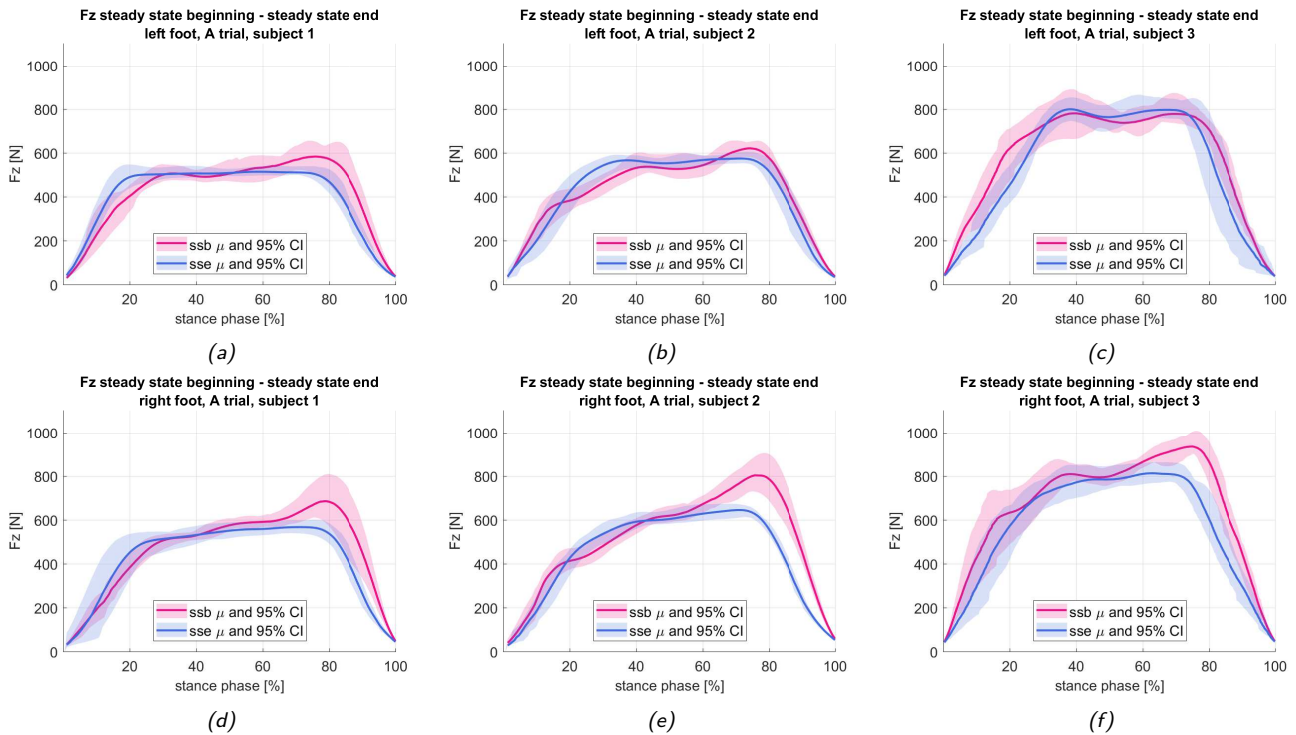


Figure 7.2:  $F_z$  in comparison 1:  $F_z$  in steady state long steps (ssb in A trials; includes sse from B trials) is in red,  $F_z$  in steady state short steps (sse in A trials; includes ssb from B trials) is in blue. Solid lines depict the mean, shaded areas the 95% confidence interval. Top row: left feet, bottom row: right feet. From left to right: subject 1, 2 and 3. X-axes show time, expressed as percentage of stance phase. Y-axes show force in Newton.

**Left foot** In subjects 1 and 2 the push-off  $F_z$  bump is slightly higher for long than for short steps, see 7.2 (a) and (b). However, the push-off bump is not necessarily the maximum  $F_z$  value in a step; especially for the small steps. Subject 3 does not show any difference, see figure (c).

**Right foot** There is a clear difference with the left foot here. First of all, the  $F_z$  push-off bump is the  $F_z$  maximum value for each step. Secondly, this push-off force is clearly higher in the long steps group (red) than in the short steps group (blue) for all three subjects, see figures (d), (e) and (f).

**Metrics** The following metrics based on  $F_z$  will be investigated further: the maximum  $F_z$  per step and the timing of the maximum  $F_z$ . See next section 7.1.2.

### 7.1.2 Value and timing of the peak Fz

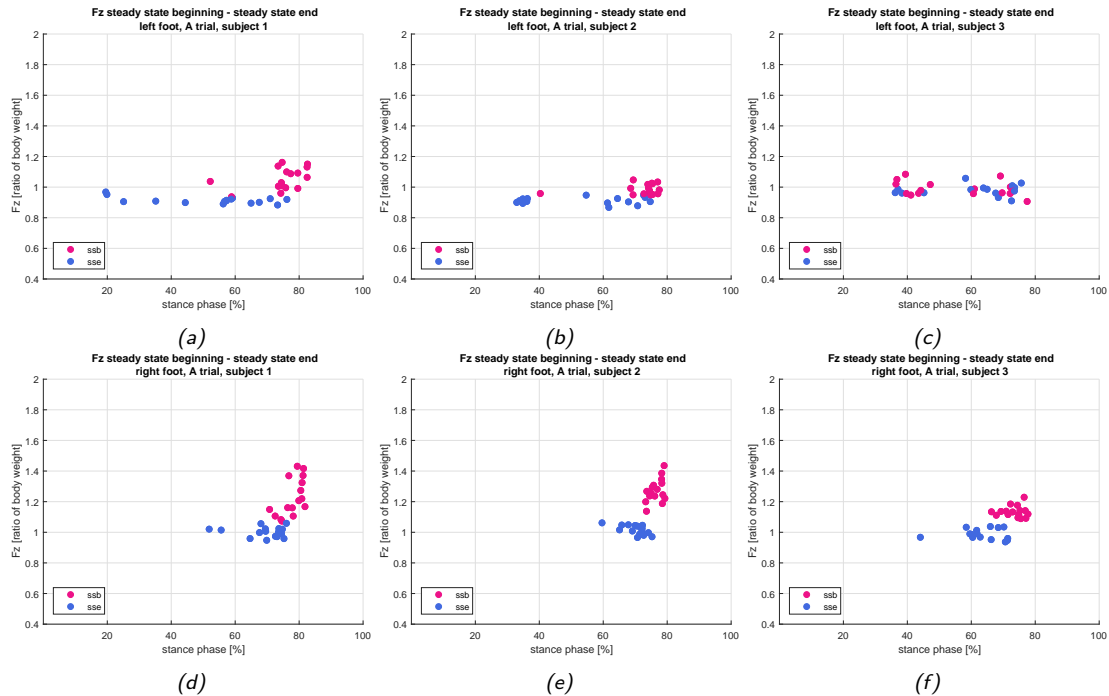


Figure 7.3: Timing and value of the maximum Fz. *ssb* contains all steady state long steps from both A and B trials; *sse* contains all short steps from both A and B trials. The maximum Fz value (y-axis) has been expressed as a ratio of the subject's body weight. The timing of the occurrence of this peak (x-axis) has been expressed as percentage of the stance phase. Top row: left foot, bottom row: right foot. From left to right: subjects 1, 2 and 3.

**Left foot** As the two top left figures of figure 7.3 show, both timing and value of the maximum Fz in a step are quite nicely clustered for the long steps (*ssb*) of subjects 1 and 2. For these subjects' short steps (*sse*), the value of the maximum Fz also seems similar over the different trials, but the timing is much more variable, as shown by the horizontal spread of the blue dots. In the short steps, the maximum Fz can occur anywhere between roughly 20-80% of the stance phase. For subject 3, both timing and value of the maximum Fz does not differentiate between the long and short steps.

**Right foot** For all three subjects, the long steps and short steps clearly form different clusters in the timing-value plane, see bottom three figures. The short steps form a cluster that is wider horizontally than vertically, while the long steps form clusters that are wider vertically than horizontally (except for subject 3). For all three subjects, it appears that during long steps, the maximum Fz occurs later in the stance phase than during short steps.

**Metrics** Thus far it seems that both timing and value of the maximum Fz per step in the right foot are good metrics.

### 7.1.3 Box plots

Below metrics for comparison 1 are presented in box plots as explained in section 5.4.1.

**Timing of Fz peak** For the left foot, the difference is less convincing (only for subject 1 the boxes do not overlap, while for subject 3 there is likely no difference at all) than for the right foot (for none of the subjects the boxes overlap). Therefore, timing of the Fz peak value in the right foot seems a valid metric.

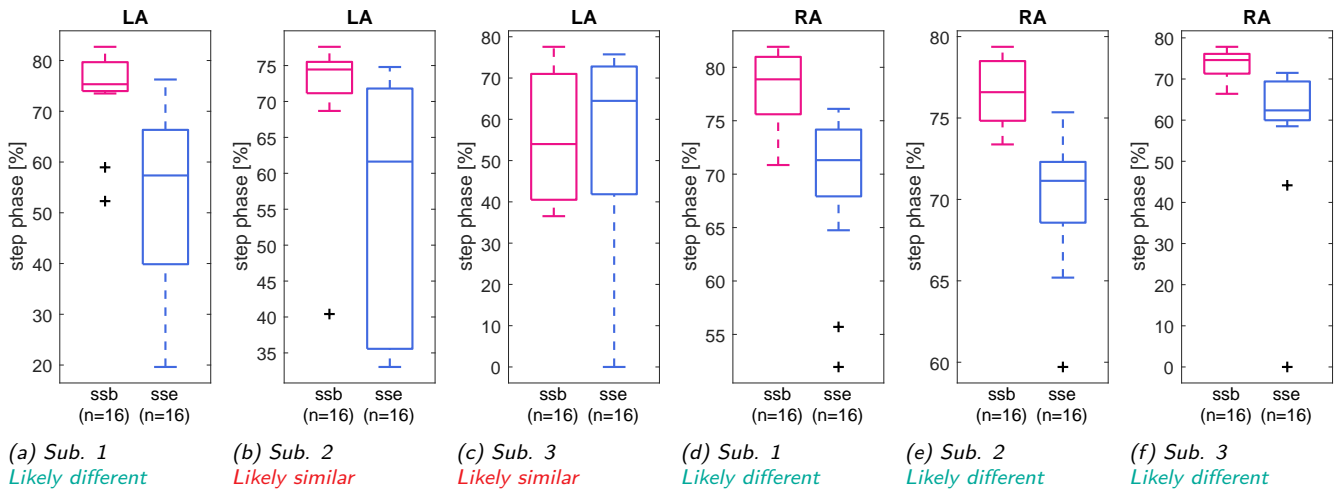


Figure 7.4: Timing (in percentage of the stance phase) of the Fz peak value. *ssb* contains all steady state long steps from both A and B trials; *sse* contains all short steps from both A and B trials. Left three figures: left foot. Right three figures: right foot.

**Value of Fz peak** For the left foot the difference is convincing for subjects 1 and 2 (boxes do not overlap), but no difference can be spotted for subject 3. For the right foot the difference is clear for all three subjects: neither boxes nor whiskers overlap. Value of the right foot Fz peak seems a valid metric.

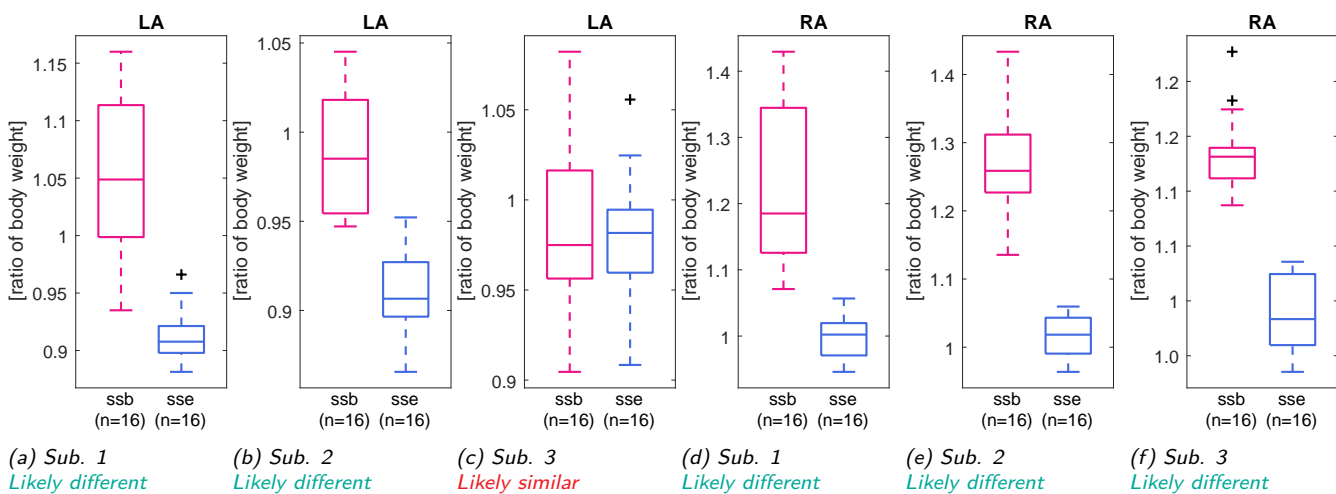


Figure 7.5: Fz peak value. *ssb* contains all steady state long steps from both A- and B-trials; *sse* contains all short steps from both A- and B-trials. Maximum Fz has been expressed as a ratio of subject's body weight. Left three figures: left foot. Right three figures: right foot.

## 7.2 CoP X: x-coordinate of the center of pressure

### 7.2.1 Overlay plots

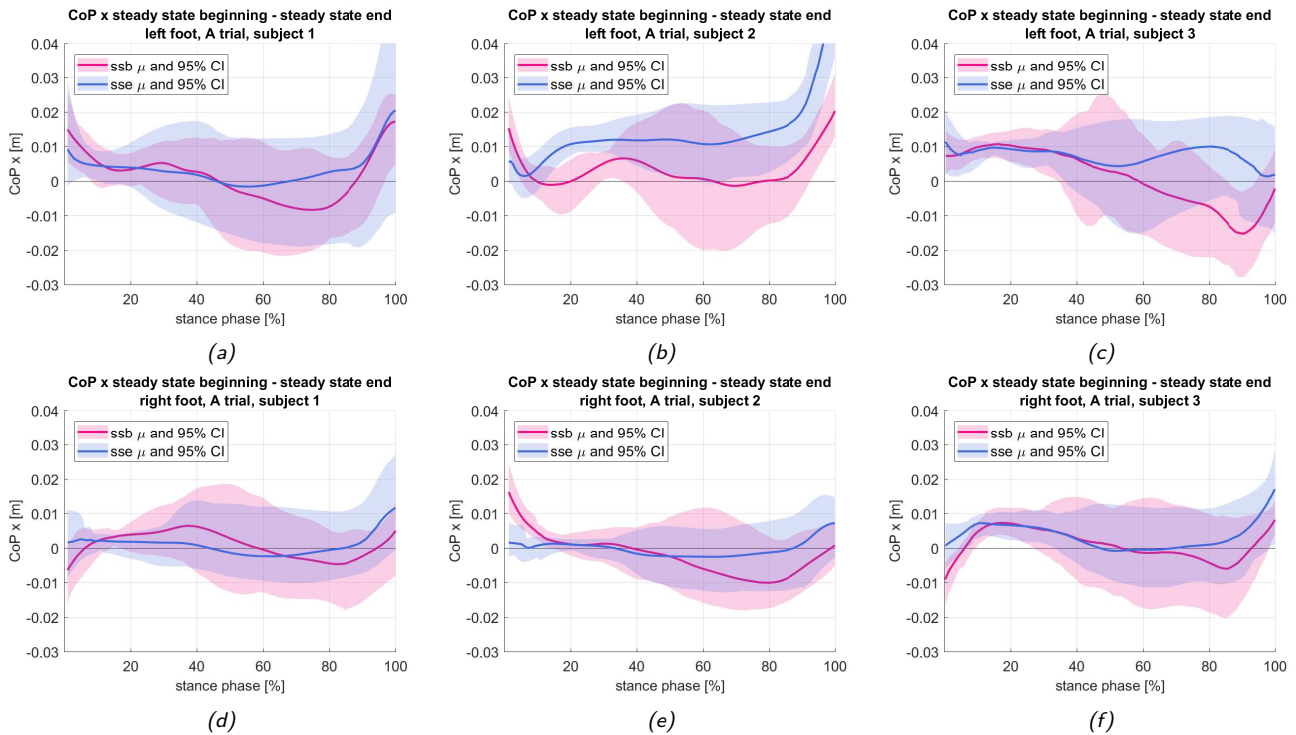


Figure 7.6: CoP X in comparison 1: CoP X in steady state long steps (ssb in A-trials; includes sse from B-trials) is in red, CoP X in steady state short steps is in blue. Solid lines depict the mean, shaded areas the 95% confidence interval. Top row: left feet, bottom row: right feet. From left to right: subject 1, 2 and 3. X-axes show time, expressed as percentage of stance phase. Y-axes show x-coordinate of the CoP in meters.

**Left foot** Especially subjects 1 and 2 show a CoP X pattern where the CoP moves more outward (lateral direction; positive x-coordinate) towards the end of the stance phase in the small steps. See figures 7.6a and 7.6b. For subject 2, there is a very big difference in the CoP X rise from 0-100% of stance phase. For subjects 1 and 2, the CoP X is more positive at 0% of stance phase in ssb than in sse.

**Right foot** Like the left foot, the x-coordinate of the CoP moves more outward (positive x-direction) in short steps than in long steps. There is also a discernible difference in the CoP x-coordinate at 0% of stance phase; however the difference is the other way around for subjects 1 and 3, and subject 2. See figures 7.6d, 7.6e and 7.6f.

**Metrics** The first metrics based on the CoP X proposed: CoP X at 100% of stance phase, CoP X at heel strike, CoP X slope between 0-100% of stance phase. The CoP pattern shows a high variety between steps of the same group, which can be seen in the broad CI's of figure 7.6. Therefore we will look at the CoP patterns plotted separately for each step before deciding which other CoP X metrics to choose, see section 7.2.2.



## 7.2.2 CoP X: peaks indicated

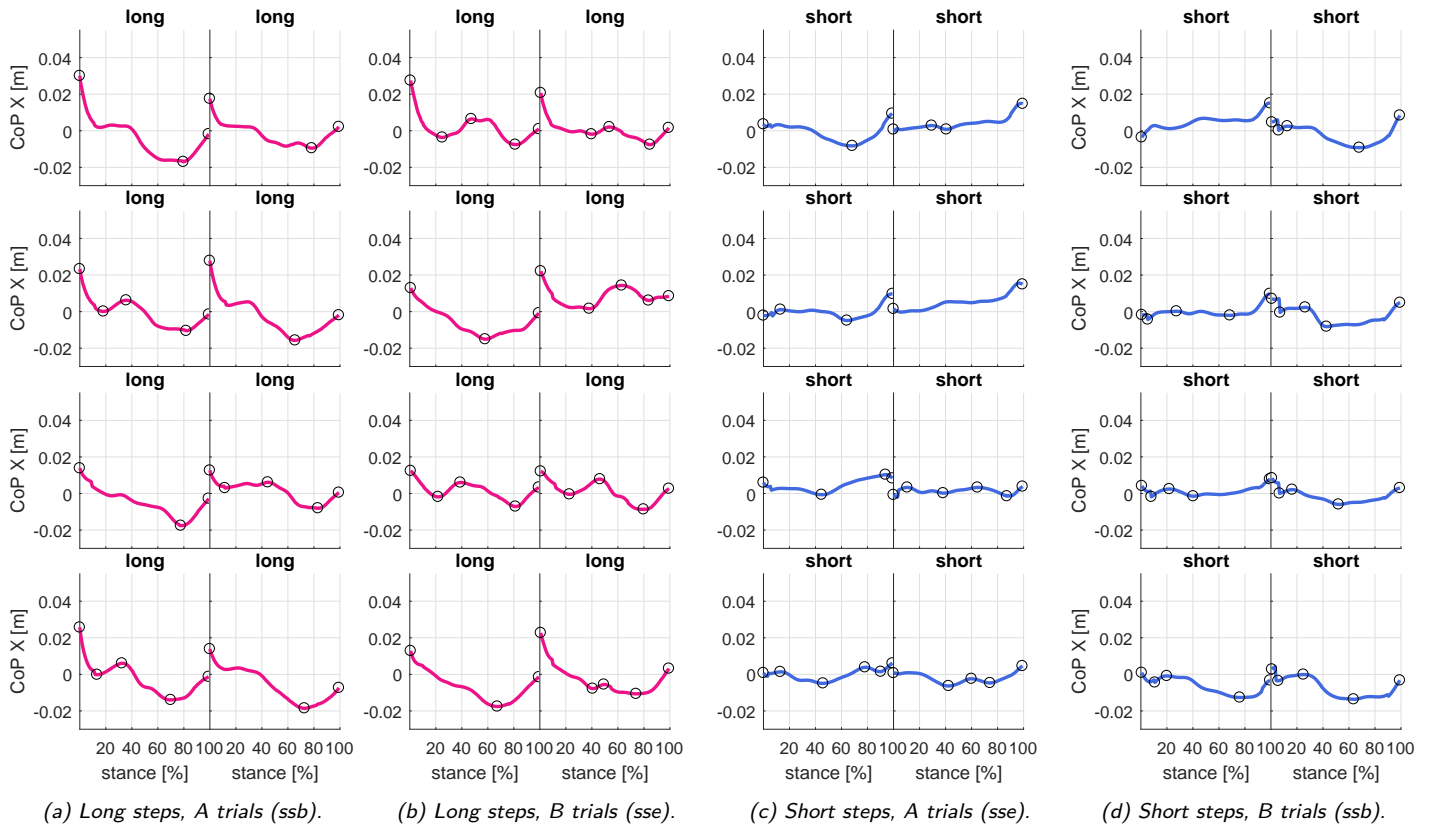


Figure 7.7: Subject 2: steady state steps from all trials (4 A-trials, 4 B-trials) shown separately, including peaks found with a minimum prominence of 2mm, for the right foot. X-axes show time, expressed as percentage of stance phase. Y-axes show the x-coordinate of the CoP in meters. Colors correspond to the step groups defined previously.

Shown in figure 7.7 is the trajectory of the CoP X of the right foot of subject 2 during long steps ((a) and (b)) and during short steps ((c) and (d)). Matlab was used to find the peaks with a minimum prominence of 2mm of these graphs, which are indicated with a black circle. To avoid confusion by showing a large number of similar figures, the graphs showing the same for the left foot and the other subjects are omitted here. Figure 7.8 shows a number of figures in which steps 2 (long step, steady state) and 7 (short step, steady state) are plotted on top of each other. The selection of plots shown is random; different trials from different subjects are shown. These plots (fig. 7.8) are included to give the reader a sense of how the CoP X metrics were selected; by comparing specific steps, rather than the mean and CI's as seen in figure 7.6.

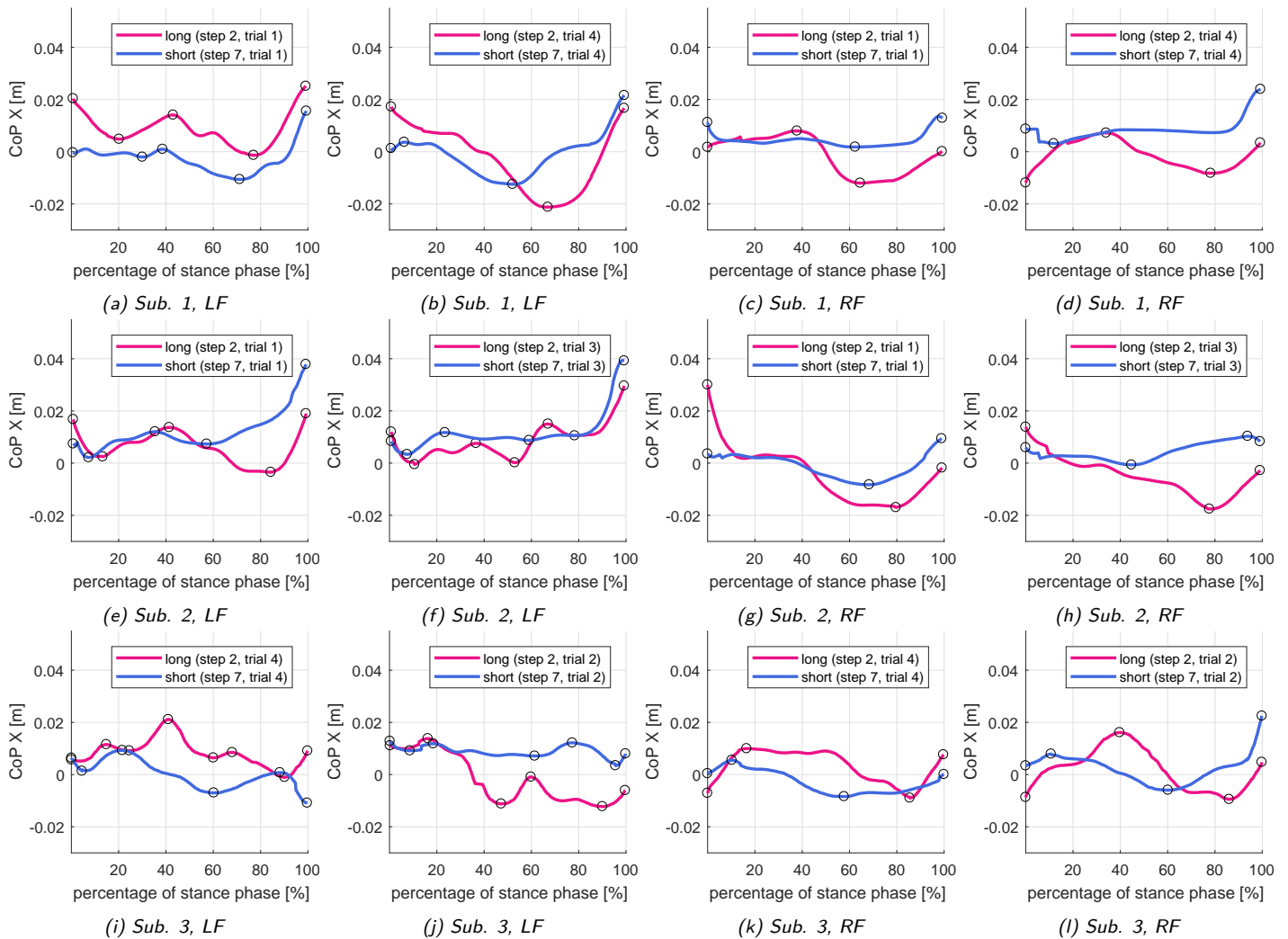


Figure 7.8: A random selection of plots such as in figure 7.7, where one steady state long step and one steady state short step have been plotted on top of each other. Each figure contains one step 2 from one of the A-trials, and one step 7 from one of the A-trials, from a single subject.

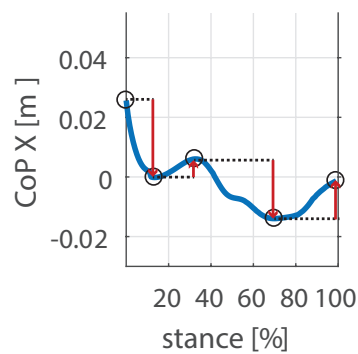


Figure 7.9: The red arrows represent the rises between peaks. The metric 'absolute sum of rises' adds the absolute values of all these arrows per step.

**Metrics** Thus, the following metrics are proposed:

- CoP X at heel strike (0% of stance phase).
- Maximum difference between the values of any two peaks in a step (highest peak and lowest valley).
- The sum of the rises between all peaks in a step (absolute values). See figure 7.9 for a visual clarification.
- The CoP X rise from 0% to 100% of the stance phase.
- The rise between the 1st and 2nd peak (0% of stance phase to following peak).

### 7.2.3 Box plots

**Difference between highest peak and lowest valley in a step** See the boxplots in figure 7.10. Left foot: this might be a viable metric for subjects 2 and 3. However, the possible effect occurs in another direction for either subject: for subject 2, there are higher peaks and lower valleys in short steps, while for subject 3 the bigger peak-to-valley distances occur in long steps. Right foot: there is only a likely difference for subject 2. All in all, this metric does not seem to have a lot of merit.

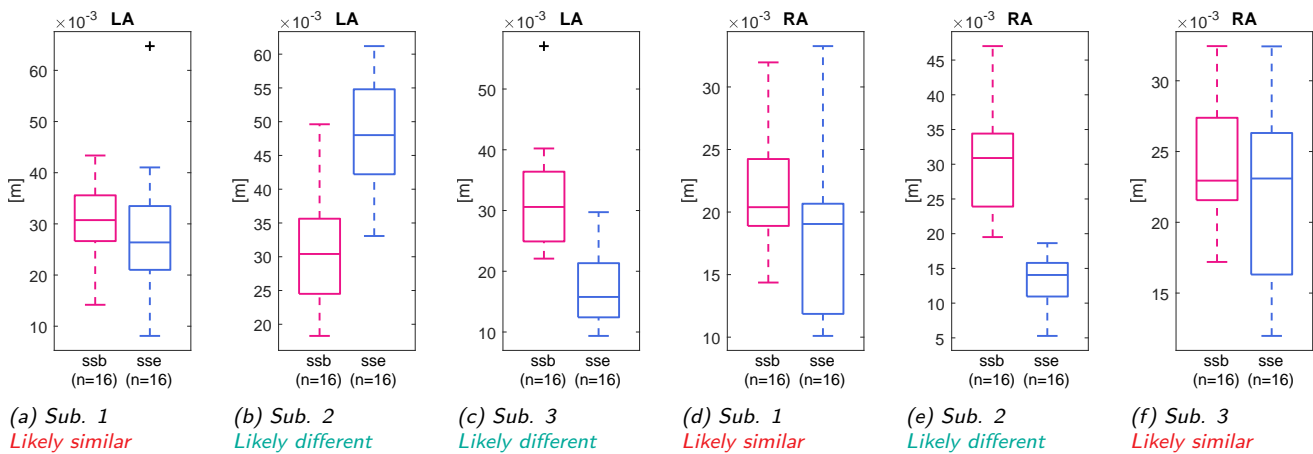


Figure 7.10: CoP X: maximum difference between any two peaks in a step. *ssb* contains all steady state long steps from both A- and B-trials; *sse* contains all short steps from both A- and B-trials. The y-axes display the difference between the highest peak and lowest valley of CoP X in a step. Left three figures: left foot. Right three figures: right foot.

**Sum of rises between CoP X peaks** See figure 7.9 for a visual explanation of this metric, and figure 7.11 for the resulting box plots. The results for this metric are promising: only the boxes for sub. 2's left foot data overlap. Also the differences are in the same direction for all subjects.

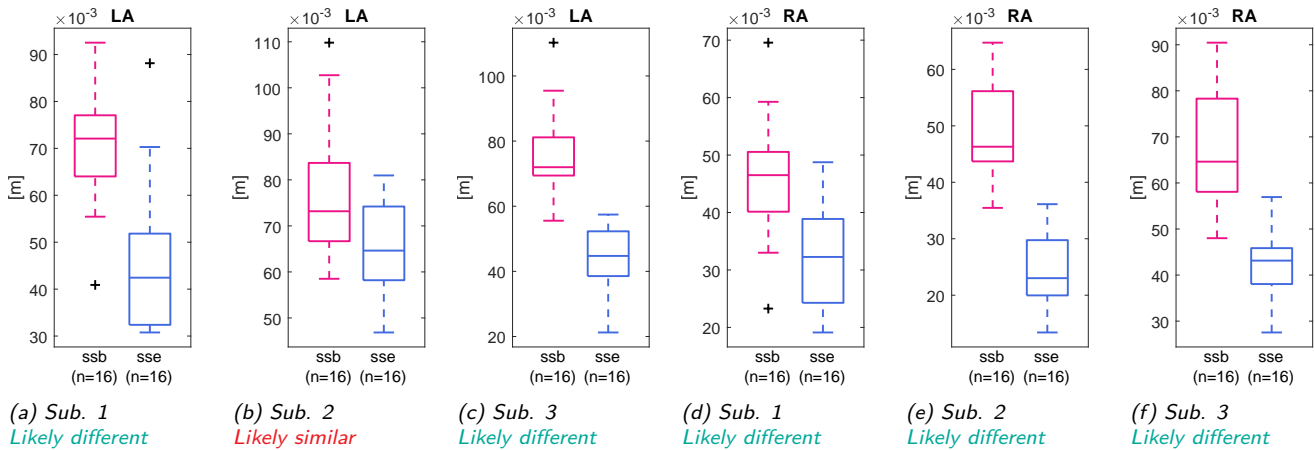


Figure 7.11: CoP X, absolute sum of rises between peaks. *ssb* contains all steady state long steps from both A- and B-trials; *sse* contains all short steps from both A- and B-trials. The y-axes display the sum of all the rises (absolute values) between peaks in a step. Left three figures: left foot. Right three figures: right foot.

**CoP X at 0% of stance phase** For the right foot this seems a good metric, see figure 7.12. For none of the three subjects the two boxes overlap. For the left foot only the box plot corresponding to subject 2 indicates a likely difference. Again, the direction of the likely difference is not the same for all subjects.

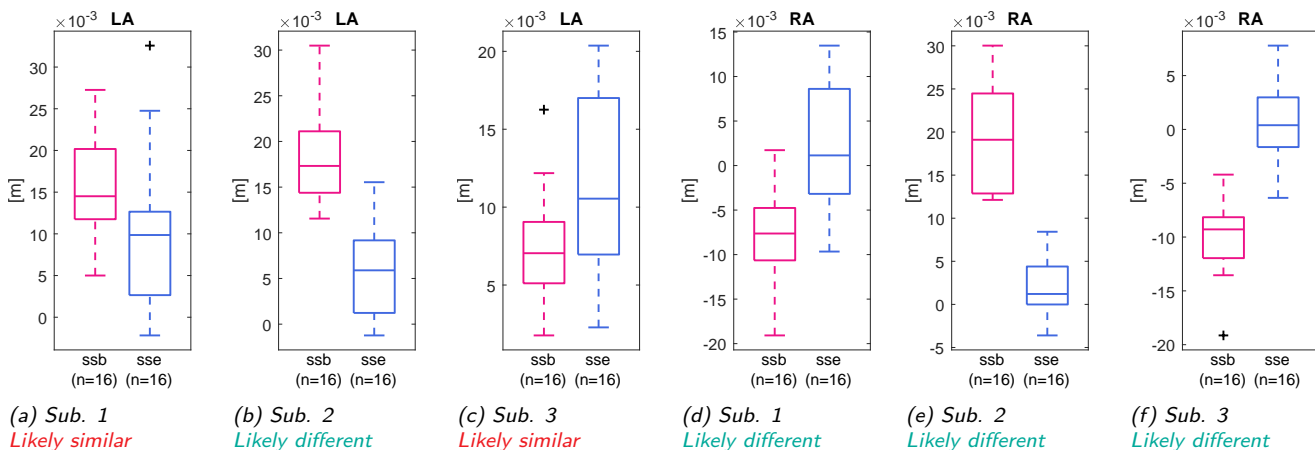


Figure 7.12: CoP X at foot strike. *ssb* contains all steady state long steps from both A- and B-trials; *sse* contains all short steps from both A- and B-trials. The y-axes display the value of the CoP X at foot strike (0% of stance phase). Left three figures: left foot. Right three figures: right foot.

**Rise between 0% of stance phase and the following peak** This seems a promising metric, especially for the right foot. It should be noted that again, the differences are not the same for the three subjects: whereas subject 1, for example, shows a positive rise in long steps as opposed to a negative rise in short steps (right foot), subject 2 (right foot) shows a positive rise for both long and short steps; however the rise during long steps is bigger.

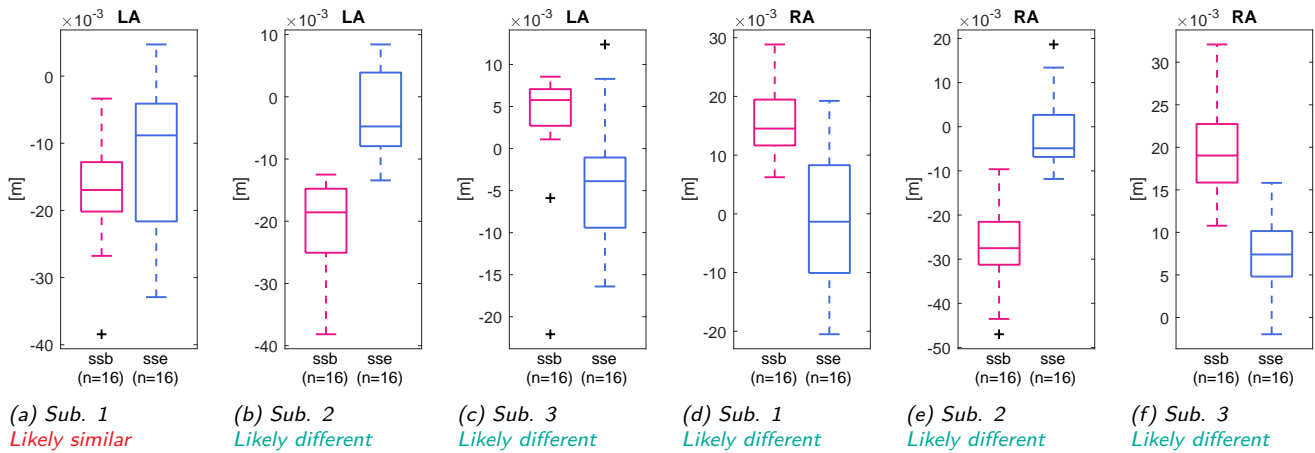


Figure 7.13: CoP X, rise between 0% of stance phase and the next peak. ssb contains all steady state long steps from both A- and B-trials; sse contains all short steps from both A- and B-trials. The y-axes display the difference in value of the CoP X at foot strike (0% of stance phase) and the next CoP X peak. Left three figures: left foot. Right three figures: right foot.

**Total rise during stance phase** This is the total rise from 0-100% of the stance phase. There is only a potential difference for subject 2: for both feet, the total rise is much greater in short steps than in long steps. This metric will not be considered henceforward, since there is no likely difference for the other two subjects.

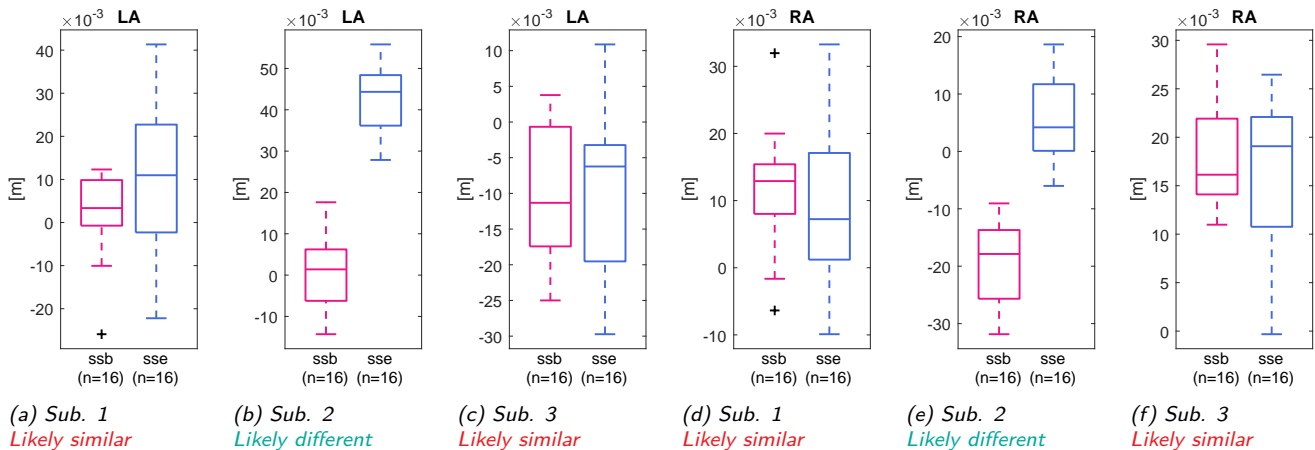


Figure 7.14: CoP X total rise during stance phase. ssb contains all steady state long steps from both A- and B-trials; sse contains all short steps from both A- and B-trials. The y-axes display the difference between the value of the CoP X at foot strike (0% of stance phase) and at foot lift (100% of stance phase). Left three figures: left foot. Right three figures: right foot.

## 7.3 CoP Y: y-coordinate of the center of pressure

### 7.3.1 Overlay plots

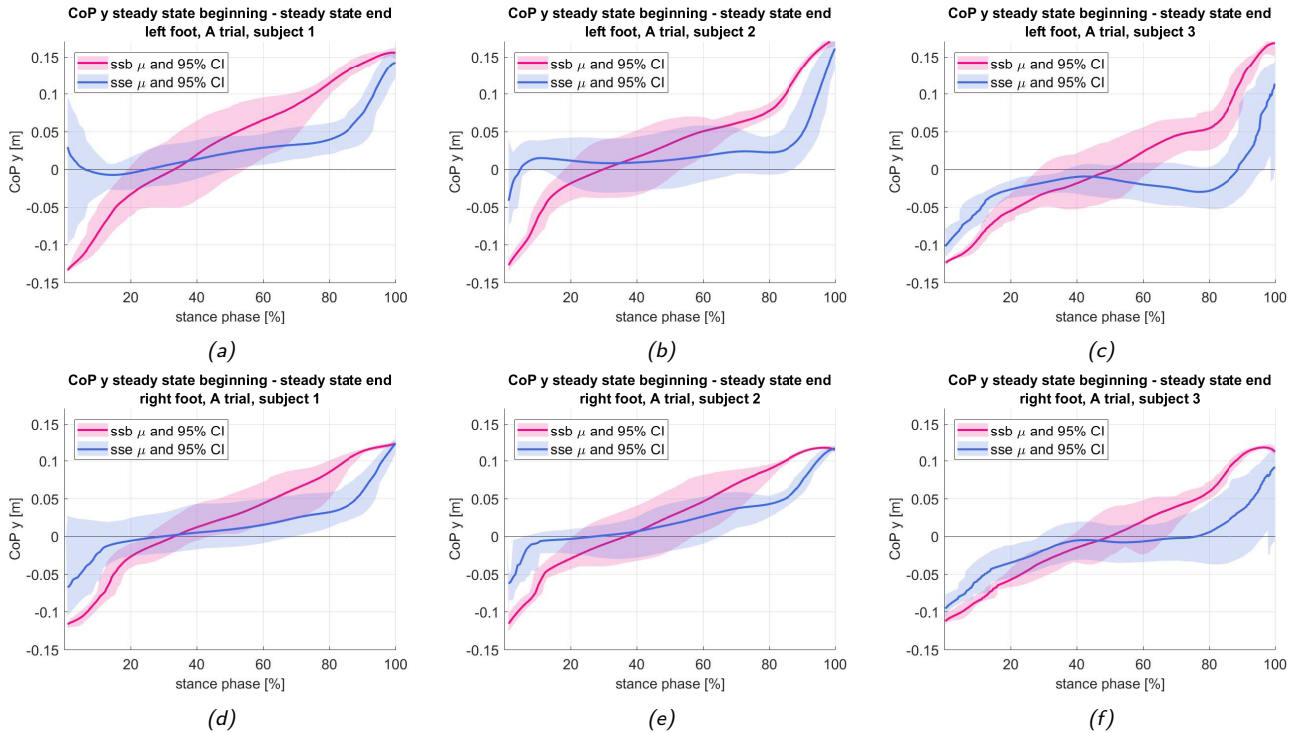


Figure 7.15: CoP Y in comparison 1: CoP Y in steady state long steps (ssb in A-trials; includes sse from B-trials) is in red, CoP Y in steady state short steps is in blue. Solid lines depict the mean, shaded areas the 95% confidence interval. Top row: left feet, bottom row: right feet. From left to right: subject 1, 2 and 3. X-axes show time, expressed as percentage of stance phase. Y-axes show y-coordinate of the CoP in meters.

**Left foot** The CoP Y at 0% of phase stance is clearly different for all three subjects, regardless of the broad CI for subject 1 at this moment. Also for all three there is a notable difference between the slopes from 0-20%, 20-80% and 80-100% of stance phase. See figures 7.15a, 7.15b and 7.15c.

**Right foot** As for the left foot, the CoP Y at 0% of phase stance is clearly different for all three subjects. Also for all three there is a notable difference between the rises from 0-20%, 20-80% and 80-100%. See figures 7.15d, 7.15e and 7.15f.

**Metrics** The metrics for CoP Y are based directly on what we see in figure 7.15: CoP Y at 0% and the slopes from 0-20%, 20-80% and 80-100% of stance phase.

### 7.3.2 Box plots

**CoP Y at 0% of stance phase** The box plots belonging to this metric, figure 7.16, reveal a clear likely difference: no overlapping boxes and often not even overlapping whiskers. All three subjects show this likely difference, in both feet.

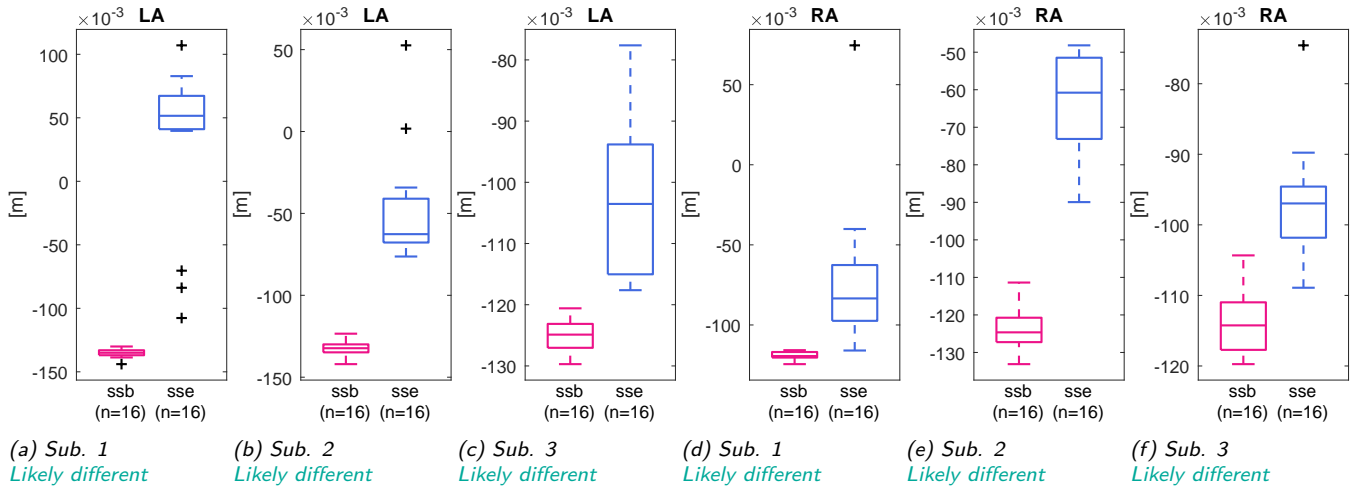


Figure 7.16: CoP Y at 0% of stance phase. *ssb* contains all steady state long steps from both A- and B-trials; *sse* contains all short steps from both A- and B-trials. The y-axes display the value of CoP Y at foot strike (0% of stance phase). Left three figures: left foot. Right three figures: right foot.

**CoP Y rise from 0% to 20% of stance phase** We see a very clear likely difference for the left foot of subject 1, smaller/no differences in the other cases.

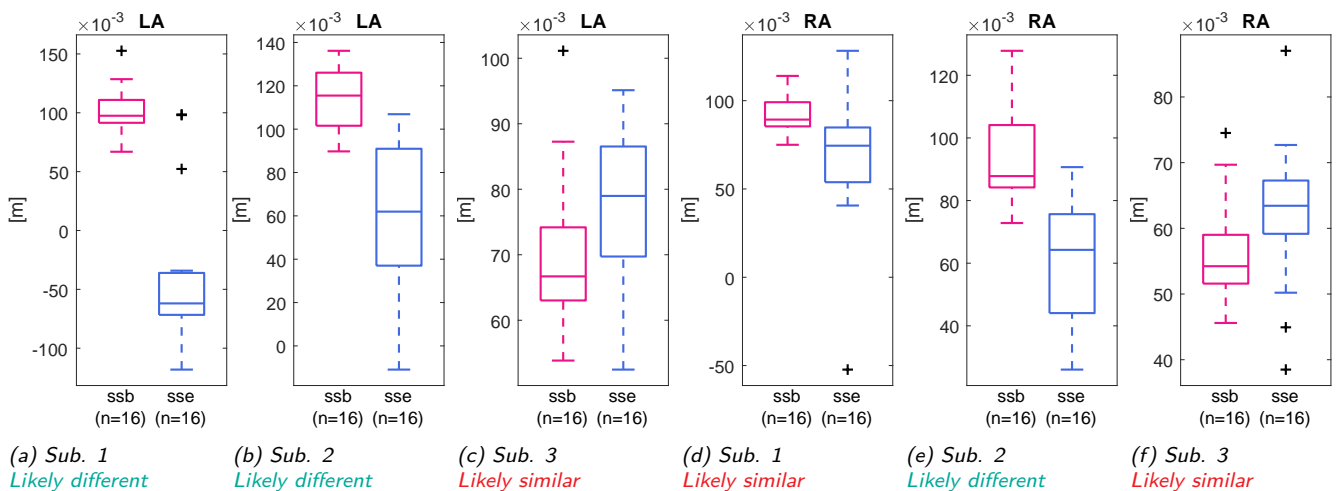


Figure 7.17: CoP Y rise from 0% to 20% of stance phase. *ssb* contains all steady state long steps from both A- and B-trials; *sse* contains all short steps from both A- and B-trials. The y-axes display the difference between the value of CoP Y at foot strike (0% of stance phase) and at 20% of stance phase. Left three figures: left foot. Right three figures: right foot.

**CoP Y rise from 20% to 80% of stance phase** This is very clearly a viable metric: both for left and right feet of all three subjects, neither boxes nor whiskers overlap.

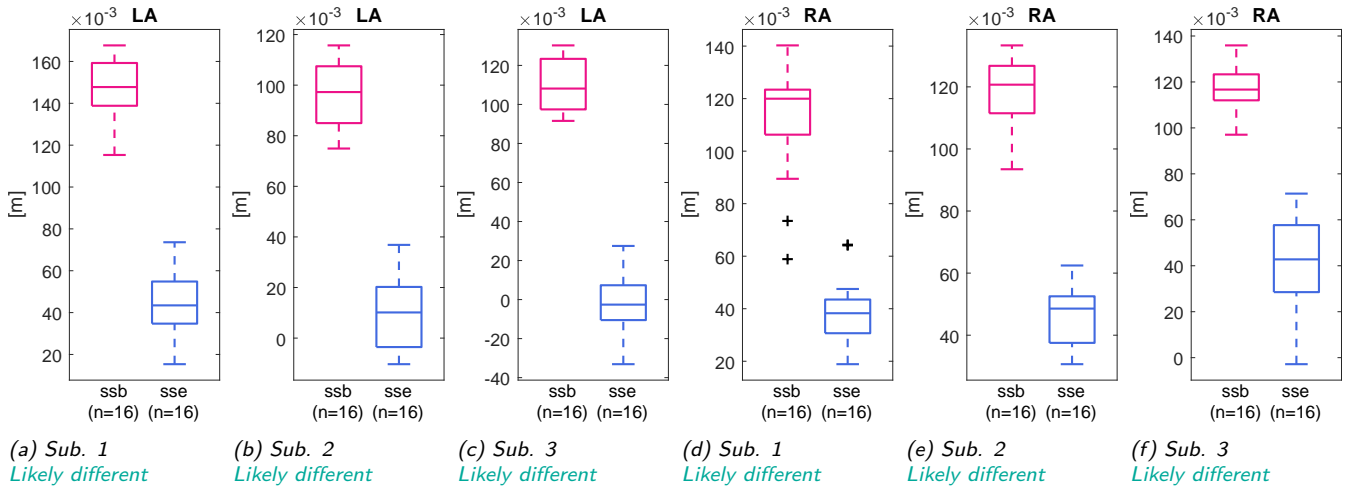


Figure 7.18: CoP Y rise from 20% to 80% of stance phase. *ssb* contains all steady state long steps from both A- and B-trials; *sse* contains all short steps from both A and B trials. The y-axes display the difference between the value of CoP Y at 20% and 80% of stance phase. Left three figures: left foot. Right three figures: right foot.

**CoP Y rise from 80% to 100% of stance phase** This metric also shows a clear potential difference for both feet of all three subjects.

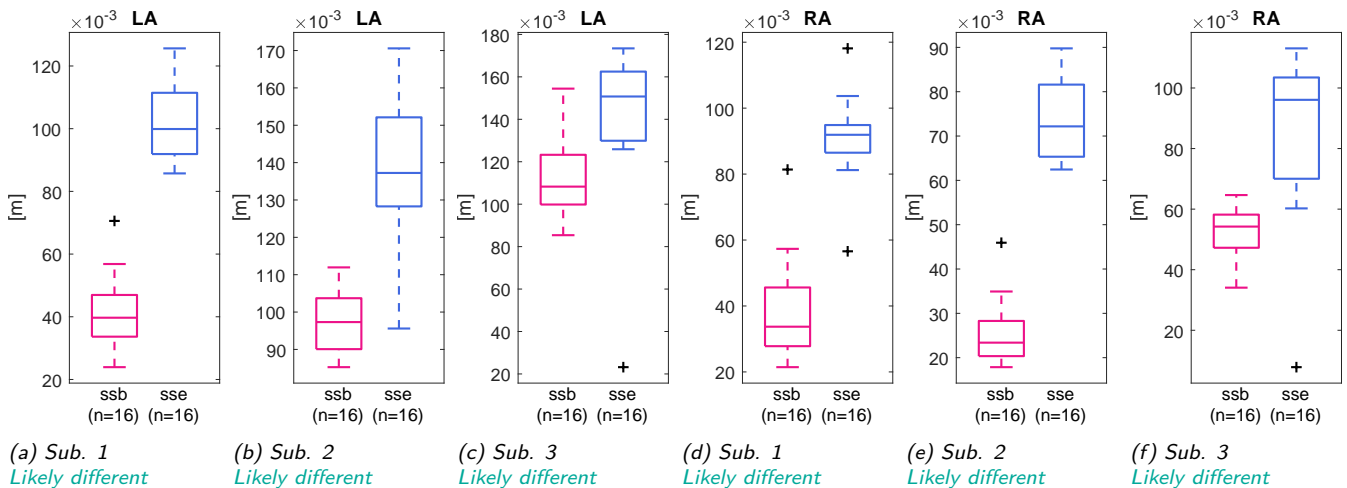


Figure 7.19: CoP Y rise from 80% to 100% of stance phase. *ssb* contains all steady state long steps from both A- and B-trials; *sse* contains all short steps from both A- and B-trials. The y-axes display the difference between the value of CoP Y at 80% and 100% of stance phase in meters. Left three figures: left foot. Right three figures: right foot.



## 7.4 Conclusions

**Question 1.** *Can the pressure pattern possibly be used to distinguish extreme steady state long from extreme steady state short steps?*

Now we can answer **question 1: Yes, the pressure pattern can distinguish between steady state long and steady state short steps** - at least when the difference between long and short steps is quite extreme (A- and B-trials).

Parameter	Metric \ Subject	L			R			Likely difference for all three subjects?	
		1	2	3	1	2	3	L	R
Fz	Timing of peak value	ld	ls	ls	ld	ld	ld	no	yes
	Value of peak	ld	ld	ls	ld	ld	ld	no	yes
CoP X	Max peak - min valley	ls	ld	ld	ls	ld	ls	no	no
	Sum of rises	ld	ls	ld	ld	ld	ld	no	yes
	Value at 0%	ls	ld	ls	ld	ld	ld	no	yes
	Rise peak 1-2	ls	ld	ld	ld	ld	ld	no	yes
CoP Y	Netto rise 0-100%	ls	ld	ls	ls	ld	ls	no	no
	Value at 0%	ld	ld	ld	ld	ld	ld	yes	yes
	Rise 0-20%	ld	ld	ls	ls	ld	ls	no	no
	Rise 20-80%	ld	ld	ld	ld	ld	ld	yes	yes
	Rise 80-100%	ld	ld	ld	ld	ld	ld	yes	yes

Table 7.1: Summary of the box plots presented in this chapter. *ld* = likely different, *ls* = likely similar. Likely different means that for this subject there is likely a difference in this metric between steady state long steps and steady state short steps. Likely similar means that there is probably no such difference. Whether there is a likely difference for all three subjects for a certain metric (L or R foot are considered separately) is indicated in the rightmost columns.

Table 7.1 lists the metrics that show a likely difference in comparison 1, and whether this difference can be seen in both feet and in all three subjects. We expect that the biggest effect of step size on these metrics will be found when comparing the steady states of A- and B-trials. Therefore, we now eliminate from further consideration any metrics that do not indicate a likely difference in comparison 1. We will continue into the following chapter with the following metrics:

- Fz: timing in stance phase of peak value (right foot)
- Fz: value of peak value (right foot)
- CoP X: sum of the rises (right foot)
- CoP X: value at 0% of stance phase (right foot)
- CoP X: rise between 1st and 2nd peak (right foot)
- CoP Y: value at 0% of stance phase (both feet)
- CoP Y: rise from 20% to 80% of stance phase (both feet)
- CoP Y: rise from 80% to 100% of stance phase (both feet)

It should be noted that even if a metric shows a likely difference between ssb and sse for all three subjects, the difference is not necessarily in the same direction for all subjects.

## Chapter 8

# Comparing the steady state beginning to the pre-transition step

**Question 2.** *Can the pressure pattern possibly be used to identify a change in step length before it happens?*

- ⇒ What metrics identified in answering question 1, show a likely difference between the steady state beginning and pre-transition step group?
- ⇒ Do these metrics show a likely difference in this comparison, for both feet?
- ⇒ Do these metrics show a likely difference in this comparison, for all three subjects?

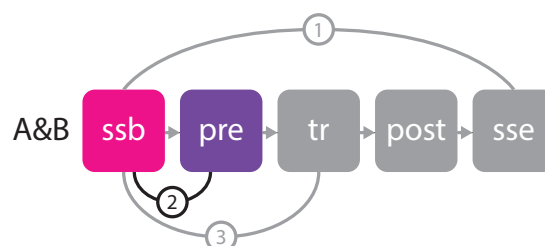


Figure 8.1: In comparison 2 the steady state beginning step group is compared to the pre-transition step group.

## 8.1 Fz: vertical force component

As was concluded from the previous chapter, for the Fz-based metrics, only the right foot will be considered:

- Fz: timing in stance phase of peak value (right foot)
- Fz: value of peak value (right foot)

### 8.1.1 A-trials

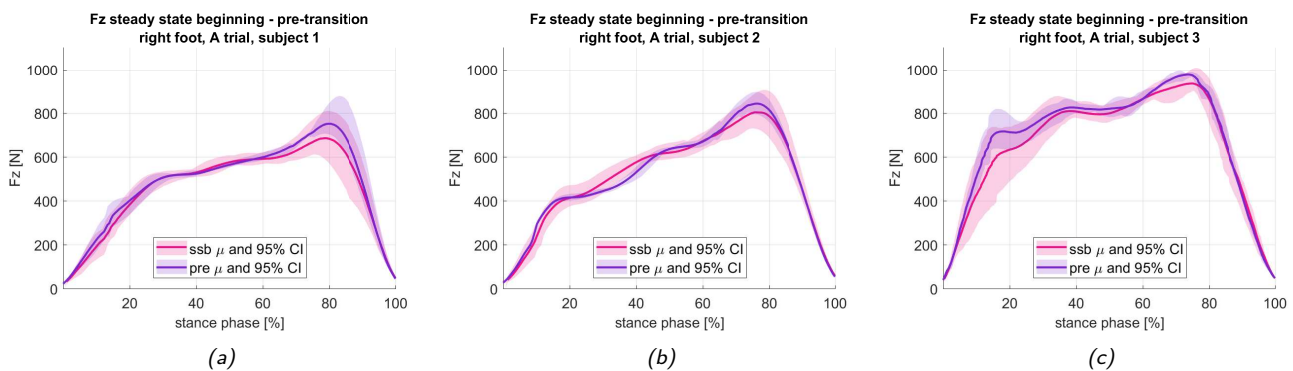


Figure 8.2: Fz mean and confidence interval for the steady state beginning steps (red) and the pre-transition steps (purple). Each figure depicts another subject. All three figures are about the right foot in A-trials (beginning with long steps). *ssb* contains steady state long steps from A- and B-trials. *pre* contains pre-transition steps from A-trials alone. Y-axes represent the Fz in Newton, while the x-axes represent time expressed as a percentage of stance phase.

Figure 8.2 shows the same kind of overlay plots as were used in the previous chapter. Immediately, we notice that the rather clear difference in Fz "bump" that was seen when comparing the steady states is absent here. We see however, a similar small difference for all three subjects: the pre-transition mean shows a *higher Fz bump in the pre-transition steps than in the steady state long steps*. This is quite interesting, since it is opposite to what we had expected: apparently the Fz-pattern does not start to become more like the steady state end Fz-pattern in the pre-transition steps. Rather, it looks like a more extreme version of the steady state beginning Fz-pattern. It may be interesting to take a closer look at the data using box plots. However, it is clear from figure 8.2 that the timing of the maximum Fz value is not a viable metric in this case: the Fz peaks lie very close together.

Figure 8.3 shows comparison 2, A-trials, of the metric maximum Fz for the right foot in boxplots. It indicates that there is only a likely difference for subject 3.

### 8.1.2 B-trials

Figure 8.4 shows that in B-trials, the Fz pattern of the pre-transition step group is extremely similar to the steady state beginning group. For all three subjects (especially sub. 1 and 2) the lines representing the mean Fz lie so closely together (sometimes not even distinguishable from each other) that we can safely conclude that for B-trials Fz-based metrics cannot be used to distinguish pre-transition steps from steady state beginning steps.

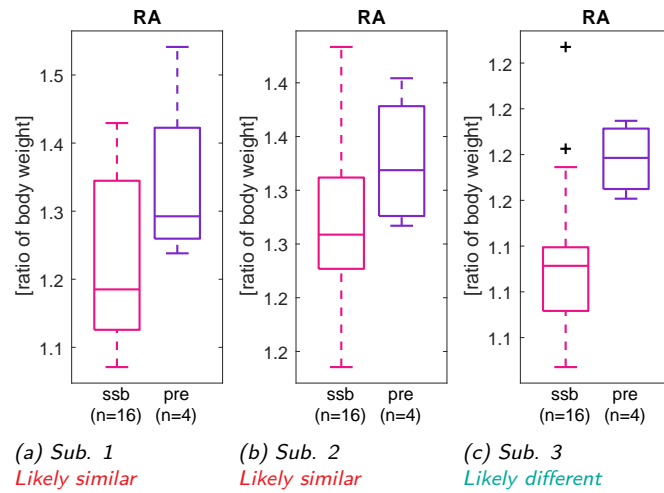


Figure 8.3: Value of the maximum  $F_z$  for each step, right foot, A-trials. *ssb* contains all steady state long steps from both A- and B-trials; *sse* contains all pre-transition steps from only A-trials. Maximum  $F_z$  has been expressed as a ratio of subject's body weight.

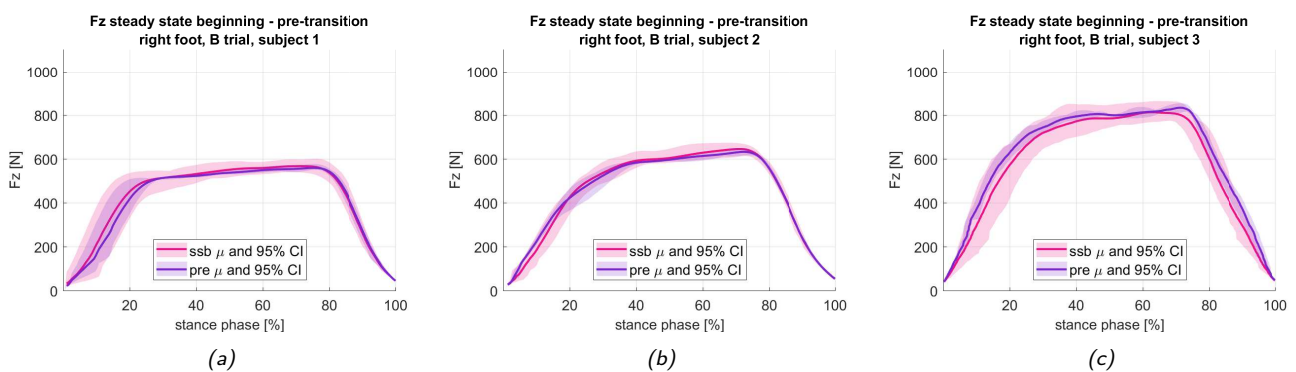


Figure 8.4:  $F_z$  mean and confidence interval for the steady state beginning steps (red) and the pre-transition steps (purple). Each figure depicts another subject. All three figures are about the right foot in B-trials (beginning with short steps). Y-axes represent the  $F_z$  in Newton, while the x-axes represent time expressed as a percentage of stance phase.

## 8.2 CoP X: x-coordinate of the center of pressure

As for the  $F_z$ , again only the right foot will be considered in this comparison. Since the overlay plots were able to show us so very little for comparison 1, we will skip them in this chapter and move straight to the box plots for the following metrics:

- CoP X: sum of the rises (right foot)
- CoP X: value at 0% of stance phase (right foot)
- CoP X: rise between 1st and 2nd peak (right foot)

### 8.2.1 A-trials

None of the three metrics show any difference between the steady state beginning step group and the pre-transition step group, in A-trials. See figures 8.5, 8.6 and 8.7.

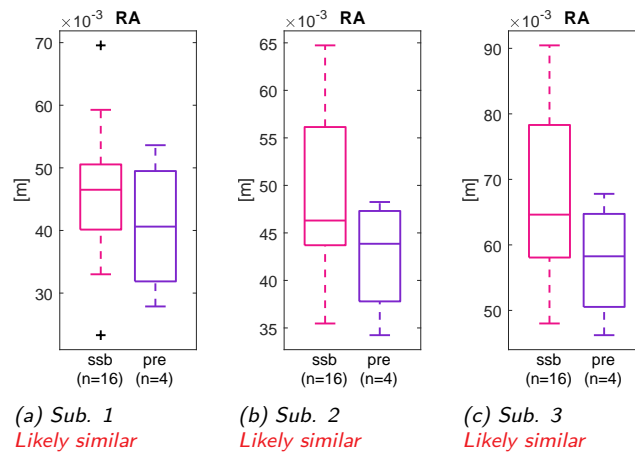


Figure 8.5: CoP X, absolute sum of rises, right foot, A-trials, comparison 2. *ssb* contains all steady state long steps from both A- and B-trials; *pre* contains pre-transition steps from A-trials only.

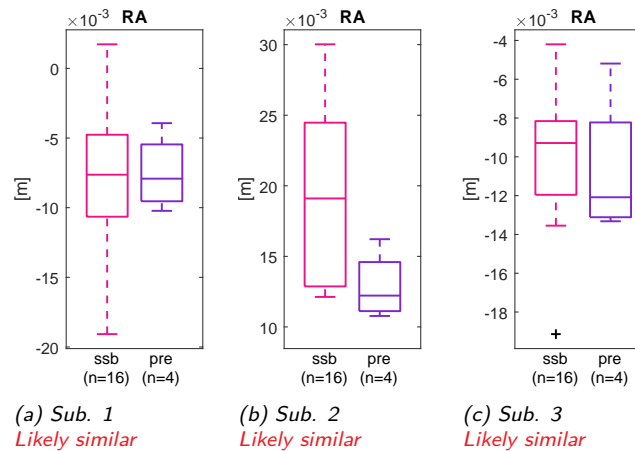


Figure 8.6: CoP X at foot strike (0% of stance phase), right foot, A-trials, comparison 2. *ssb* contains all steady state long steps from both A- and B-trials; *pre* contains pre-transition steps from A-trials only.

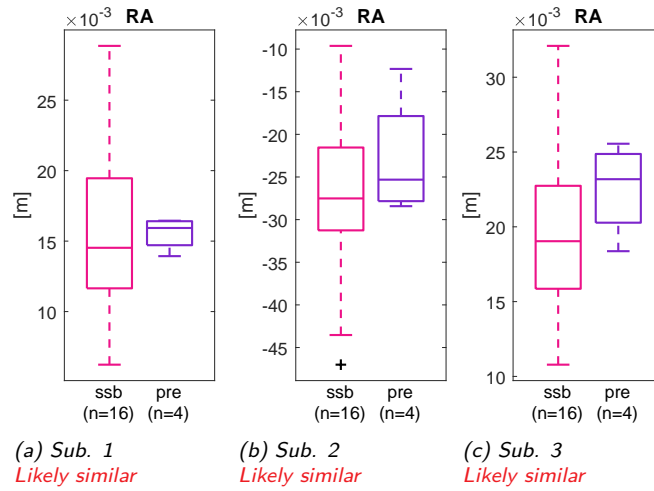


Figure 8.7: CoP X, rise between peak at 0% of stance phase and following peak, right foot, A-trials, comparison 2. *ssb* contains all steady state long steps from both A and B trials; *pre* contains pre-transition steps from A-trials only.

## 8.2.2 B-trials

As for the A-trials, none of the three metrics show any difference between the steady state beginning step group and the pre-transition step group. See figures 8.8, 8.9 and 8.10.

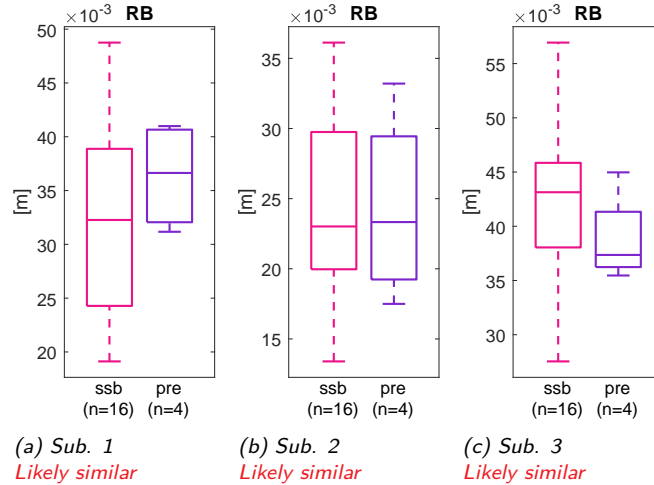


Figure 8.8: CoP X, absolute sum of rises between peaks, right foot, B-trials, comparison 2. *ssb* contains all steady state short steps from both A- and B-trials; *pre* contains pre-transition steps from B-trials only.

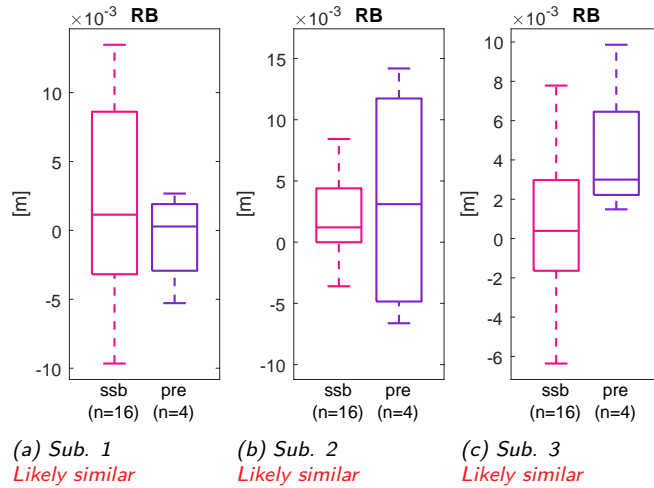


Figure 8.9: CoP X at foot strike, right foot, B-trials, comparison 2. *ssb* contains all steady state short steps from both A- and B-trials; *pre* contains pre-transition steps from B-trials only.

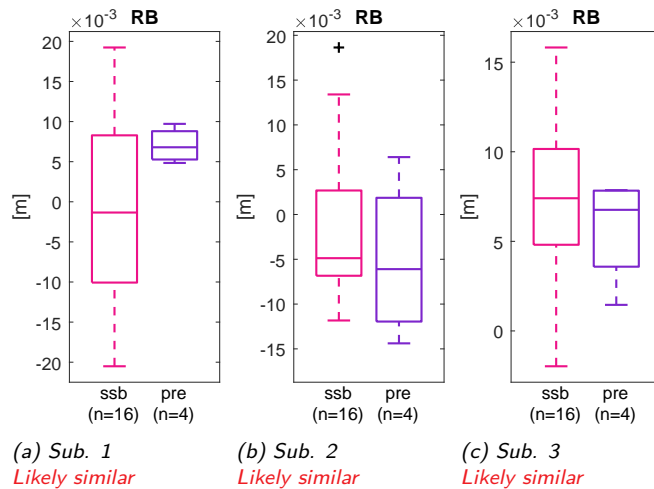


Figure 8.10: CoP X, rise between peak at 0% of stance phase and following peak, right foot, B-trials, comparison 2. *ssb* contains all steady state short steps from both A- and B-trials; *pre* contains pre-transition steps from B-trials only.

## 8.3 CoP Y: y-coordinate of the center of pressure

Three CoP Y-based metrics will be considered - for both feet. These are:

- CoP Y: value at 0% of stance phase (both feet)
- CoP Y: rise from 20% to 80% of stance phase (both feet)
- CoP Y: rise from 80% to 100% of stance phase (both feet)

### 8.3.1 A-trials

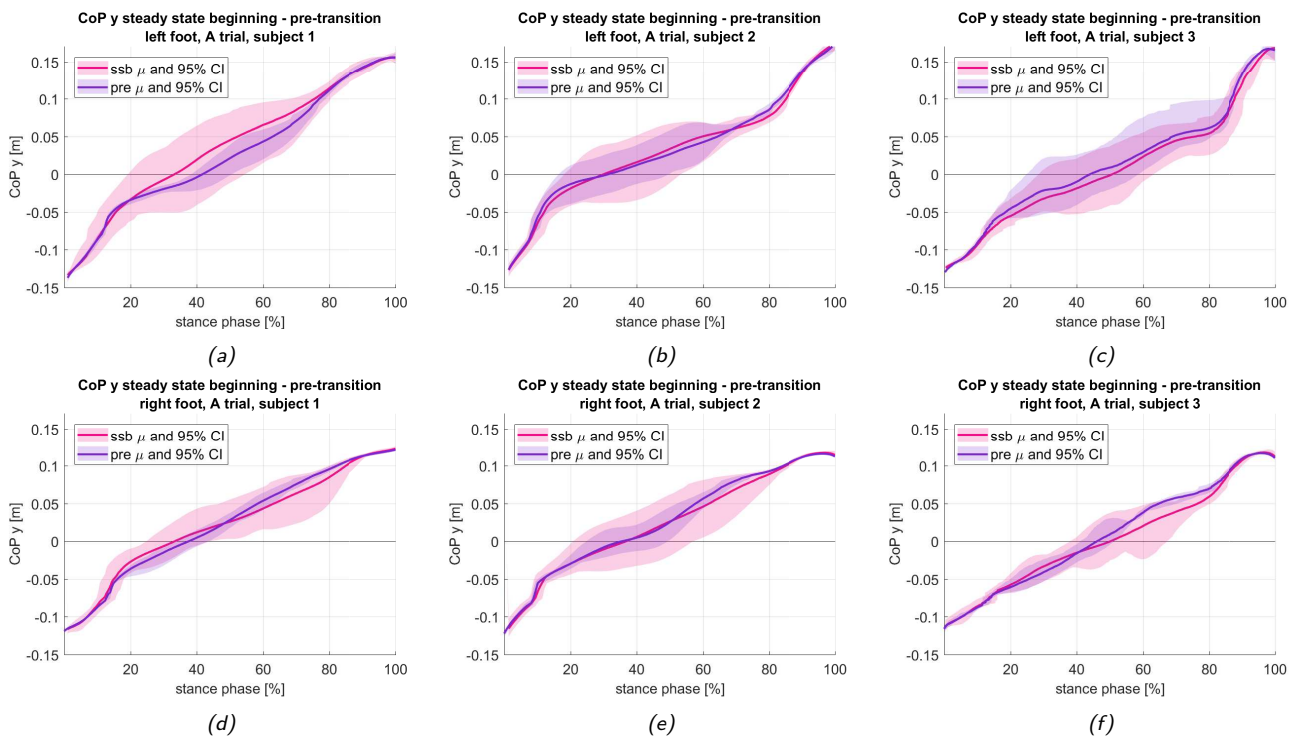


Figure 8.11: CoPY in comparison 2, A-trials: CoP Y in steady state long steps (ssb in A-trials; includes sse from B-trials) is in red, CoP Y in pre-transition steps, A-trials, is in purple. Solid lines depict the mean, shaded areas the 95% confidence interval. Top row: left feet, bottom row: right feet. From left to right: subject 1, 2 and 3. X-axes show time, expressed as percentage of stance phase. Y-axes show y-coordinate of the CoP in meters.

The red and purple lines in figure 8.11 lie so close together, that without further analysis, it can be assumed that no CoP Y-based metrics can distinguish between steady state long steps and pre-transition steps.

### 8.3.2 B-trials

The red and purple lines in figure 8.12 lie so close together, that without further analysis, it can be assumed that most CoP Y-based metrics cannot distinguish between steady state short steps and pre-transition steps. However, it may be interesting to take a closer look at the CoP Y value at 0% of stance phase, see figure 8.13. Indeed, it there is a likely difference for subjects 2 and 3, for the left foot.



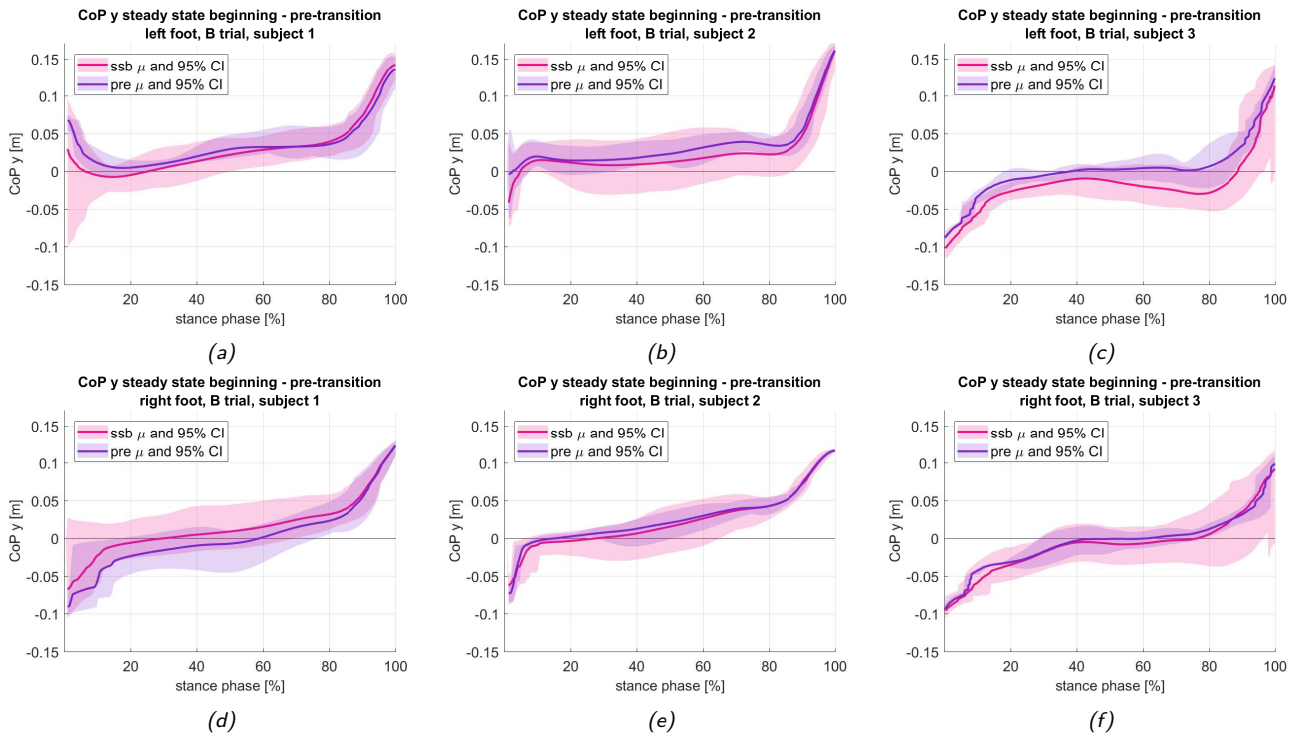


Figure 8.12: CoP Y in comparison 2: CoP Y in steady state short steps (ssb in B-trials; includes sse from A-trials) is in red, CoP Y in pre-transition steps, B-trials, is in purple. Solid lines depict the mean, shaded areas the 95% confidence interval. Top row: left feet, bottom row: right feet. From left to right: subject 1, 2 and 3. X-axes show time, expressed as percentage of stance phase. Y-axes show y-coordinate of the CoP in meters.

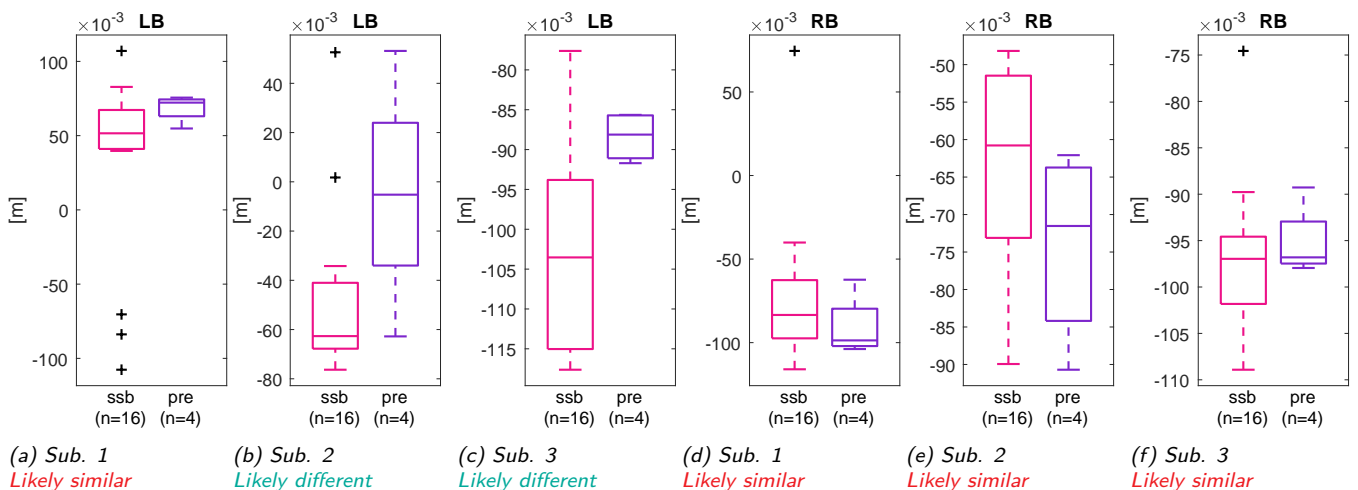


Figure 8.13: CoP Y at 0% of stance phase, comparison 2, B-trials. ssb contains all steady state long steps from both A- and B-trials; pre contains all short steps from B-trials only. The y-axes display the value of CoP Y at foot strike (0% of stance phase). Left three figures: left foot. Right three figures: right foot.

## 8.4 Conclusions

**Question 2.** *Can the pressure pattern possibly be used to identify a change in step length before it happens?*

As becomes clear at a glance at table 8.1, there are no metrics that show a likely difference between the steady state step groups and the pre-transition step groups, for neither A-trials nor B-trials. Therefore, we can conclude that **no, it does not seem possible to predict a change in step length before it happens, from the pressure pattern.**

A-trials		L			R			Likely difference for all three subjects?	
Parameter	Metric \ Subject	1	2	3	1	2	3	L	R
Fz	Timing of peak value	-	-	-	ls	ls	ls	-	no
	Value of peak	-	-	-	ls	ls	ld	-	no
CoP X	Sum of rises	-	-	-	ls	ls	ls	-	no
	Value at 0%	-	-	-	ls	ls	ls	-	no
CoP Y	Rise peak 1-2	-	-	-	ls	ls	ls	-	no
	Value at 0%	ls	ls	ls	ls	ls	ls	no	no
	Rise 20-80%	ls	ls	ls	ls	ls	ls	no	no
	Rise 80-100%	ls	ls	ls	ls	ls	ls	no	no

B-trials		L			R			Likely difference for all three subjects?	
Parameter	Metric \ Subject	1	2	3	1	2	3	L	R
Fz	Timing of peak value	-	-	-	ls	ls	ls	-	no
	Value of peak	-	-	-	ls	ls	ls	-	no
CoP X	Sum of rises	-	-	-	ls	ls	ls	-	no
	Value at 0%	-	-	-	ls	ls	ls	-	no
CoP Y	Rise peak 1-2	-	-	-	ls	ls	ls	-	no
	Value at 0%	ls	ld	ld	ls	ls	ls	no	no
	Rise 20-80%	ls	ls	ls	ls	ls	ls	no	no
	Rise 80-100%	ls	ls	ls	ls	ls	ls	no	no

Table 8.1: Summary of the metrics presented in this chapter. *ld* = likely different, *ls* = likely similar. Likely different means that there is likely a difference in this metric between steady state long steps and steady state short steps, for this subject. Likely similar means that there is probably not such a difference. If there is such a likely difference for all three subjects for a certain metric (L or R foot are considered separately), this is indicated in the rightmost columns. A dash indicates that this metric for the condition at hand, was already dismissed in chapter 7, or in studying the overlay plots; no boxplots were made.

## Chapter 9

# Comparing the steady state beginning to the transition step

**Question 3.** *Can the pressure pattern possibly be used to identify a change in step length while it is happening?*

- ⇒ What metrics identified in answering question 1, show a likely difference between the steady state beginning and transition step group?
- ⇒ Do these metrics show a likely difference in this comparison, for both feet?
- ⇒ Do these metrics show a likely difference in this comparison, for all three subjects?

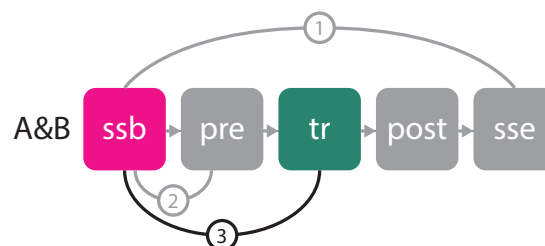


Figure 9.1: In comparison 3 the steady state beginning step group is compared to the transition step group.

## 9.1 Fz: vertical force component

The actual transition in step length takes place during stance phase of the left foot. Therefore, the left foot will be considered for all metrics in this chapter, even if no differences in these metrics were found for the left foot in chapter 7 (comparison 1):

- Fz: timing in stance phase of peak value (both feet)
- Fz: value of peak value (both feet)

### 9.1.1 A-trials

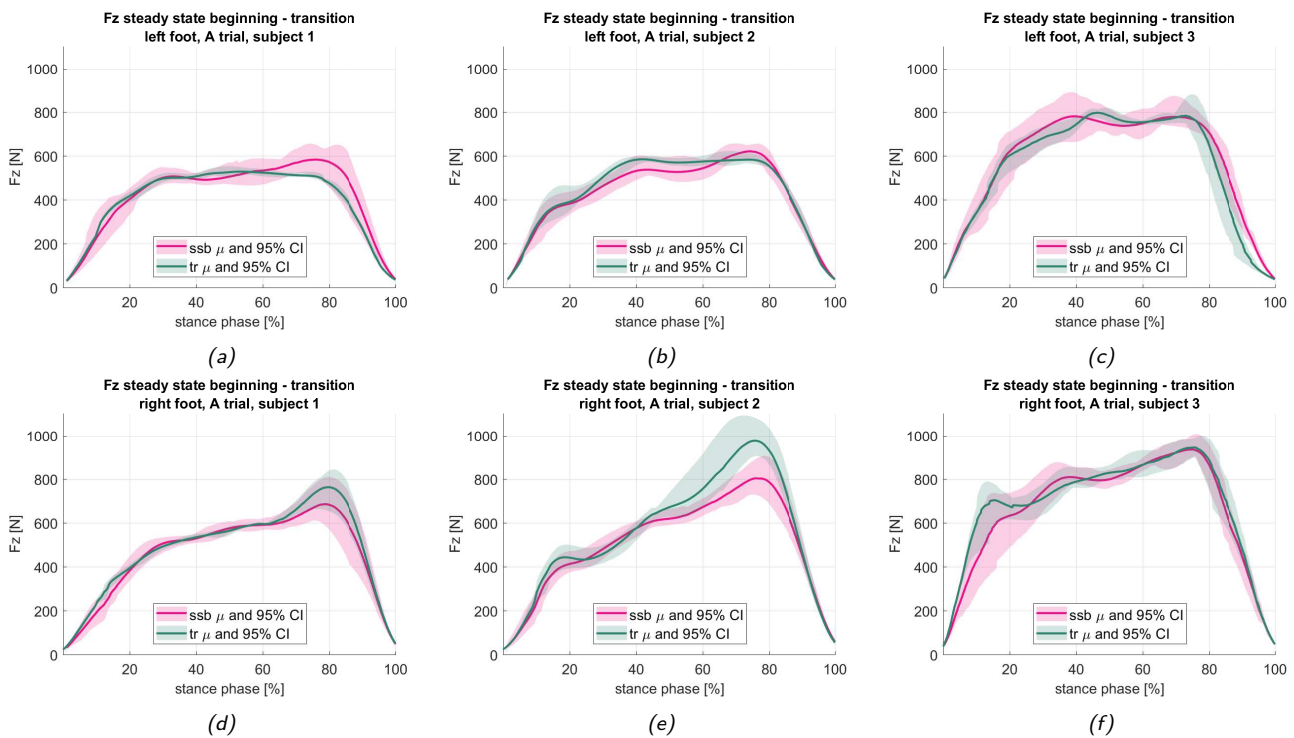


Figure 9.2: Fz mean and 95% CI for the steady state beginning steps (red) and the transition steps (green), A-trials (beginning with long steps). Top row: left foot, bottom row: right foot. From left to right: subject 1 to 3. ssb contains steady state long steps from A- and B-trials. tr contains transition steps from A-trials alone. Y-axes represent the Fz in Newton, while the x-axes represent time expressed as a percentage of stance phase.

**Left foot** For subjects 1 and 2, there might be a difference between the two step groups in the timing of the maximum Fz; it seems as though the maximum Fz occurs earlier in the transition step than in the ssb. The box plots (figure 9.4) affirm this observation only for subject 1. The difference in the value of the maximum Fz seems negligible for all subjects bar subject 1, an observation that is confirmed by the box plots as well (figure 9.3).

**Right foot** In subject 2's data we see a clear difference in the height of the "Fz bump"; we see a similar but smaller effect in subject 1 and nothing like it in subject 3. Indeed the box plots, see figure 9.3, reflect these observations. The overlap plots clearly show there is no difference in the timing of the maximum Fz for the right foot so there is no need to present the box plots in this case.

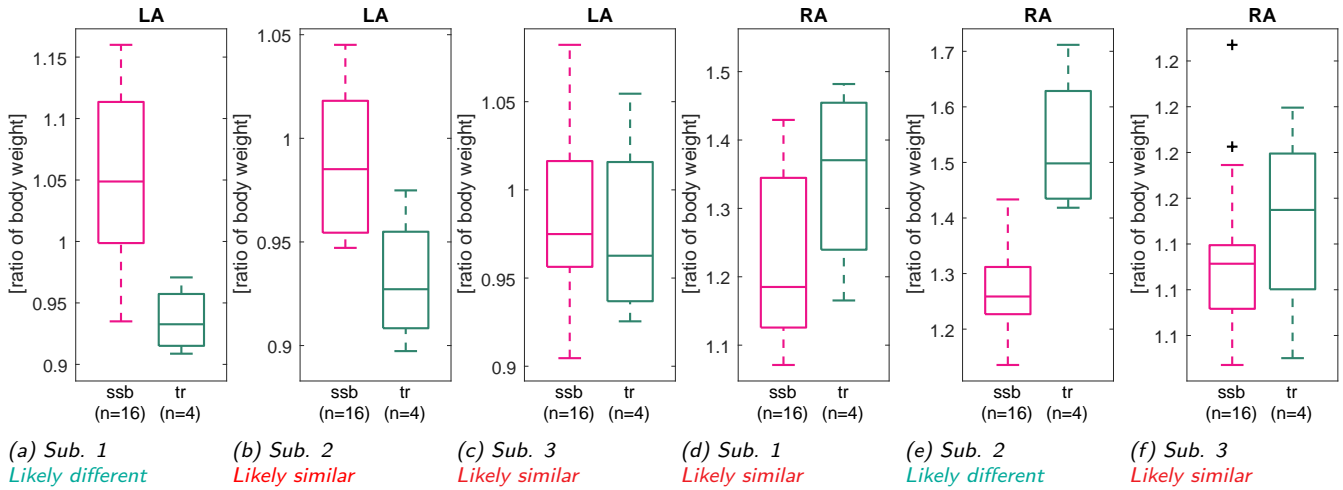


Figure 9.3: Fz peak value in a step, comparison 3, A-trials, right foot. ssb contains all steady state long steps from both A- and B-trials; tr contains transition steps from A-trials alone. Maximum Fz has been expressed as a ratio of subject's body weight.

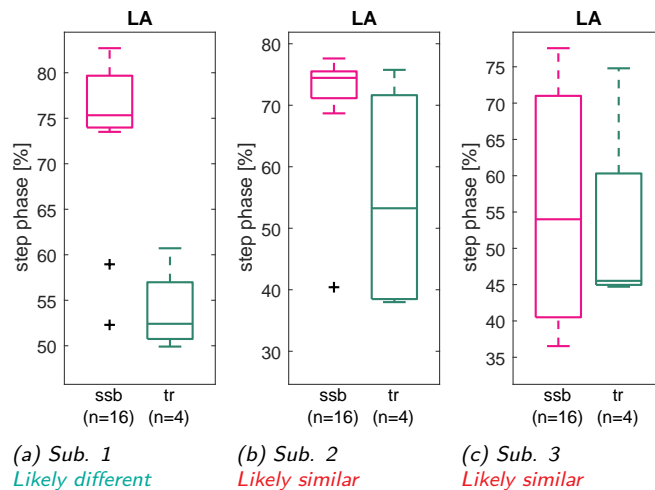


Figure 9.4: Timing (in percentage of the stance phase) of the Fz peak value, comparison 3, A-trials, left foot. ssb contains all steady state short steps from both A- and B-trials; tr contains all transition steps from A-trials.

## 9.1.2 B-trials

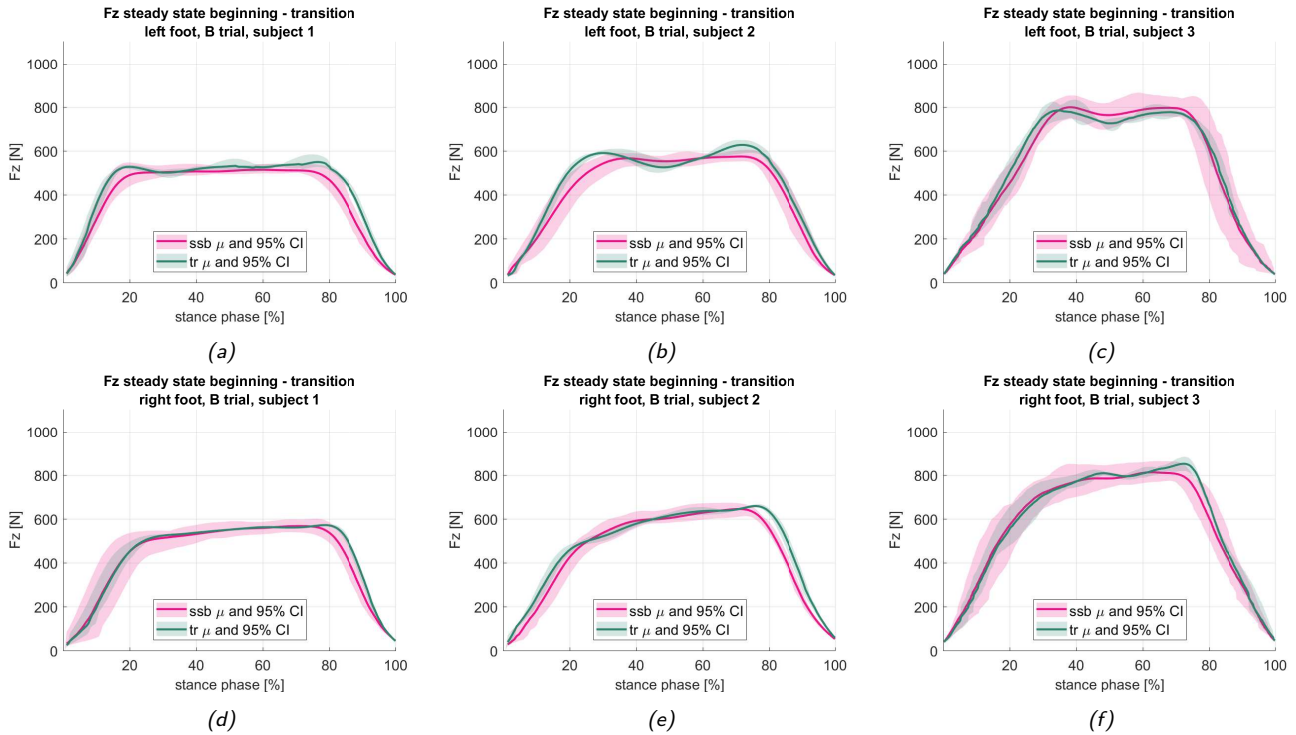


Figure 9.5:  $F_z$  mean and 95% CI for the steady state beginning steps (red) and the transition steps (green). *ssb* contains all steady state short steps from both A- and B-trials; *tr* contains transition steps from B-trials alone. Y-axes represent the  $F_z$  in Newton, while the x-axes represent time shown as a percentage of stance phase. From left to right: subjects 1 to 3. Top row: left foot, bottom row: right foot.

The  $F_z$  bumps are nearly indistinguishable in these images (figure 9.5); mean and CI of both step groups neatly overlap. It is not necessary to display the box plots for this data.

## 9.2 CoP X: x-coordinate of the center of pressure

Again, the following metrics are considered and we move directly to the boxplots:

- CoP X: sum of the rises
- CoP X: value at 0% of stance phase
- CoP X: rise between 1st and 2nd peak

### 9.2.1 A-trials

Virtually all metrics are likely similar over the two step groups compared here. Clearly CoP X-based metrics are not capable of distinguishing a transition step from a steady state long step. See figures 9.6, 9.7 and 9.8.

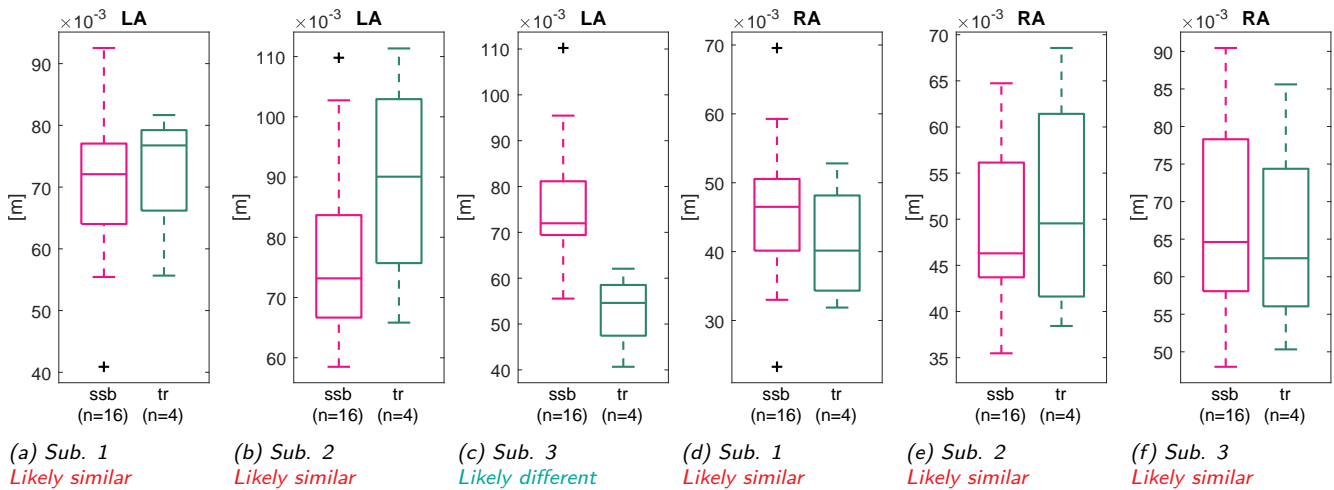


Figure 9.6: CoP X, absolute sum of rises, A-trials, comparison 3. ssb contains all steady state long steps from both A- and B-trials; tr contains transition steps from A-trials only. Left three figures: left foot. Right three figures: right foot.

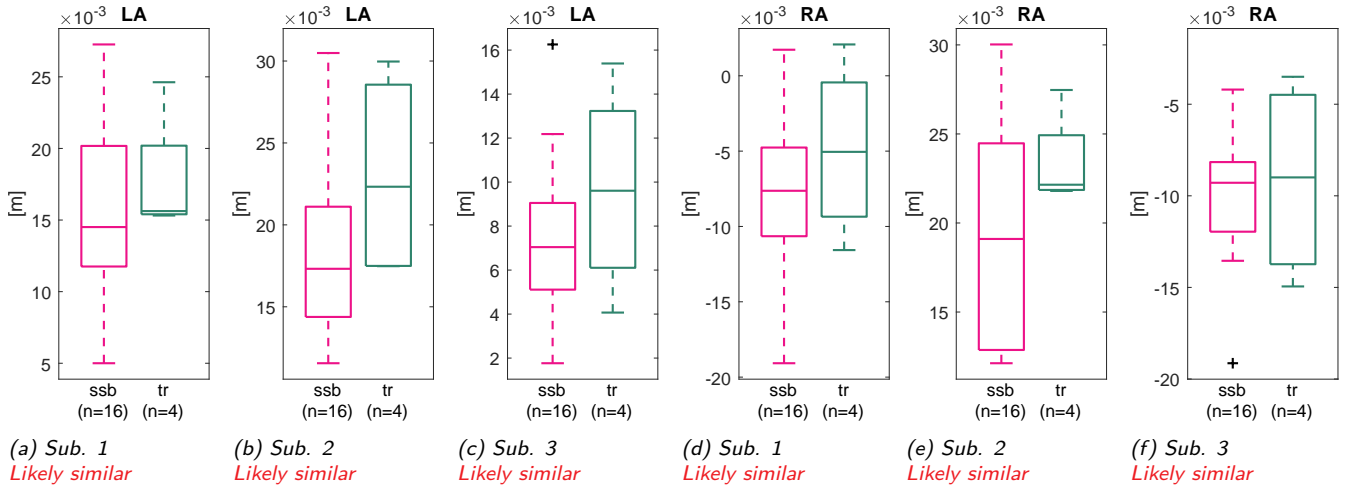


Figure 9.7: CoP X at foot strike, A-trials, comparison 3. *ssb* contains all steady state long steps from both A- and B-trials; *tr* contains transition steps from A-trials only. Left three figures: left foot. Right three figures: right foot.

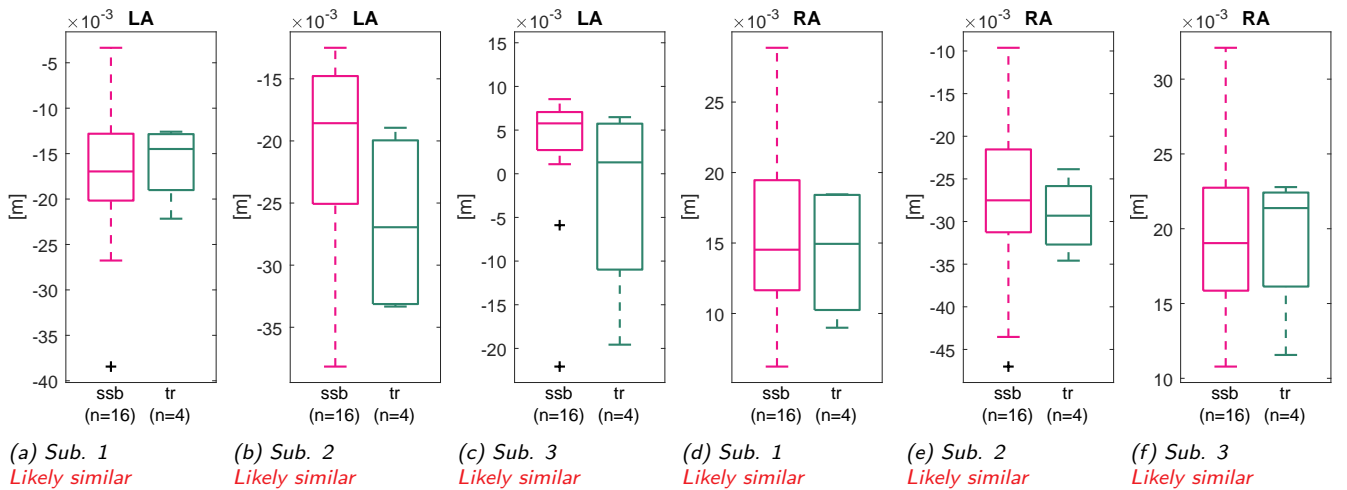


Figure 9.8: CoP X, rise between peak at 0% of stance phase and following peak, A-trials, comparison 3. *ssb* contains all steady state long steps from both A- and B-trials; *tr* contains transition steps from A-trials only. Left three figures: left foot. Right three figures: right foot.



### 9.2.2 B-trials

For B-trials, only the sum of the rises looks like a viable metric: it shows a likely difference for all three subjects in the left foot. The other two metrics show negative results, as in the A-trials. See figures 9.9, 9.10 and 9.11.

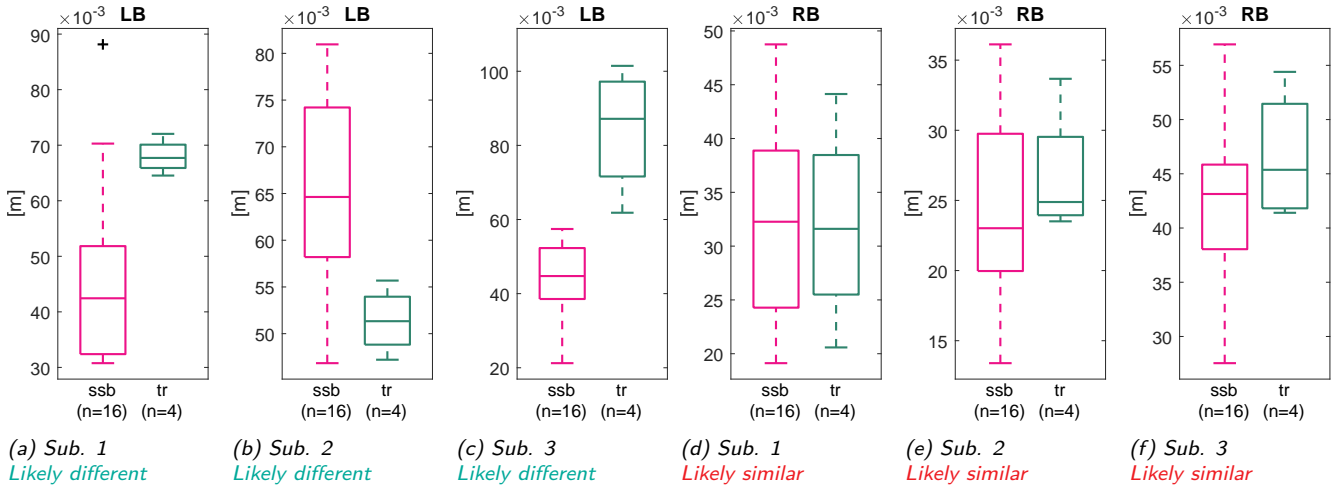


Figure 9.9: CoP X, absolute sum of rises between peaks, B-trials, comparison 2. ssb contains all steady state short steps from both A- and B-trials; tr contains transition steps from B-trials only. Left three figures: left foot, right three figures: right foot.

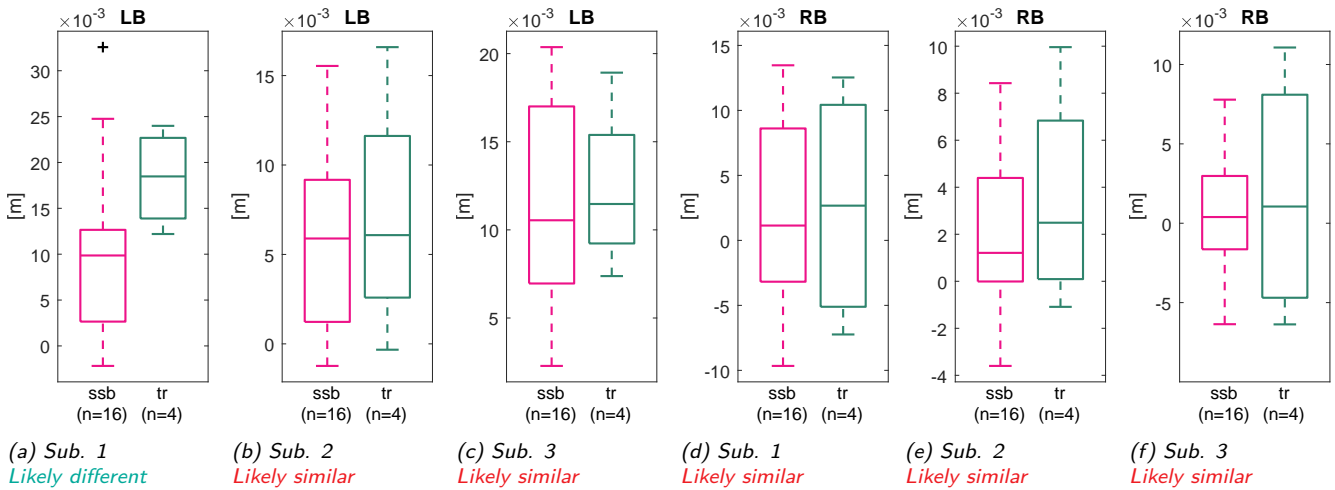


Figure 9.10: CoP X at foot strike, B-trials, comparison 3. ssb contains all steady state short steps from both A and B trials; tr contains transition steps from B-trials only. Left three figures: left foot. Right three figures: right foot.

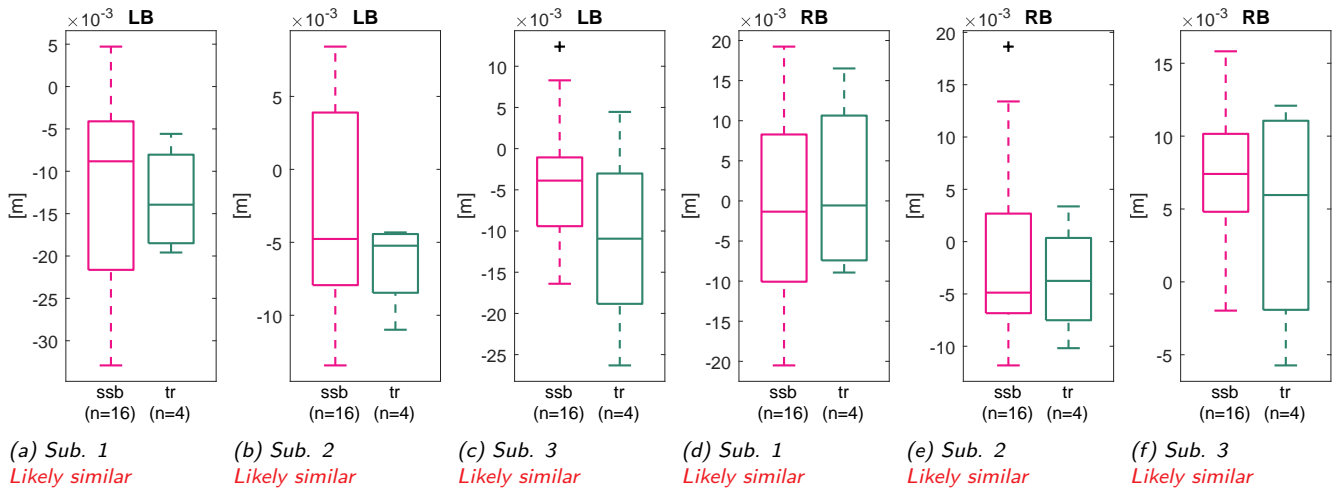


Figure 9.11: CoP X, rise between peak at 0% of stance phase and following peak, B-trials, comparison 3. ssb contains all steady state short steps from both A and B trials; tr contains transition steps from B-trials only. Left three figures: left foot. Right three figures: right foot.

### 9.3 CoP Y: y-coordinate of the center of pressure

Three CoP Y-based metrics will be considered - for both feet. These are:

- CoP Y: value at 0% of stance phase (both feet)
- CoP Y: rise from 20% to 80% of stance phase (both feet)
- CoP Y: rise from 80% to 100% of stance phase (both feet)

#### 9.3.1 A-trials

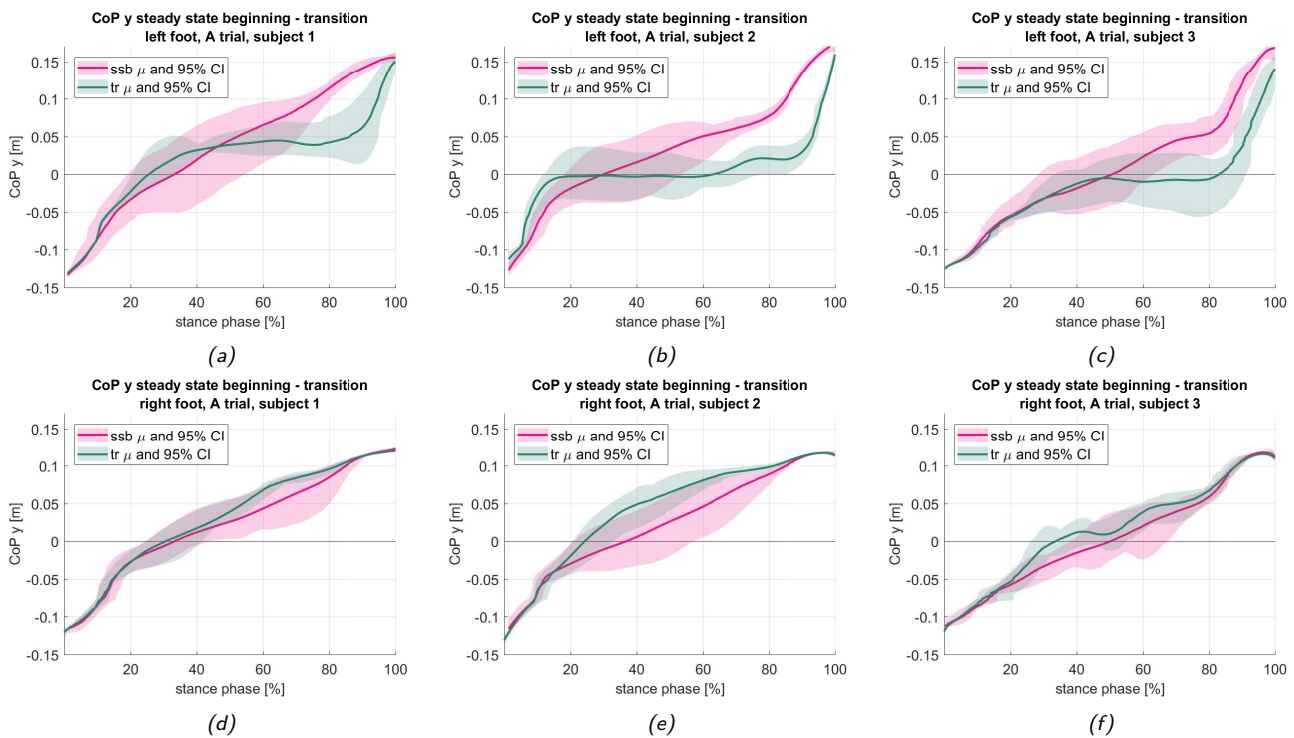


Figure 9.12: CoP Y in comparison 3, A-trials: CoP Y in steady state long steps (ssb in A-trials; includes sse from B-trials) is in red, CoP Y in transition steps, A-trials, is in green. Solid lines depict the mean, shaded areas the 95% CI. Top row: left feet, bottom row: right feet. From left to right: subject 1, 2 and 3. X-axes show time, expressed as percentage of stance phase. Y-axes show y-coordinate of the CoP in meters.

Looking at figure 9.12, we see a difference between the left and right feet patterns. It is probable that this has to do with the difference in step length between the left and right feet in the transition step: the left foot makes a swing of 130cm (a regular long step), while the right foot makes a swing of 85cm (the actual transition step). Based on figure 9.12 we take a closer look at two metrics: CoP Y rise from 20-80% of stance phase and the rise from 80-100% of stance phase: figures 9.13 and 9.14. These box plots indicate a likely difference for both metrics in the left feet of all three subjects.

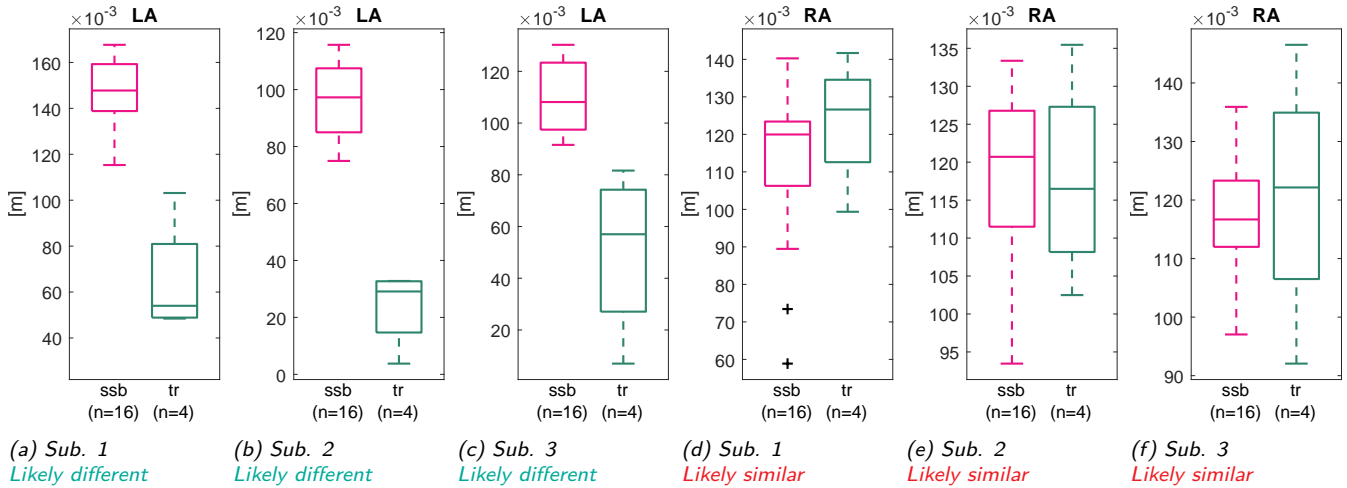


Figure 9.13: CoP Y rise from 20% to 80% of stance phase, comparison 3. *ssb* contains all steady state long steps from both A- and B-trials; *tr* contains transition steps from A-trials only. The y-axes display the difference between the value of CoPY at 20% and 80% of stance phase. Left three figures: left foot. Right three figures: right foot.

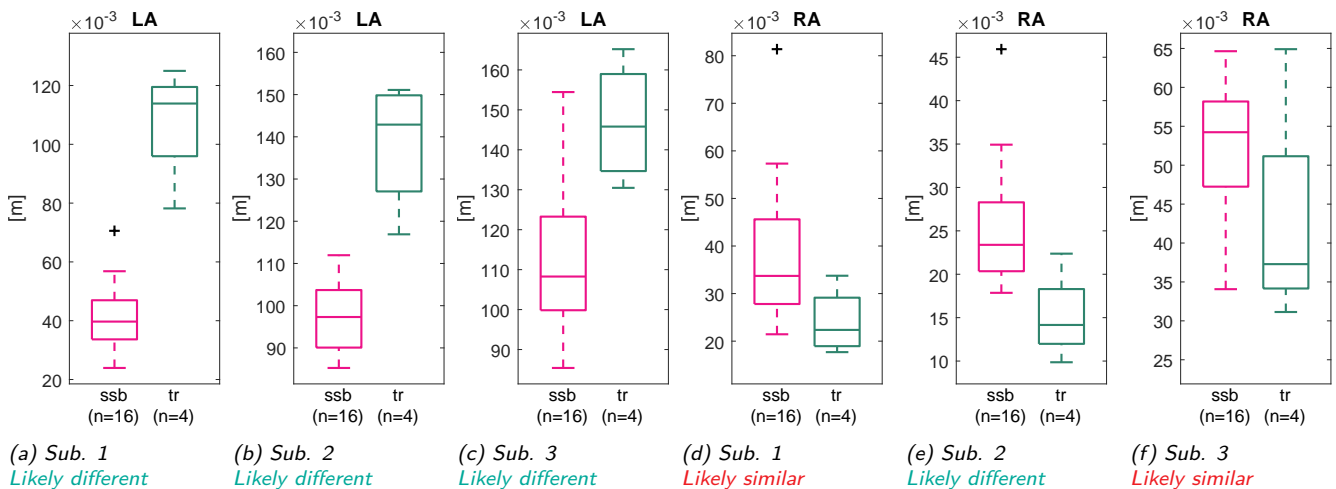


Figure 9.14: CoP Y rise from 80% to 100% of stance phase, comparison 3. *ssb* contains all steady state long steps from both A- and B-trials; *tr* contains transition steps from A-trials only. The y-axes display the difference between the value of CoP Y at 20% and 80% of stance phase. Left three figures: left foot. Right three figures: right foot.

### 9.3.2 B-trials

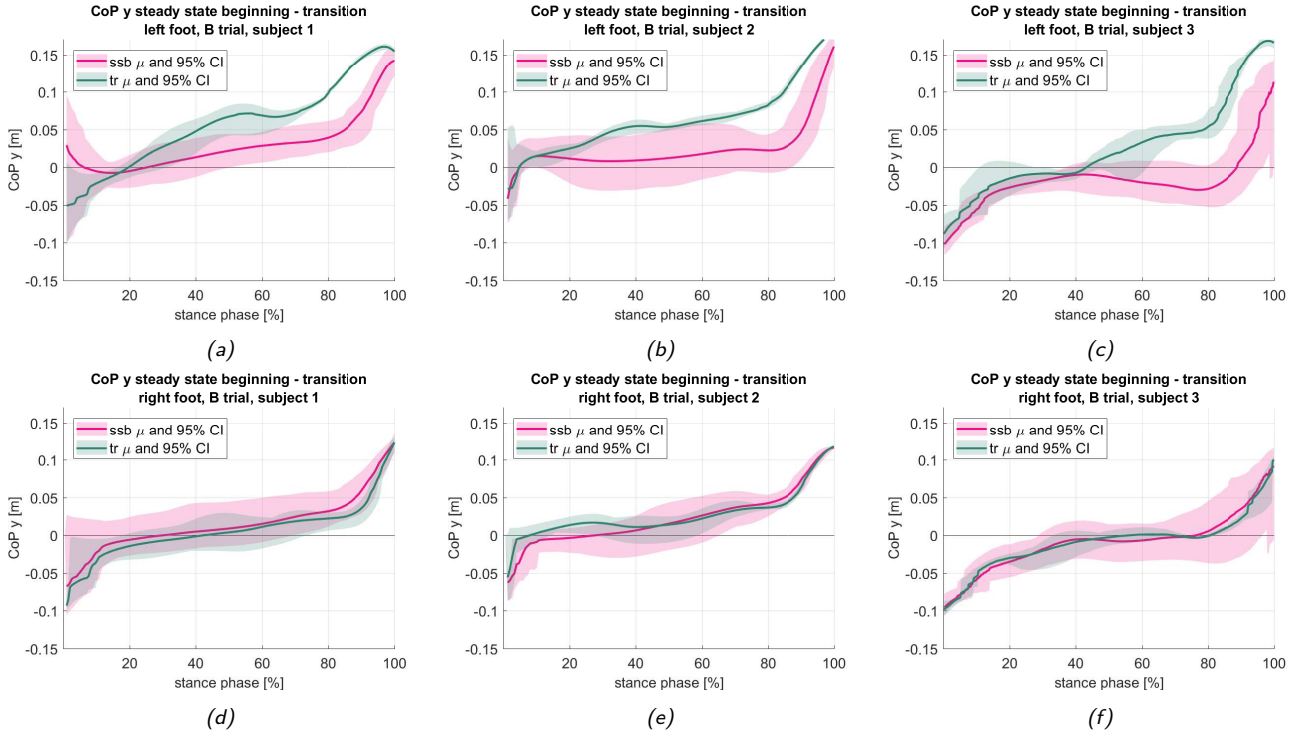


Figure 9.15: CoP Y in comparison 3: CoP Y in steady state short steps (ssb in B-trials; includes sse from A-trials) is in red, CoP Y in transition steps, B-trials, is in green. Solid lines depict the mean, shaded areas the 95% CI. Top row: left feet, bottom row: right feet. From left to right: subject 1, 2 and 3. X-axes show time, expressed as percentage of stance phase. Y-axes show y-coordinate of the CoP in meters.

Based on figure 9.15 we take a look at all three CoP Y-based metrics for the left foot only: figures 9.16 to 9.18. The latter two box plots indicate a likely difference for all three subjects.

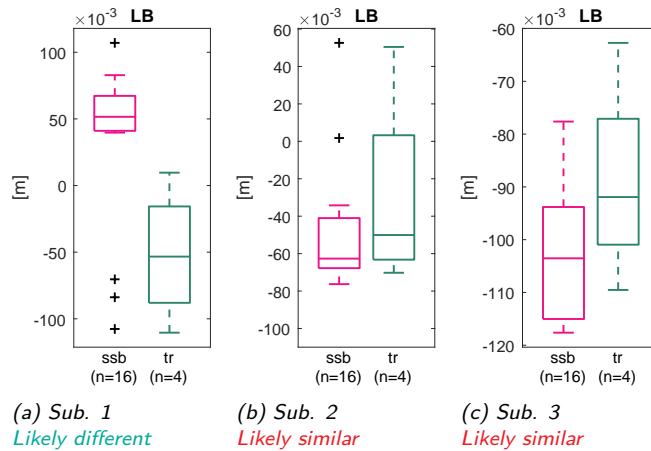


Figure 9.16: CoP Y at 0% of stance phase, comparison 2, B-trials, left foot. ssb contains all steady state long steps from both A- and B-trials; tr contains transition steps from B-trials only. The y-axes display the value of CoP Y at foot strike (0% of stance phase).

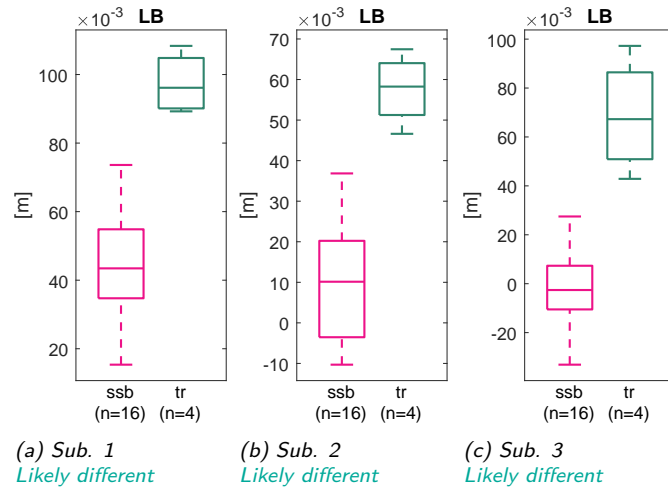


Figure 9.17: CoP Y rise from 20% to 80% of stance phase, comparison 3, B-trials, left foot. *ssb* contains all steady state long steps from both A- and B-trials; *tr* contains transition steps from B-trials only. The y-axes display the difference between the value of CoP Y at 20% and 80% of stance phase.

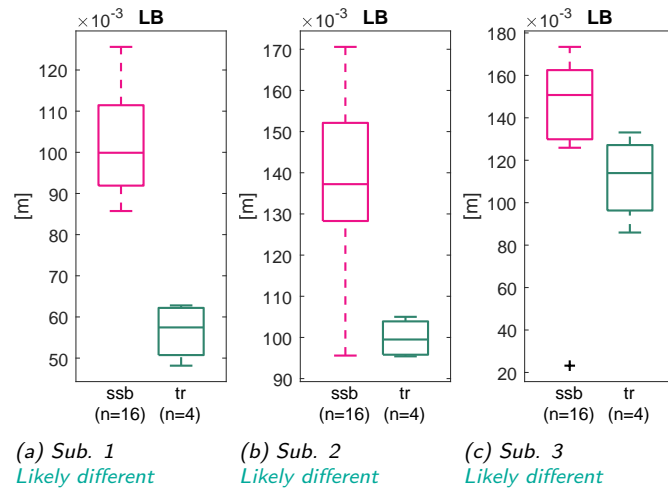


Figure 9.18: CoP Y rise from 80% to 100% of stance phase, comparison 3, B-trials, left foot. *ssb* contains all steady state long steps from both A- and B-trials; *tr* contains transition steps from B-trials only. The y-axes display the difference between the value of CoP Y at 80% and 100% of stance phase.

## 9.4 Conclusions

**Question 3.** *Can the pressure pattern possibly be used to identify a change in step length while it is happening?*

Table 9.1, which summarizes the results from this chapter, can help to answer **question 3: yes, it is possible to identify a change in step length while it is happening by using the pressure pattern, but there are only a few metrics that can be used for this end**, which are CoP Y rise from 20-80% of step phase and CoP Y rise from 80-100% of step phase in A-trials and the same plus CoP X sum of rises for B-trials. These metrics show a likely difference between steady state beginning steps and the transition step in the left foot for all three subjects.

A-trials		L			R			Likely difference for all three subjects?	
Parameter	Metric \ Subject	1	2	3	1	2	3	L	R
Fz	Timing of peak value	ld	ls	ls	-	-	-	no	no
	Value of peak	ld	ls	ls	ls	ld	ls	no	no
CoP X	Sum of rises	ls	ls	ld	ls	ls	ls	no	no
	Value at 0%	ls	ls	ls	ls	ls	ls	no	no
	Rise peak 1-2	ls	ls	ls	ls	ls	ls	no	no
CoP Y	Value at 0%	-	-	-	-	-	-	no	no
	Rise 20-80%	ld	ld	ld	ls	ls	ls	yes	no
	Rise 80-100%	ld	ld	ld	ls	ld	ls	yes	no

B-trials		L			R			Likely difference for all three subjects?	
Parameter	Metric \ Subject	1	2	3	1	2	3	L	R
Fz	Timing of peak value	-	-	-	-	-	-	no	no
	Value of peak	-	-	-	-	-	-	no	no
CoP X	Sum of rises	ld	ld	ld	ls	ls	ls	yes	no
	Value at 0%	ld	ls	ls	ls	ls	ls	no	no
	Rise peak 1-2	ls	ls	ls	ls	ls	ls	no	no
CoP Y	Value at 0%	ld	ls	ls	-	-	-	no	no
	Rise 20-80%	ld	ld	ld	-	-	-	yes	no
	Rise 80-100%	ld	ld	ld	-	-	-	yes	no

Table 9.1: Summary of the box plots presented in this chapter. *ld* = likely different, *ls* = likely similar. Likely different means that there is likely a difference in this metric between steady state long steps and steps in the transition group, for this subject. Likely similar means that there is probably not such a difference. If there is a likely difference for all three subjects for a certain metric (L or R foot are considered separately), this is indicated in the rightmost columns. A dash (-) signifies that this metric was eliminated without the need of studying the boxplots; it was either discarded at the end of chapter 7 or by looking at the overlay plots such as fig. 9.15.

## Chapter 10

# The moderate track: C- and D-trials

**Question 4.** *Can the pressure pattern possibly be used to distinguish between steady state long and steady state short steps, when the difference in step length is less extreme?*

- ⇒ What metrics identified in answering question 1, show a likely difference between moderate steady state long and moderate steady state short steps?
- ⇒ Do these metrics show a likely difference in this comparison, for both feet?
- ⇒ Do these metrics show a likely difference in this comparison, for all three subjects?

After thoroughly analysing the A- and B-trials, in chapters 7, 8 and 9, this chapter will briefly consider the C- and D-trials. In the C- and D-trials the subjects traversed the moderate track, where the difference between long and short steps was smaller than in the extreme track used for A- and B-trials. Since in the A- and B-trials hardly any effects were found for comparisons 2 and 3, for trials C- and D only the steady states will be compared. This is comparison 4, see figure 10.1.

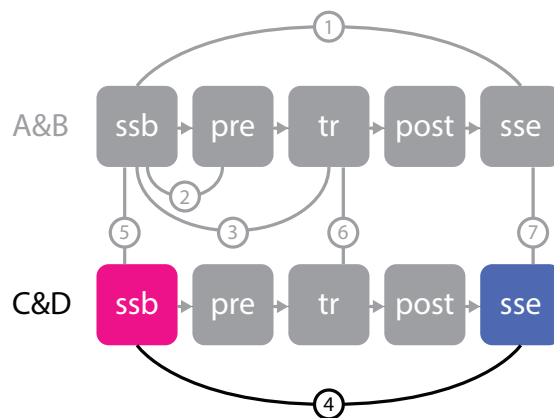


Figure 10.1: Comparison 4.



## 10.1 Fz: vertical force component

### 10.1.1 Overlay plots

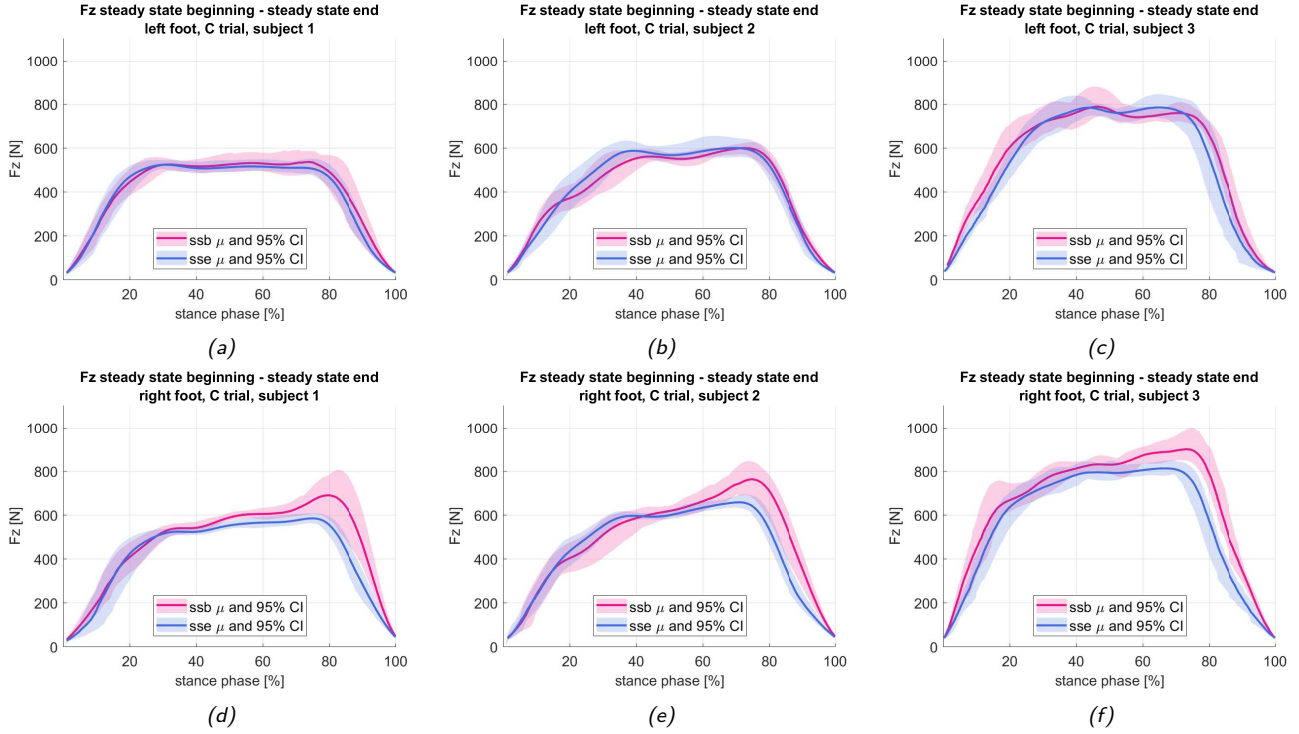


Figure 10.2:  $F_z$  in comparison 4, C&D-trials:  $F_z$  in steady state long steps (ssb in C-trials; includes sse from D-trials) is in red,  $F_z$  in steady state short steps (sse in C-trials; includes ssb from D-trials) is in blue. Solid lines depict the mean, shaded areas the 95% confidence interval. Top row: left feet, bottom row: right feet. From left to right: subject 1, 2 and 3. X-axes show time, expressed as percentage of stance phase. Y-axes show force in Newton.

**Left foot** The red and blue lines for the red foot lie very closely together; no further attention will be paid to the  $F_z$ -metrics for the left foot in this comparison.

**Right foot** As in comparison 1, in the right foot, we see the  $F_z$ -bumps around 75% of stance phase here as well, in the ssb group. Moreover, it seems that the maximum  $F_z$  occurs later in the step phase in ssb steps than in sse steps. So for the right foot, we will take a look at the boxplots for maximum  $F_z$  and timing of maximum  $F_z$ .

### 10.1.2 Box plots

**Timing of Fz peak** As figure 10.2 already hinted, this metric shows a likely difference for subjects 1 and 2 only.

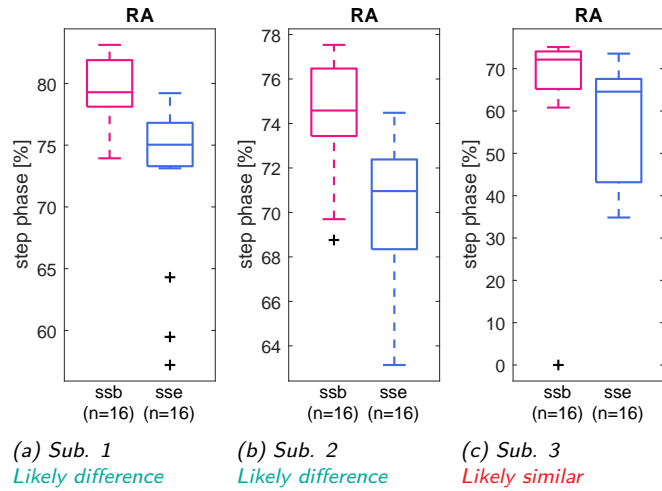


Figure 10.3: Timing (in percentage of the stance phase) of the Fz peak value for the right foot. ssb contains all steady state long steps from both C- and D-trials; sse contains all steady state short steps from both C- and D-trials.

**Value of Fz peak** As in comparison 1, this is again a good metric in comparison 4: a likely difference can be seen in figure 10.4 for all three subjects.

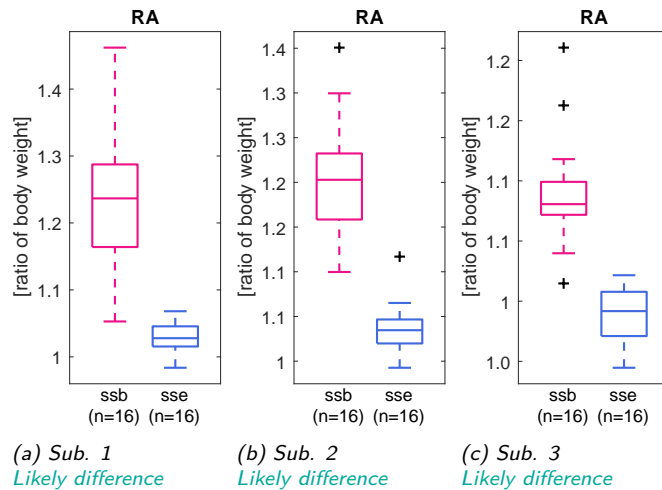


Figure 10.4: Value of the maximum Fz in each step, right foot, comparison 4. ssb contains all steady state long steps from both C- and D-trials; sse contains all steady state short steps from both C- and D-trials. Maximum Fz has been expressed as a ratio of subject's body weight.

## 10.2 CoP X: x-coordinate of the center of pressure

### 10.2.1 Overlay plots

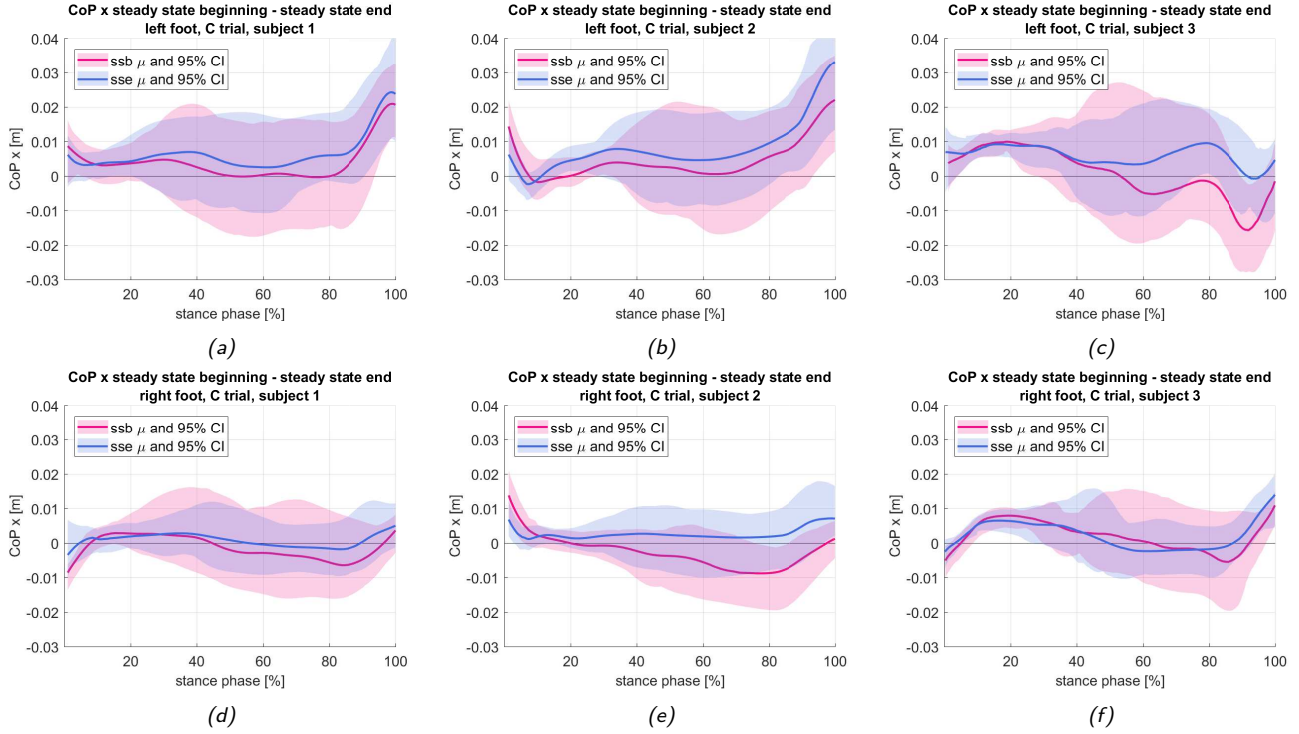


Figure 10.5: CoP X in comparison 4: CoP X in steady state long steps (ssb in C-trials; includes sse from D-trials) is in red, CoP X in steady state short steps is in blue. Solid lines depict the mean, shaded areas the 95% confidence interval. Top row: left feet, bottom row: right feet. From left to right: subject 1, 2 and 3. X-axes show time, expressed as percentage of stance phase. Y-axes show x-coordinate of the CoP in meters.

As in comparison 1, it can again be noticed that the CoP X CIs are very broad. It seems as though in these trials, as in the A- and B-trials, there is a large difference between left and right feet. Thus, again, the boxplots are presented on the next few pages, to take a more detailed look at the metrics based on the x-coordinate of the CoP that were validated in chapter 7:

- CoP X: sum of the rises (right foot)
- CoP X: value at 0% of stance phase (right foot)
- CoP X: rise between 1st and 2nd peak (right foot)

### 10.2.2 Box plots

**Sum of rises between CoP X peaks** The boxes overlap for none of the three subjects, indicating that also when step size difference is moderate, this is a good metric to differentiate between steady state long and short steps.

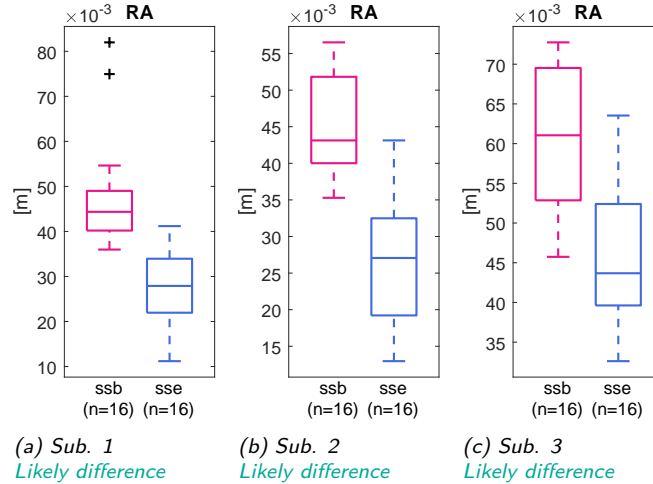


Figure 10.6: CoP X, absolute sum of rises between peaks. *ssb* contains all steady state long steps from both C- and D-trials; *sse* contains all steady state short steps from both C- and D-trials. The y-axes display the sum of all the rises between peaks in a step.

**CoP X at 0% of stance phase** This metric does not perform so well for moderately long and short steps. There is only a likely difference for subject 2; for the other two subjects, the boxes partly overlap.

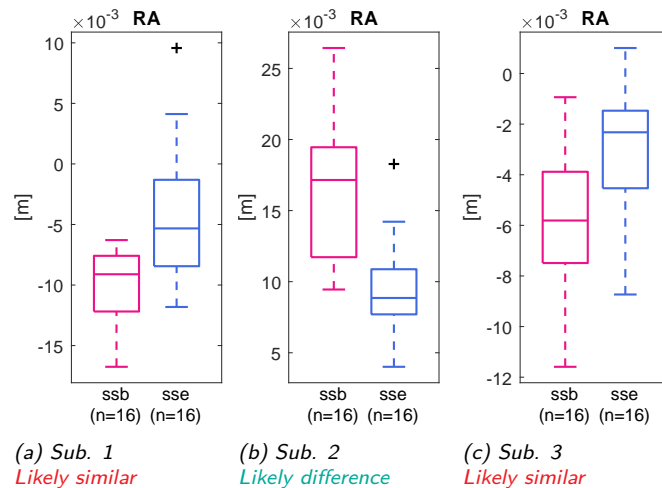


Figure 10.7: CoP X at foot strike. *ssb* contains all steady state long steps from both C- and D-trials; *sse* contains all short steps from both C- and D-trials. The y-axes display the value of the CoP X at foot strike (0% of stance phase).

**Rise between 0% of stance phase and the following peak** As for the previous metric, again there is only a likely difference for subject 2.

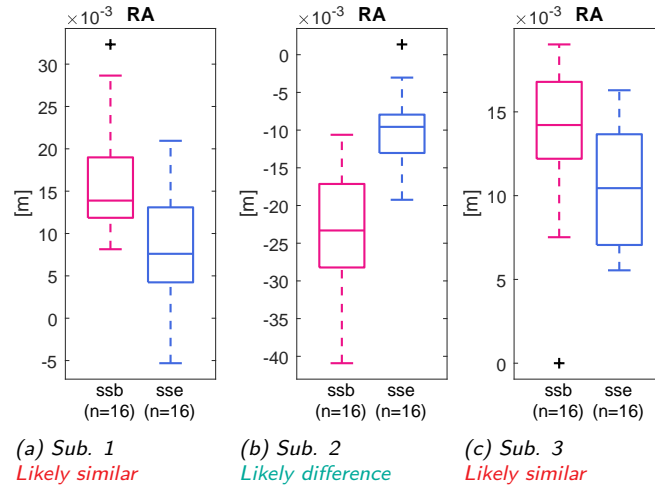


Figure 10.8: CoP X, rise between 0% of stance phase and the next peak, right foot. *ssb* contains all steady state long steps from both C- and D-trials; *sse* contains all steady state short steps from both C- and D-trials. The y-axes display the difference in value of the CoP X at foot strike (0% of stance phase) and the next CoP X peak.

## 10.3 CoP Y: y-coordinate of the center of pressure

### 10.3.1 Overlay plots

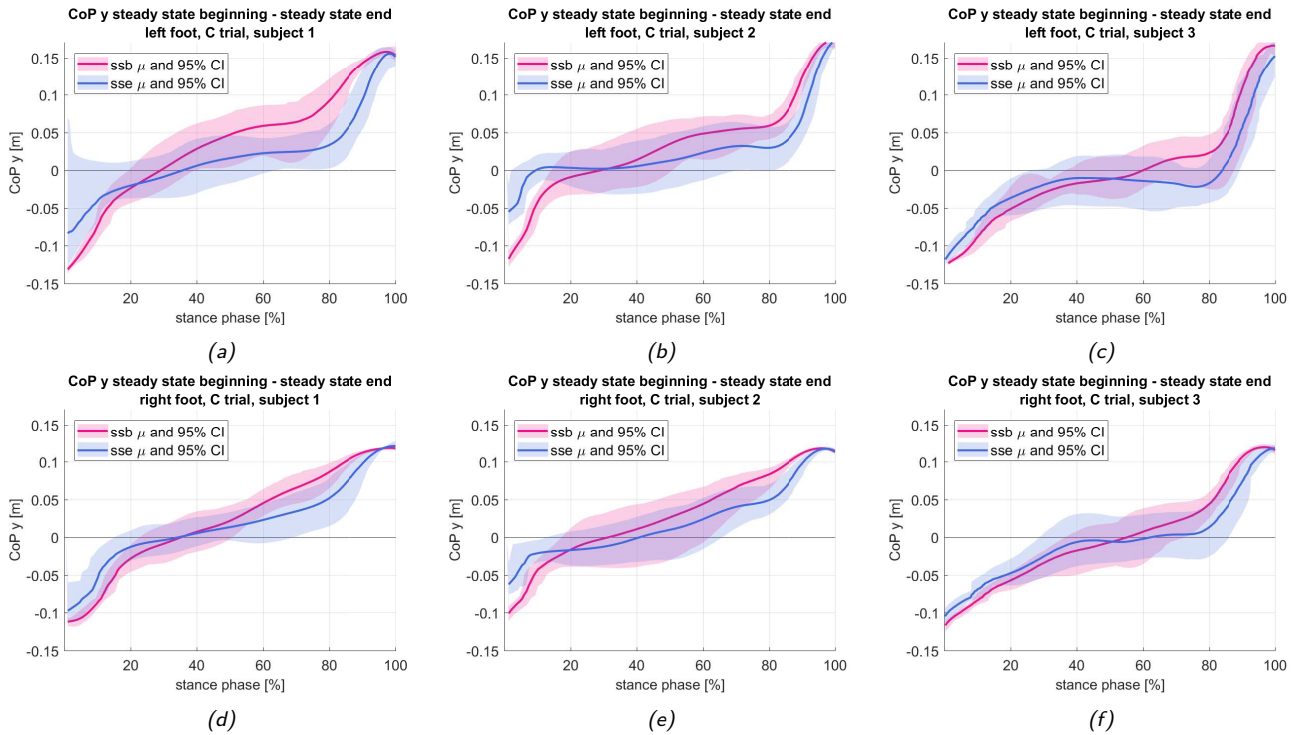


Figure 10.9: CoP Y in comparison 4: CoP Y in steady state long steps (ssb in C-trials; includes sse from D-trials) is in red, CoP Y in steady state short steps (sse in D-trials; includes sse from C-trials) is in blue. Solid lines depict the mean, shaded areas the 95% CI. Top row: left feet, bottom row: right feet. From left to right: subject 1, 2 and 3. X-axes show time, expressed as percentage of stance phase. Y-axes show y-coordinate of the CoP in meters.

As expected, similar patterns as in comparison 1 (chapter 7, figure 7.15) can be observed, but the red (long steady state) and blue (short steady state) lines do not diverge as much from each other as in comparison 1. Still, there is a good chance that the metrics will show some likely differences, so the box plots are studied.

### 10.3.2 Box plots

**CoP Y at 0% of stance phase** The differences are especially large for subject 2, as could already be seen in figure 10.9. For the left foot, there is a likely difference for all three subjects.

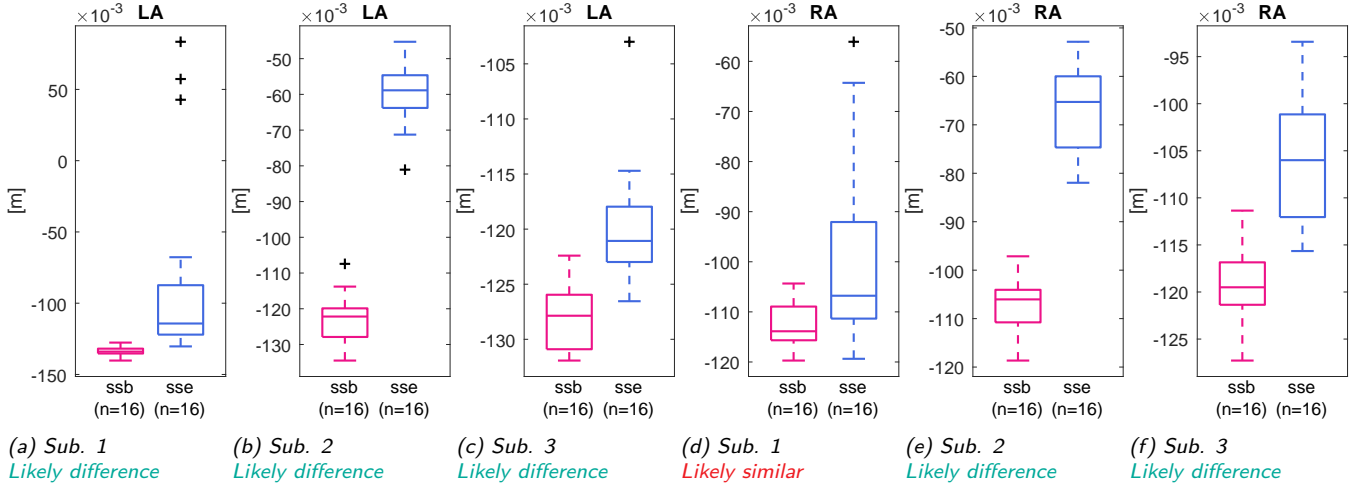


Figure 10.10: CoP Y at 0% of stance phase, comparison 4. *ssb* contains all steady state long steps from both C- and D-trials; *sse* contains all short steps from both C- and D-trials. The y-axes display the value of CoP Y at foot strike (0% of stance phase). Left three figures: left foot. Right three figures: right foot.

**CoP Y rise from 20% to 80% of stance phase** None of the boxes in the plots in figure 10.11 overlap; this metric still has value, when the difference in step size is less extreme than in comparison 1. Still, for all three subjects the box whiskers overlap; this was not the case in comparison 1 (figure 7.18). So it seems that as step length differences become less extreme, so do pressure pattern differences become smaller.

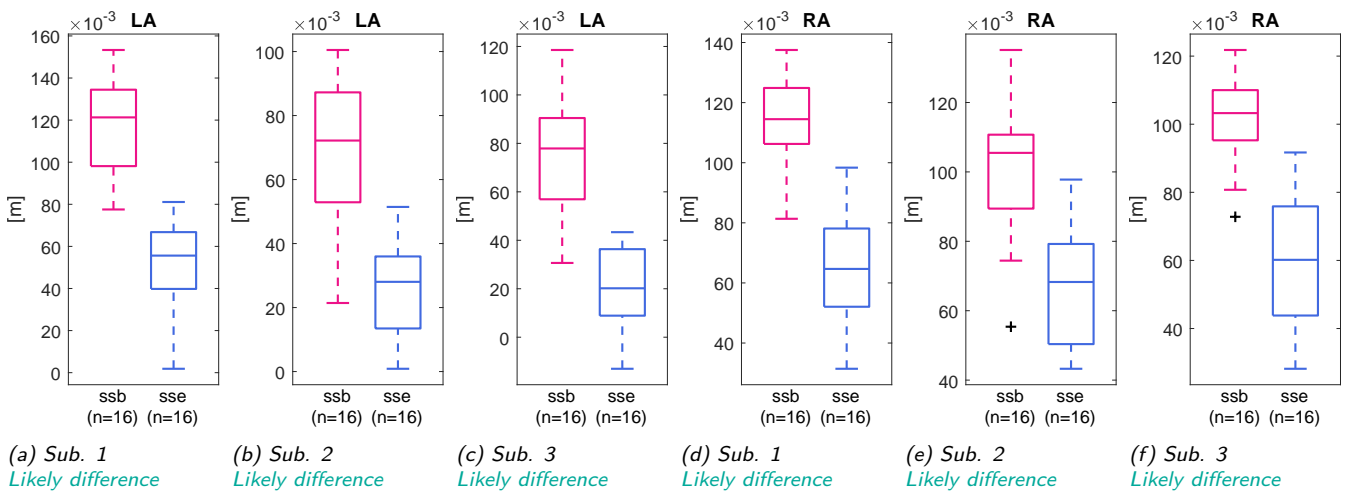


Figure 10.11: CoP Y rise from 20% to 80% of stance phase, comparison 4. *ssb* contains all steady state long steps from both C- and D-trials; *sse* contains all short steps from both C- and D-trials. The y-axes display the difference between the value of CoP Y at 20% and 80% of stance phase. Left three figures: left foot. Right three figures: right foot.

**CoP Y rise from 80% to 100% of stance phase** Again, no overlapping boxes for all three subjects, both for left and right feet.

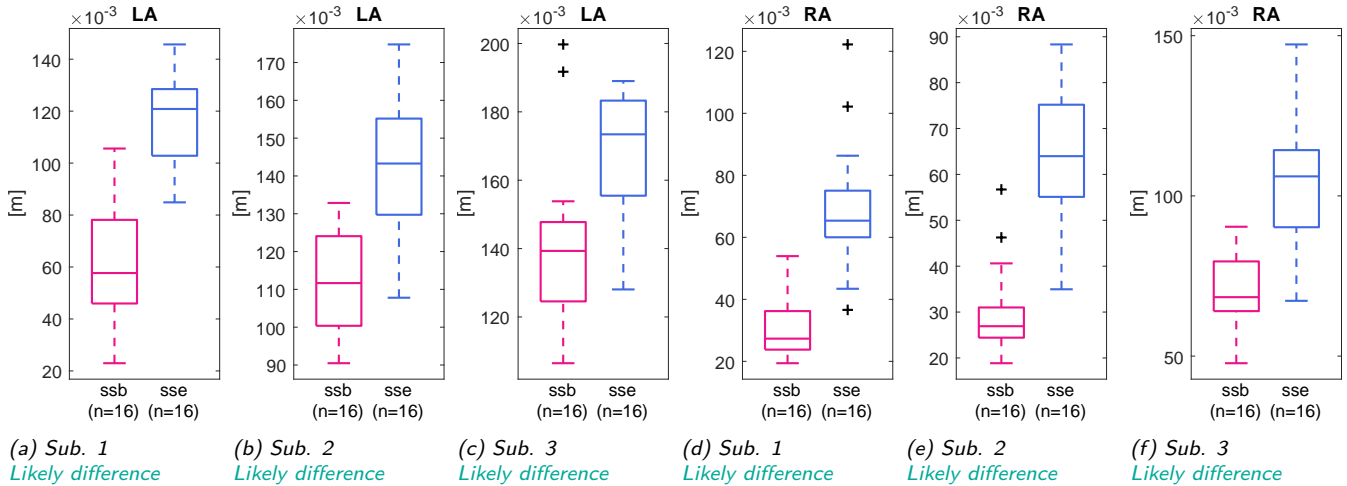


Figure 10.12: CoP Y rise from 80% to 100% of stance phase, comparison 4. *ssb* contains all steady state long steps from both C- and D-trials; *sse* contains all short steps from both C- and D-trials. The y-axes display the difference between the value of CoP Y at 80% and 100% of stance phase. Left three figures: left foot. Right three figures: right foot.



## 10.4 Conclusions

**Question 4.** *Can the pressure pattern possibly be used to distinguish between steady state long and steady state short steps, when the difference in step length is less extreme?*

Steady states		L			R			Likely difference for all three subjects?	
Parameter	Metric \ Subject	1	2	3	1	2	3	L	R
Fz	Timing of peak value	-	-	-	ld	ld	ls	-	no
	Value of peak	-	-	-	ld	ld	ld	-	yes
CoP X	Sum of rises	-	-	-	ld	ld	ld	-	yes
	Value at 0%	-	-	-	ls	ld	ls	-	no
CoP Y	Rise peak 1-2	-	-	-	ls	ld	ls	-	no
	Value at 0%	ld	ld	ld	ls	ld	ld	yes	no
	Rise 20-80%	ld	ld	ld	ld	ld	ld	yes	yes
	Rise 80-100%	ld	ld	ld	ld	ld	ld	yes	yes

Table 10.1: Summary of the box plots presented in this chapter. *ld* = likely different, *ls* = likely similar. Likely different means that there is likely a difference in this metric between steady state long steps and steady state short steps, for this subject. Likely similar means that there is probably no such difference. If there is a likely difference for all three subjects for a certain metric (L or R foot are considered separately), this is indicated in the rightmost columns.

Table 10.1, which summarizes the metrics discussed in this chapter like in previous chapters, answers the research question for this chapter. **Yes, the pressure pattern can be used to distinguish between steady state long and steady state short steps, when the difference in step length is moderate.** All metrics identified in chapter 7 show an effect of step size in the current comparison as well. However, only the Fz peak value and CoP X sum of rises for the right foot, CoP Y value at 0% for the left foot and CoP Y rise 20-80% and CoP Y rise 80-100% for both feet, show a likely difference for all three subjects.

# Chapter 11

## Comparing the extreme to the moderate track

Finally, we will have a look at how the A- and B-trials differ from the C- and D-trials. In the C- and D-trials, the long steps are less long than in the A- and B-trials (110cm vs. 130cm swing) and the short steps are less short (60cm vs. 40cm swing). The transition steps, however, are of the same length; 85cm swing. The actual 85cm-transition step takes place during the stance phase of the left foot; therefore this chapter will only consider the left feet. The research question for this chapter is:

**Question 5.** *Does the pressure pattern of the transition step depend on the length of the steps before/after it?*

- ⇒ Is there a difference in pressure pattern between transition steps from extremely long to extremely short steps, and moderately long to moderately short steps?
- ⇒ Is there a difference in pressure pattern between transition steps from extremely short to extremely long steps, and moderately short to moderately long steps?
- ⇒ Is there a difference in pressure pattern between extreme/moderate long steps?
- ⇒ Is there a difference in pressure pattern between extreme/moderate short steps?

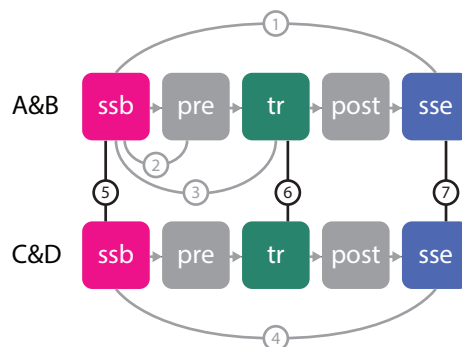


Figure 11.1: In comparisons 5, 6 and 7 three step groups from the A&B trials are compared to the same step groups from the C&D trials.

## 11.1 Comparison 6

### 11.1.1 Comparing the transition steps from A- and C-trials

See images (d) for Fz, (e) for CoP X and (f) for CoP Y of figure 11.2 (subject 1). Similar images for subjects 2 and 3 can be found in Appendix C C.1 (subject 2) and C.2 (subject 3).

**Fz** No notable difference for all three subjects.

**CoP X** Higher value at start of stance phase of A-trial for all three subjects. Higher value at end of stance phase of A-trials for subjects 2 and 3.

**CoP Y** No notable difference for subjects 1 and 3. Slightly higher values in second half of stance phase for subject 2 in C-trials.

### 11.1.2 Comparing the transition steps from B- and D-trials

See images (g) for Fz, (h) for CoP X and (i) for CoP Y of figures 11.2 (subject 1), C.1 (subject 2) and C.2 (subject 3).

**Fz** No notable difference for all three subjects.

**CoP X** Higher values throughout stance phase in B-trials for subjects 1 and 2. No discernible difference for subject 3.

**CoP Y** Higher values throughout stance phase in B-trials for all three subjects.

## 11.2 Comparisons 5 and 7

### 11.2.1 Comparing the moderately to extremely long steps

See images (a) for Fz, (b) for CoP X and (c) for CoP Y of figures 11.2 (subject 1), C.1 (subject 2) and C.2 (subject 3).

**Fz** No notable difference for all three subjects.

**CoP X** Higher values at start of stance phase in extreme trials for subjects 1 and 3. No discernible difference for subject 2.

**CoP Y** No notable differences for all three subjects.

### 11.2.2 Comparing the moderately to extremely short steps

See images (j) for Fz, (k) for CoP X and (l) for CoP Y of figures 11.2 (subject 1), C.1 (subject 2) and C.2 (subject 3).

**Fz** No notable difference for all three subjects.

**CoP X** Higher value at start of stance phase in extreme trials for subjects 1 and 3. Higher values throughout stance phase of extreme trials for subject 2.

**CoP Y** No notable differences for all three subjects.

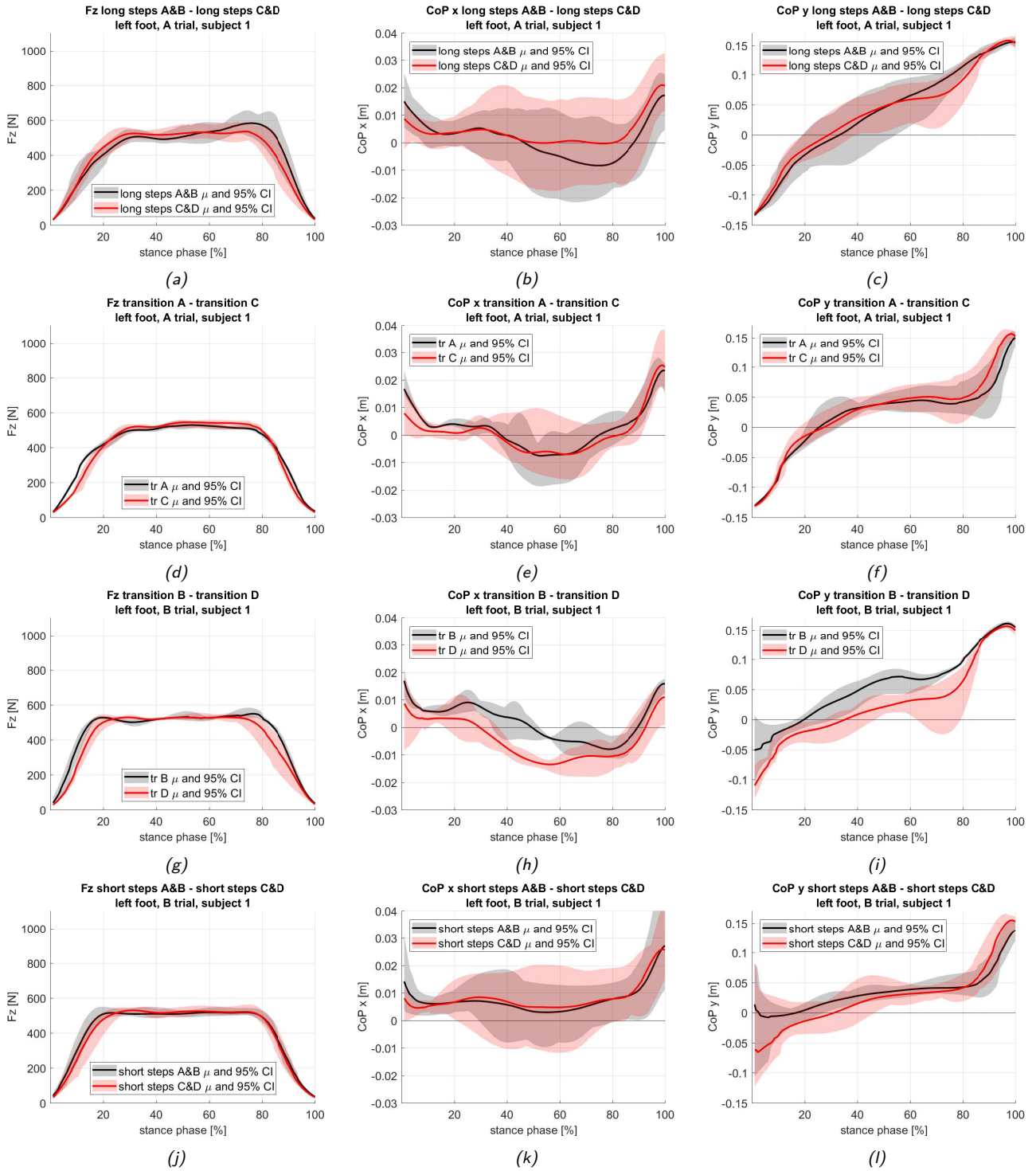


Figure 11.2: The three parameters  $F_z$ ,  $CoP_x$  and  $CoP_y$ , comparisons 5, 6 and 7, subject 1, left foot. Black: A- and/or B-trials. Red: C- and/or D-trials. Top row: steady state long steps from A&B compared to steady state long steps from C&D. Second row: transition A compared to transition C. Third row: transition B compared to transition D. Bottom row: steady state short steps from A&B compared to steady state short steps from C&D. From left to right:  $F_z$ ,  $CoP_x$ ,  $CoP_y$ . Solid lines: mean values. Shaded areas: 95% CI.

### 11.3 Conclusions

**Question 5.** *Does the pressure pattern of the transition step depend on the length of the steps before/after it?*

Overall, the differences between the extreme (A and B) and moderate (C and D) trials are very small. One thing that stands out, is that in the extreme trials, the CoP X seems to incline towards higher values. Apparently subjects sway more to the side when the steps they take are of unusual size. Another thing that stands out, is that in the B-trial transition steps, the CoP Y is consistently higher for all three subjects than in the D-trial transition steps. This possible difference cannot be seen when comparing the extremely long/short steps to the moderately long/short steps, respectively. This is an interesting observation, since it might indicate that the pressure pattern recorded during a transition step depends on the length of the steps that come before or after the transition step. A similar potential difference between the transition steps in A- and C-trials cannot be seen. So, to answer the four sub-questions specifically:

↳ *Is there a difference in pressure pattern between transition steps from A- and C-trials?*  
Hardly. CoP X at 0% of stance phase is slightly higher in A-trial transition steps than in C-trial transition steps.

↳ *Is there a difference in pressure pattern between transition steps from B- and D-trials?*  
Potentially. For all three subjects there is a notable difference in CoP Y. Also, some difference in CoP X pattern for two of the three subjects.

↳ *Is there a difference in pressure pattern between extreme/moderate long steps?*  
Hardly. CoP X at 0% of stance phase is slightly higher in A-trial transition steps than in C-trial transition steps, for two of the three subjects.

↳ *Is there a difference in pressure pattern between extreme/moderate short steps?*  
Hardly. In the extremely short steps, CoP X inclines more outward than in the moderately short steps.

To answer the main research question of this chapter:

**When transitioning from short to long steps, the length of steps before/after the transition step may have an influence on the pressure pattern of the transition step. When transitioning from long to short steps, the length of steps before/after the transition step does not seem to be of influence.**

**Part IV**  
**Concluding**

# Chapter 12

## Conclusions

The main research question was:

**Main question.** *Is there potential in using the pressure pattern to intuitively control step length in semi-autonomous exoskeletons?*

This question cannot be answered with a definite yes or no yet. There is some potential in intuitively controlling exoskeleton step length using the pressure pattern in the foot soles. The pressure pattern changes with step length for healthy subjects walking with crutches. However, the pressure pattern does not change before the actual change in step length takes place, and may therefore simply be the effect of the change in base of support (BoS) formed by the feet excluding crutches (fBoS), which changes with step length. There are small changes in pressure pattern during the transition steps; these may also be due to the altering fBoS. In other words: different step lengths can be associated with different pressure patterns. It is unknown if these changes in pressure pattern are merely the result of the changes in fBoS, and can only occur if and when the fBoS changes - or if the pressure pattern changes could occur independently of a changing fBoS. With this in mind, the metrics derived from the CoP X are very interesting. When step length changes, the fBoS formed by the feet changes along with it - but only in the y-direction. Any effects on the metrics based on CoP X are therefore less likely to be solely the effect of the altered BoS. Questions such as this will be discussed in the next and final chapter.

Presently, the conclusions drawn from chapters 7 to 11 will be summarized, highlighting how these sub-conclusions contribute to the main conclusion.

**Question 1.** *Can the pressure pattern possibly be used to distinguish extreme steady state long from extreme steady state short steps?*

Yes, this is possible. Eight metrics were identified that show likely differences between the steady state long and steady state short steps for all three subjects. This means that when the difference between a long and short step is quite large, the pressure pattern can be used to differentiate between the two. It can be concluded that even when people walk using crutches, there is a correlation between step length and pressure pattern recorded in the foot soles. This indicates that using this pressure pattern as a signal to control step length in exoskeletons has potential.

**Question 2.** *Can the pressure pattern possibly be used to identify a change in step length before it happens?*

No, this is not possible. No metrics were identified that show a likely difference between steady state steps and pre-transition steps for all three subjects. This conclusion decreases confidence in the potential of using the pressure pattern as an input to control

step length. Effects in the pressure patterns are not identified until step length - and thus the BoS - have started changing. It remains unknown if such pressure pattern alterations *could* even occur without the altered step length/BoS. It is therefore unsure if a paraplegic walking in an exoskeleton could produce such pressure pattern changes to control step length.

**Question 3.** *Can the pressure pattern possibly be used to identify a change in step length while it is happening?*

Yes, this is possible. Three metrics were identified that show a likely difference between the transition steps and the ssb steps for all three subjects in the B-trials; two of these indicated a difference in the A-trials. These metrics only showed a difference in the data of the subjects' left feet. The actual transition (swing leg makes a swing of intermediate length) takes place during this left stance phase, so again, it is unsure whether this effect on the pressure pattern could occur without (i.e. prior to) the altered step length. This doubt is enlarged by the observation that in A-trials, both metrics that show a likely difference, are based on the CoP Y. In B-trials, however, a CoP X-based metric shows a likely difference.

**Question 4.** *Can the pressure pattern possibly be used to distinguish between steady state long and steady state short steps, when the difference in step length is less extreme?*

Yes, the pressure pattern can be used to distinguish between steady state long and steady state short steps, when the difference in step length is moderate. Five of the metrics identified in the extreme trials (see question 1) also show some effect of step size on pressure pattern in the moderate trials. This observation boosts confidence in the idea that these metrics can distinguish between step sizes, and are not merely the result of an unnatural gait due to prescribed steps of exaggerated lengths.

**Question 5.** *Does the pressure pattern of the transition step depend on the length of the steps before/after it?*

When transitioning from short to long steps, the length of steps before/after the transition step may have an influence on the pressure pattern of the transition step. When transitioning from long to short steps, the length of steps before/after the transition step does not seem to be of influence. Since step length before/after the transition step hardly influences the pressure pattern in the transition step, it seems that the pressure pattern is mainly the result of the actual step length as it is at the current time instance: in all trials the transition swings are 85cm. Indeed, this seems the most likely conclusion to be drawn here; any differences between the transition steps from both extreme/moderate trials, are very subtle and likely not significant.



# Chapter 13

## Discussion

At the start of this project it was established that paraplegic exoskeleton users should be able to have more control over walking parameters and that this control should be more intuitive. In order to come a little closer to this goal - the "dot on the horizon" from figure 2.1 - the study described in this report was conceived. It was concluded that the pressure pattern can be used to differentiate between long and short steps, while there are no signs that the pressure pattern changes before the actual step length change has taken place. In this chapter, it will be discussed how the limitations of and assumptions made in this study color the conclusions drawn in the previous chapter; what improvements could have been made to this study with the knowledge of hindsight; and what the next steps towards that dot on the horizon might be.

### 13.1 Assumptions

In short, the most important assumptions that were made (see section 3.1):

- A paraplegic walking in an exoskeleton can manipulate the pressure pattern while walking.
- If pressure pattern variations occur in relation to varying step length during healthy gait, this means that manipulating the pressure pattern to control step length in exoskeleton gait is an intuitive control method.
- Changing the pressure pattern remains an intuitive manipulation, even if a person cannot use their leg muscles.

Before engineers can begin to implement the proposed intuitive control strategy, the assumptions listed above will have to be validated. Due to time and technical constraints, it was not feasible to perform experiments with paraplegic subjects in this study. It also made more sense to first find out how the pressure pattern relates to step length changes in healthy walking: if no effects at all had been found, it would be useless to continue validating the above assumptions.

### 13.2 Experiment evaluation

Overall, the experiments went well. Subjects reported enjoying participating in the study; traversing the tracks correctly felt like a fun, challenging game to them. Most limitations that occurred during the experiments had to do with hardware issues:

### 13.2.1 Tethered sensors

The sensors were not wireless. The cable bundle that ran from subject to the researcher's laptop, was a big hassle to handle. The researcher had to walk alongside the subject to manage the cables, while also carrying the laptop and making sure everything ran smoothly. This way, it was sometimes hard to keep proper track of missteps and mistrials. For any future studies, wireless sensors are greatly recommended.

### 13.2.2 Rigidity of the foot plates

The choice to make the upper side of the wearable sensor shoes one rigid aluminum plate, was made because in the design of the MARCH exoskeleton at the time, the foot plates were also rigid. Unfortunately, the rigid sensor shoes caused problems in two ways. Firstly, it became harder for subjects to walk in a natural way. During normal natural gait, the foot bends and does not stay rigid. Secondly, it is probable that the rigid design of the foot plate, contributed to sensor overloading, which caused two subsequent sensors to malfunction and fail; see next paragraph. Since later MARCH exoskeletons designs feature flexible foot plates, it is highly recommended that any future studies also involve flexible sensor shoes.

### 13.2.3 Sensor failure

Twice the sensor that was in the front of the right sensor shoe, failed and could not be repaired. This was most likely due to overloading. Forces never came close to overload values (e.g. overload value for  $F_z = 4000N * 200\%$ ). Moments around the x- and y-axes however, did reach their overload values of  $35Nm * 200\%$ . These high torques occurred at 100% of stance phase. At these instances, the rear of the sensor shoe was lifted off the ground and the entire foot rotated around the front edge. This caused all forces to concentrate on this front edge; combined with the relatively high push-off forces exerted on the toes at this point, this resulted in great torques, especially around the x-axis. These torques had not been anticipated. In possible future experiments, these high moment forces could be avoided by making the foot plate flexible; this could already be achieved by creating one hinge axis that allows for rotation, as was done in the bottom plates.

## 13.3 Limitations

Due to the sensors failing, it was not possible to continue the experiments after testing four subjects. It was later found that during the fourth subject's experiment, the front right sensor had already failed to record viable data. This disrupted the original plan of testing with twelve subjects. For this reason, the scope of this study changed: it was no longer possible to perform statistical analyses on only three subjects' data. The scope of the study was therefore adjusted, making this an exploratory study.

From the assumptions and experimental problems described previously, a number of limitations follow. Firstly, there is the small number of participants that makes it impossible to say anything regarding statistical significance of the results. It must be stressed that this was an exploratory study, featuring preliminary experiments. Secondly, healthy subjects participated. This was a logical first step since we wanted to find out more about the pressure pattern in natural walking. Still, the assumptions listed in section 3.1 could not be validated with healthy subjects, but we knew this from the start. The lack of results demonstrating any predictive quality of the pressure pattern do make it extra important to justify especially the first assumption. If the current study had discovered any changes in pressure pattern prior to any actual changes in step length, the first assumption would

already have been partially ratified. Unfortunately this is not the case.

Thirdly, the crutches were not included in this study. After pilot experiments it was decided to exclude force/torque data from the crutches, which would have little value without knowledge about the position and orientation of the crutches. This was a sensible choice, but it does preclude information that could complete the picture of pressure distribution about the complete BoS.

## 13.4 The outcome

### 13.4.1 Relating the results to literature

The general shape of the Fz-graphs resembles similar graphs found in literature (Grundy, Tosh, McLeish, & Smidt, 1975; Chevalier, Hodgins, & Chockalingam, 2010; Hayafune, Hayafune, & Jacob, 1999); although in literature the Fz-pattern usually displays two clear peaks, such as is the case in figure 6.2, the bottom-center graph (green line). These two peaks are not so clearly present in most of the other Fz-graphs in this study's results. The progression of the CoP in y-direction also seems to concur with literature; the CoP Y moves forward rapidly in the beginning and end of the stance phase, moving slower in the middle of stance phase (Grundy et al., 1975; Jamshidi et al., 2010). It is harder to relate the CoP X findings from this study to those found in literature, since there is so much variation in the x-coordinate patterns in this study. Interestingly though, we see that towards the end of the stance phase, the CoP X usually moves outward in the current study. Grundy et al. (1975), Jamshidi et al. (2010) and Lugade and Kaufman (2014) show that in barefoot walking, the CoP X moves inward before toe-off; but when wearing a shoe it moves outward (Grundy et al., 1975), which concurs with the present results. In short, while results from the current study are not astonishingly strange compared to CoP trajectories found in literature, they do differ quite a bit. Several reasons can be thought of that can explain this: the rigid sensor shoes, the use of crutches, the prescribed step frequency, step lengths and step widths.

### 13.4.2 Interpreting the results

The outcome of this study is quite positive regarding the relationship between step length and pressure pattern. However, the outcomes regarding the predictive potential of pressure pattern for step length do not give positive results. All in all, it seems that the pressure pattern is highly dependent on the *actual step length as it is at this moment*, and not much influenced by intention or transition. There might be two/three metrics that seem to be able to indicate a change in step length while it is happening, but two of these metrics (CoP Y rise from 20-80% and 80-100% of stance phase) might well be the direct result of the difference in how far the weight is shifted forward due to the actual change in step length and with that BoS. Also, the CoP Y at 0% of stance phase hardly depends on the step group in comparison 3, while it does depend on step group in comparison 1. This makes sense, especially if we conclude that it is principally the current BoS that influences the pressure pattern: at 0% of transition step stance phase, the fBoS is still the same as in the pre and ssb steps. Still, there might be other reasons for the relative lack of metrics identified based on CoP X. The employed crutch strategy makes the BoS very wide in x-direction. Likely (though this has not been recorded) this width does not vary with step length. This wide and consistent BoS might have limited variations in oscillations along the x-axis. Of course, variations in fBoS along the x-axis were also checked by prescribing foot placement in y- as well as x-direction.

## 13.5 Future visions

Even though variations in the pressure pattern cannot predict step length changes, they are apparently the natural result of changes in step length. Thus, they might still constitute a control signal that can be easily taught and trained. The major advantages of such a control strategy remain: no buttons or dials will be required; it can easily and invisibly be incorporated into the exoskeleton foot plates; the required sensors will also be valuable in automatic stability control, which is another current hot topic in exoskeleton design. When a paraplegic is walking in an exoskeleton, (s)he has to be very embroiled in shifting their weight anyway. By further exploiting this focus point, it will be avoided that the user has to use other cognitive resources, such as would be the case with voice or touch control.

That is the ultimate future vision for human-exoskeleton interaction: that it does not even feel like interacting with a robot, but like natural walking. This study has showed that sensors in the foot soles can provide a wealth of information. And while no single metric has been found that can reliably predict user intention regarding step length, it is not hard to imagine a multidimensional predictor that can combine all this pressure pattern information to draw conclusions about user intention. Especially if this information would be augmented with data from a torso IMU (inertial measurement unit), force/torque sensors in the crutches and IMUs in the crutches, IMUs on the arms, etc. Strausser and Kazerooni (2010) used arm angle to control step length: such strategies may benefit from adding foot sole pressure pattern data. In combining such a multitude of potential information and making it work for us, machine learning might play a part. This might especially be so since the differences between step groups found in this study, are not always in the same direction for all subjects. This might mean that the robot would have to learn each user's intention from their movements individually. And why stop at controlling step length? Intuitively controlling step rhythm is already a likely development for the near future: several authors have already gotten positive results in this field (Jang et al., 2010; Suzuki et al., 2005; Strausser & Kazerooni, 2010; Kolakowsky-Hayner, 2013). At Project MARCH students are developing the MARCH IV, which will feature extra hip actuators that will allow medio-lateral motion of the legs, as well as ankle actuators that will enable powered foot motion. These new degrees of freedom will require novel control methods and more information about floor reaction forces and the CoP to maintain balance (the MARCH IV will also feature insole pressure sensors). These two new demands align perfectly with what pressure pattern control can offer. Furthermore, information about the pressure pattern can provide the perfect input for a feedback system designed to give the paraplegic user more feedback about the state of their lower body. Since paraplegic users cannot feel their lower limbs such feedback could greatly improve their ability to balance and their self-confidence while walking in an exoskeleton.

## 13.6 Future work

As concluded previously, the outcomes regarding the predictive potential of pressure pattern for step length do not give positive results. However, this does not mean that the metrics identified in comparison 1 (chapter 7) might not still be able to play a role in intuitive step length control. It must not be disregarded that a paraplegic in an exoskeleton cannot directly adjust the fBoS of the feet (excluding crutches) anyway. It might well be that the paraplegic - who has experienced healthy walking in the past - still intuitively associates the adjustments in weight distribution corresponding to the changes in pressure pattern observed in this study, with the matching change in step length. If this is the case, such pressure pattern manipulations would still be an intuitive control method that is easy to learn and train. Therefore, before deciding to use or discard pressure pattern as a control signal, more research is definitely necessary. Moreover, it might be that if these

experiments were repeated with more subjects, any (predictive) effects that remained hidden due to the small sample group in this study, will emerge. To continue the current line of research, the following steps are proposed:

- First, the experiments described in this study, will have to be repeated with more subjects, in order to produce a solid statistical base for the drawn conclusions. Also, as was mentioned above, results from a larger subject pool might reveal hitherto hidden effects.
- Then, the assumptions listed in section 3.1, will have to be tested. Most importantly, they will have to be tested with paraplegic users in an active semi-autonomous exoskeleton.
- If at this point, this still seems a promising design option, the system should be properly designed and implemented in a prototype for further testing.

## 13.7 Final conclusion

Metaphorically speaking, in this study, we have taken some interesting steps in the photo in figure 2.1; steps that invite us to walk a bit further towards that dot! This project has demonstrated that the pressure pattern in the foot sole can supply us with a wealth of information; on step length for sure, but perhaps about other aspects of the user's state and wishes as well. It is a research direction that is well worth exploring more deeply!

# Gratitude

Tijdens dit afstudeerproject ben ik obstakels en omwegen tegengekomen die het me niet makkelijk hebben gemaakt. Het is een lang en veelal slopend proces geweest - waar ik gelukkig veel van heb kunnen leren en ook vaak veel plezier in heb gehad. Ik wil hier graag enkele mensen bedanken zonder wie ik dit project, door alle moeilijkheden heen, nooit had kunnen afronden.

Allereerst mijn begeleider, David Abbink. Bedankt voor al je geduld, je opbouwende kritiek - waaruit altijd je vertrouwen in mijn kunnen sprak - en je optimisme.

Het team van MARCH I: ongelooflijk wat jullie vanuit niets hebben opgebouwd! Dank voor de leuke en gezellige samenwerking.

Mijn lieve huisgenoten, vier rotsen in de branding (en een flamingo) die er dagelijks voor me zijn geweest. Jullie zijn fantastisch.

Vrienden en vriendinnen, eigenlijk te veel om bij naam te noemen (wat prijs ik mijzelf gelukkig!), maar Anna en Bente pik ik er toch even uit. Bedankt voor jullie vriendschap die me door heel wat moeilijke momenten heeft gesleept. Ik kan me geen betere manier voorstellen om het einde van deze fase te vieren dan door met jullie op reis te gaan!

Julie, ik ben ontzettend trots en dankbaar om samen met jou Opt Medical te bestieren. Wat ben je toch een bikkelaar; dankjewel voor hoe je dingen zonder mij keihard hebt doorgezet.

Leon en Marie, bedankt voor de ontspannende weekenden in Eindhoven. Joric en Michelle, bedankt voor het proeflezen van delen van dit verslag.

En bovenal: papa en mama. Zonder jullie had ik dit punt op zoveel manieren niet kunnen bereiken. Mijn dank aan jullie is eindeloos.

# Appendices

## **Appendix A**

### **Protocol sheets**



## Experimental protocol

## Subject code:

		1. Explain procedure to subject:
		a. Je gaat hier straks een paar keer heen en weer lopen.
		b. Tijdens het lopen gebruik je krukken en draag je speciale zolen. Hierin zitten sensoren. Doe geen rare dingen met de zolen: de sensoren kunnen stuk.
		c. Een metronoom zal het tempo aangeven. Wanneer de metronoom wegvalt, loop je door in een logisch tempo dat goed voelt. Voordat je begint met lopen, tellen we af: 1-2-1-2. Begin altijd te lopen met rechts.
		d. Op de grond staat aangegeven waar je je voeten steeds moet neerzetten.
		e. Als je misstapt, zal het klittenband elkaar raken; we horen dan dat je misstapt en we beginnen opnieuw.
		2. Set crutches to right length.
		3. Demonstrate how to use the crutches.
		4. Give subject a moment to get used to using the crutches in this way.
		5. Put on the soles.
		6. Let subject walk back and forth on each of the 2 tracks a few times (2x back and forth on each track)
Step:	Time (s)	7. IN PILOTS: record comfortable step frequency, 2x for each step size.
1		
1		
2		
2		
3		
3		
4		
4		
		8. Add metronome to practice (2x back and forth on each track)
		9. Voordat je een track begint, til je LINKS 2s op en dan RECHTS 2s.
		10. When subject is comfortable with the procedure, continue.
# of steps:		11. Ask subject to walk 10m at comfortable step length with crutches. Count number of steps to calculate comfortable step length.
1:	2:	
		12. Condition A, B: 4-1, 1-4
		13. Condition C, D: 3-2, 2-3

1 = 20 cm      2 = 30 cm      3 = 55 cm      4 = 65 cm

Figure A.1: Protocol sheet used during experiments.

	1	2	3	4	5	6	7	8
<b>Trial</b>	1	2	3	4	5	6	7	8
<b>Condition</b>	65-20	20-65	65-20	20-65	65-20	20-65	65-20	20-65
A-B: 4-1, 1-4 65-20, 20-65								
<b>Trial</b>	1	2	3	4	5	6	7	8
<b>Condition</b>	55-30	30-55	55-30	30-55	55-30	30-55	55-30	30-55
C-D: 3-2, 2-3 55-30, 30-55								

Figure A.2: Progress sheet used during experiments.

## **Appendix B**

### **Results overview images subjects 1 and 3**

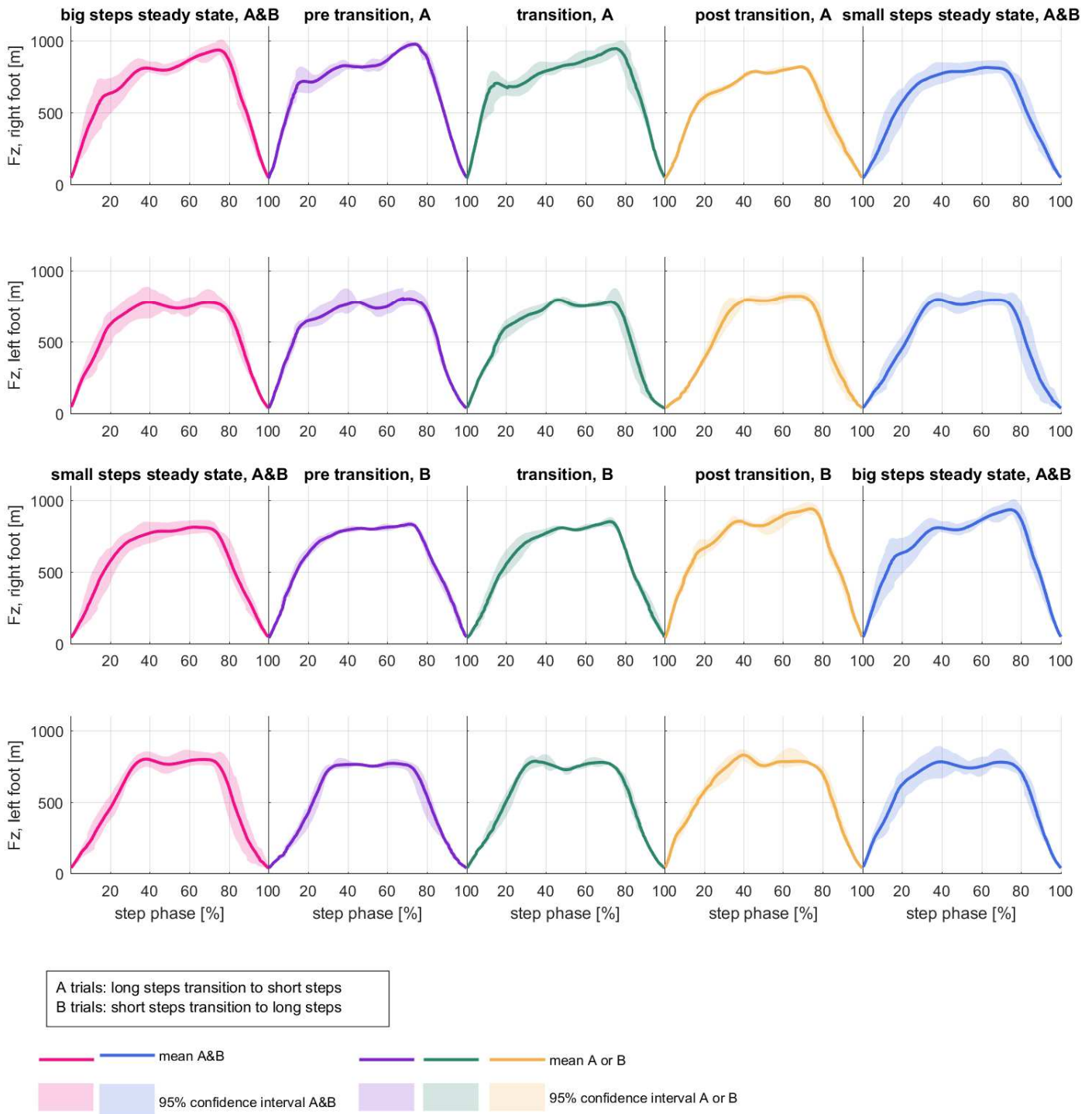


Figure B.1: Fz mean and 95% confidence interval per step group across four trials for subject 3. Different colors refer to the five step groups. Top two rows from left to right: steady state long steps (A&B), pre transition (A), transition (A), post transition (A) and steady state short steps (A&B). Bottom two rows from left to right: steady state short steps (A&B), pre transition (B), transition (B), post transition (B) and steady state long steps (A&B). First and third row from the top show left foot data, second and fourth row from the top show right foot data. X-axes show the time, expressed as percentage of stance phase. Y-axes show force in Newton.

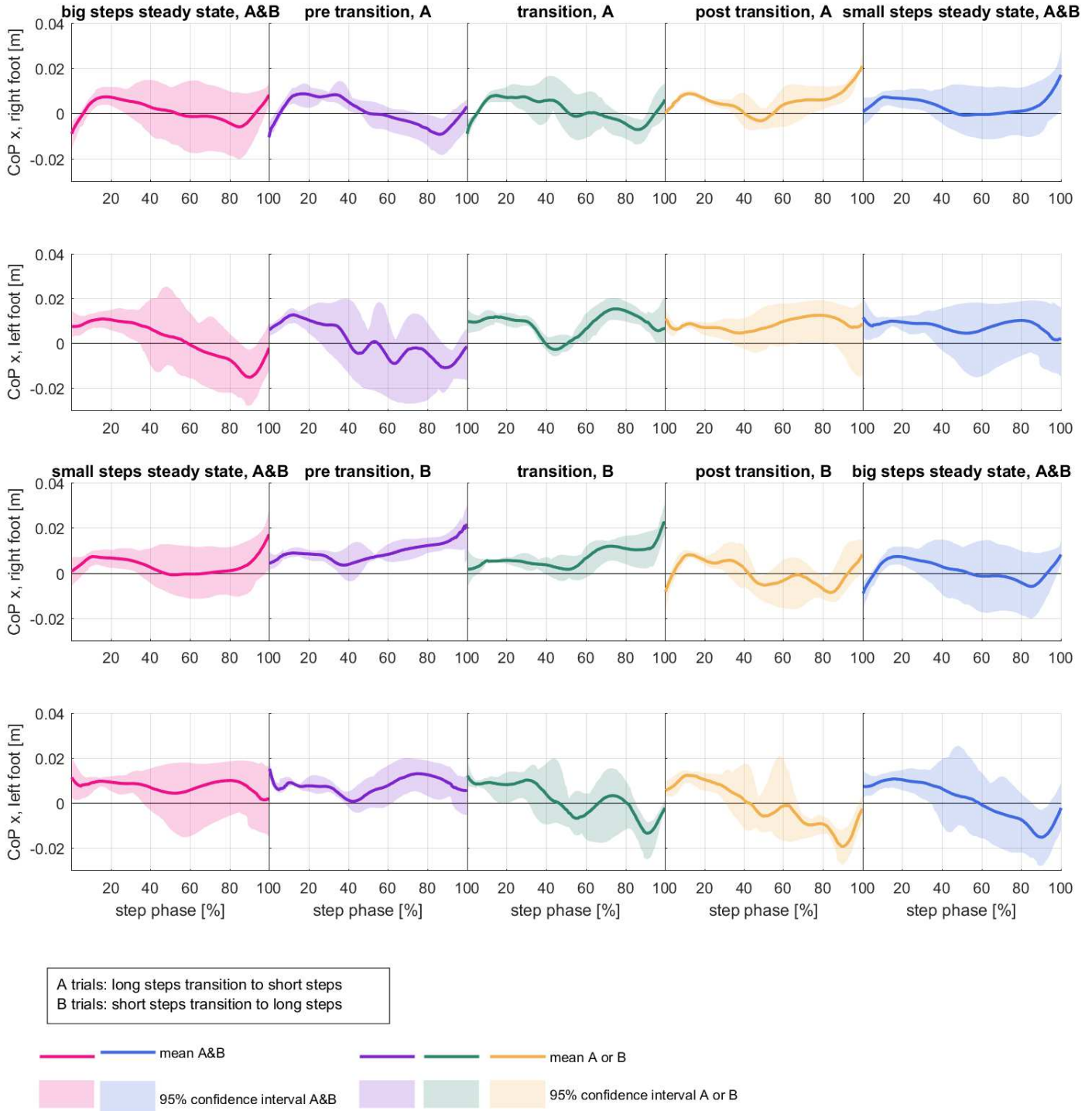


Figure B.2: CoPX mean and 95% confidence interval per step group across four trials for subject 3. Different colors refer to the five step groups. Top two rows from left to right: steady state long steps (A&B), pre transition (A), transition (A), post transition (A) and steady state short steps (A&B). Bottom two rows from left to right: steady state short steps (A&B), pre transition (B), transition (B), post transition (B) and steady state long steps (A&B). First and third row from the top show left foot data, second and fourth row from the top show right foot data. X-axes show the time, expressed as percentage of stance phase. Y-axes show force in Newton.

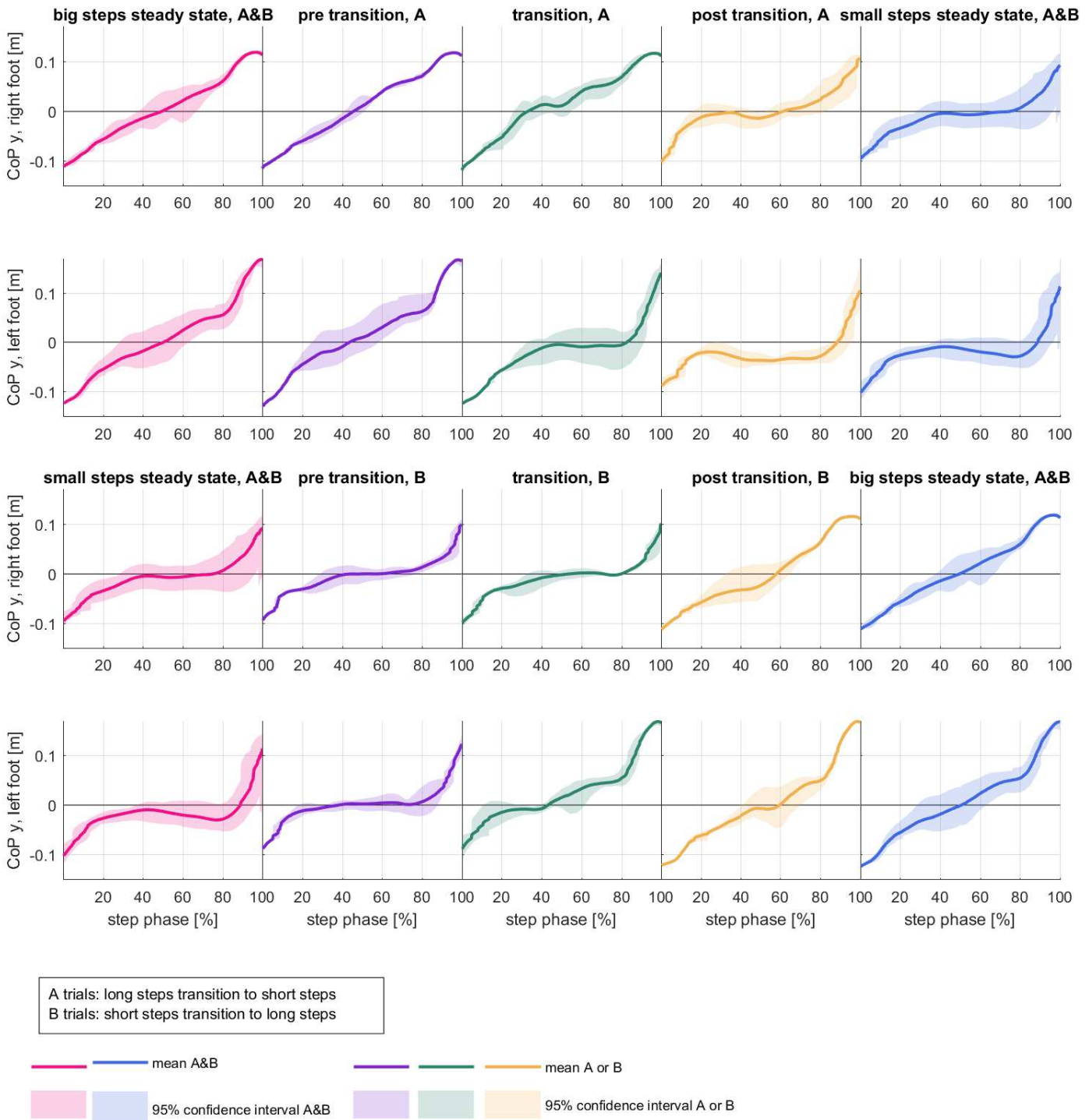


Figure B.3: CoPY mean and 95% confidence interval per step group across four trials for subject 3. Different colors refer to the five step groups. Top two rows from left to right: steady state long steps (A&B), pre transition (A), transition (A), post transition (A) and steady state short steps (A&B). Bottom two rows from left to right: steady state short steps (A&B), pre transition (B), transition (B), post transition (B) and steady state long steps (A&B). First and third row from the top show left foot data, second and fourth row from the top show right foot data. X-axes show the time, expressed as percentage of stance phase. Y-axes show force in Newton.

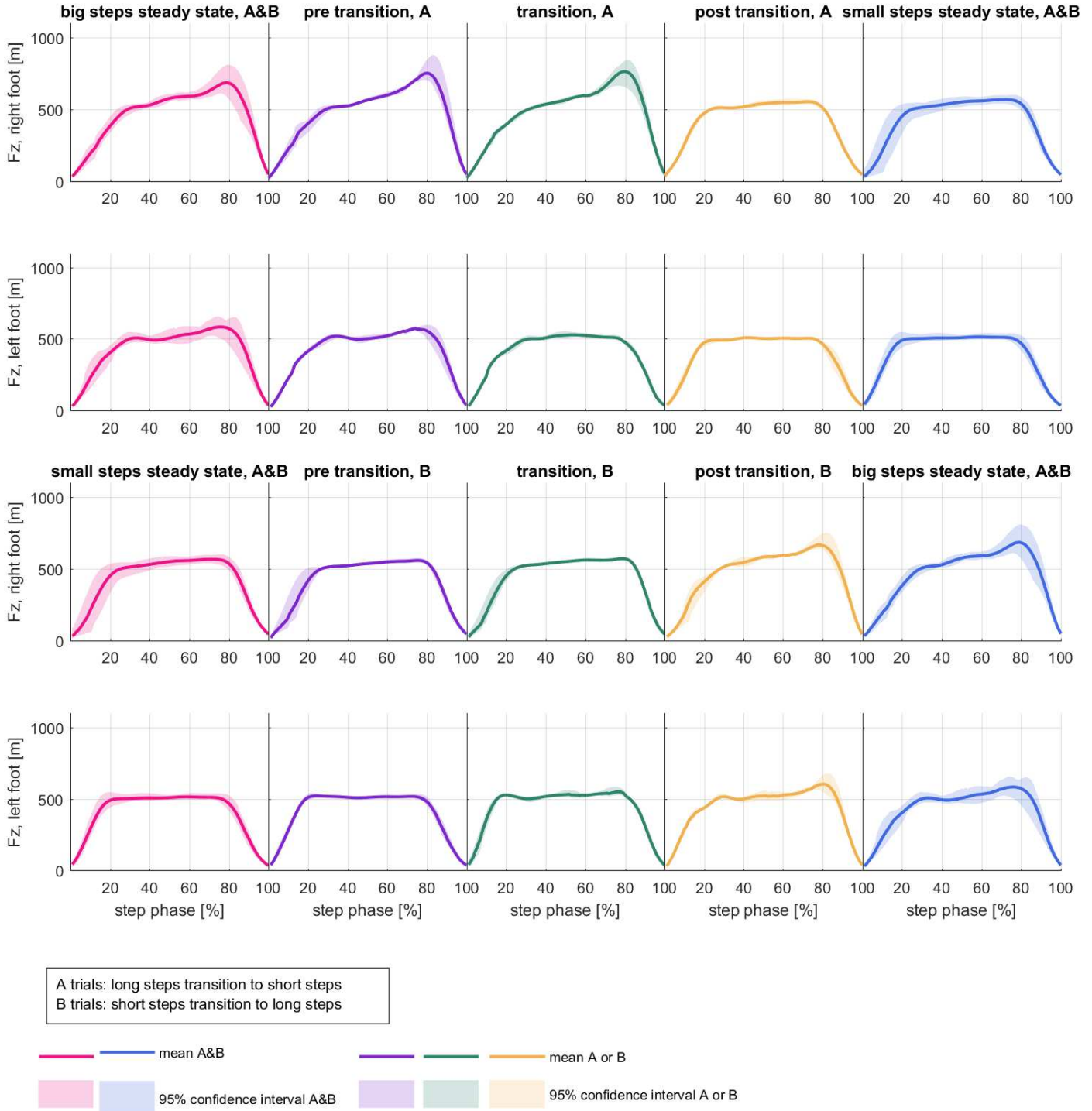


Figure B.4: Fz mean and 95% confidence interval per step group across four trials for subject 1. Different colors refer to the five step groups. Top two rows from left to right: steady state long steps (A&B), pre transition (A), transition (A), post transition (A) and steady state short steps (A&B). Bottom two rows from left to right: steady state short steps (A&B), pre transition (B), transition (B), post transition (B) and steady state long steps (A&B). First and third row from the top show left foot data, second and fourth row from the top show right foot data. X-axes show the time, expressed as percentage of stance phase. Y-axes show force in Newton.

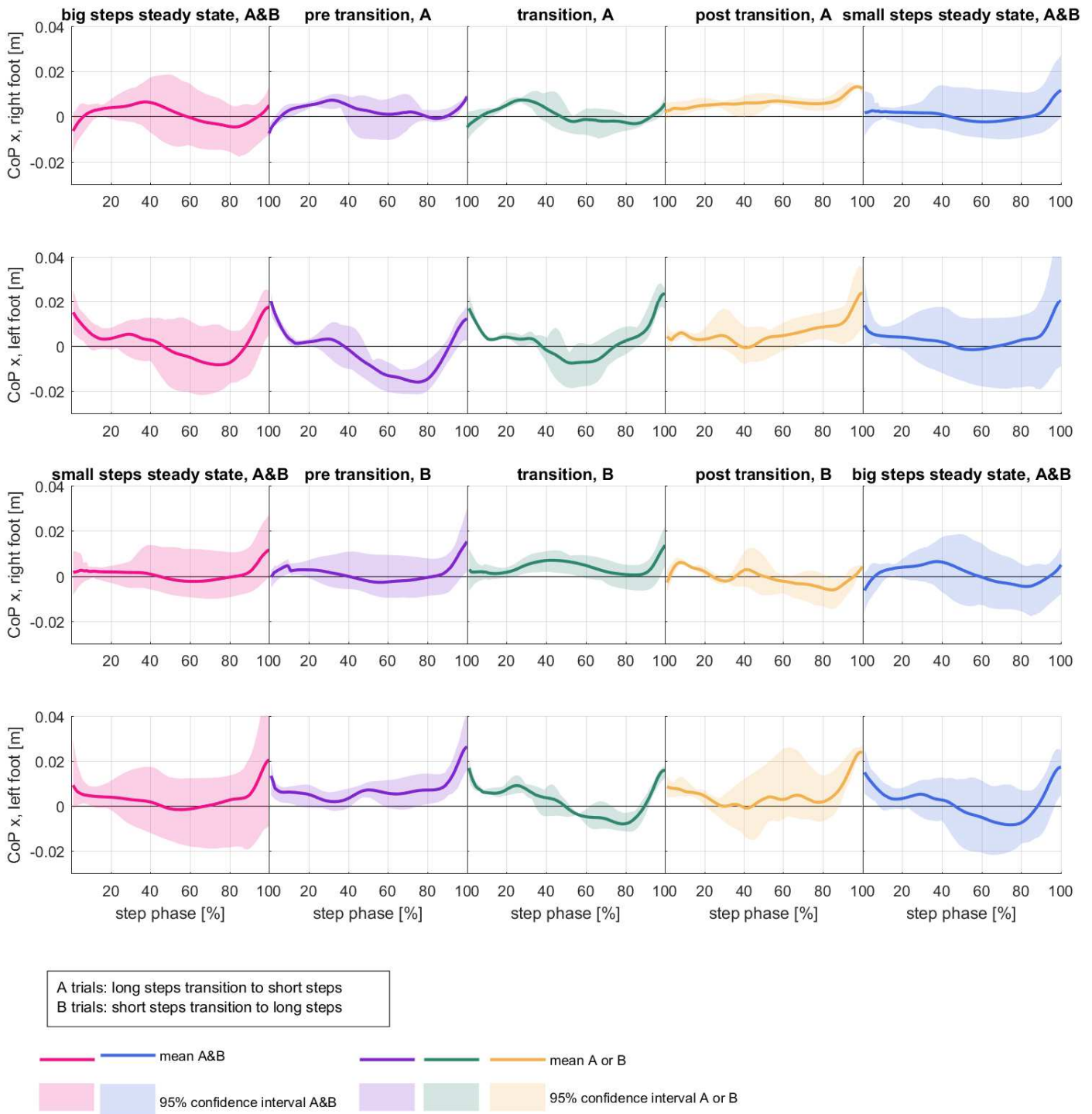


Figure B.5: CoPX mean and 95% confidence interval per step group across four trials for subject 1. Different colors refer to the five step groups. Top two rows from left to right: steady state long steps (A&B), pre transition (A), transition (A), post transition (A) and steady state short steps (A&B). Bottom two rows from left to right: steady state short steps (A&B), pre transition (B), transition (B), post transition (B) and steady state long steps (A&B). First and third row from the top show left foot data, second and fourth row from the top show right foot data. X-axes show the time, expressed as percentage of stance phase. Y-axes show force in Newton.



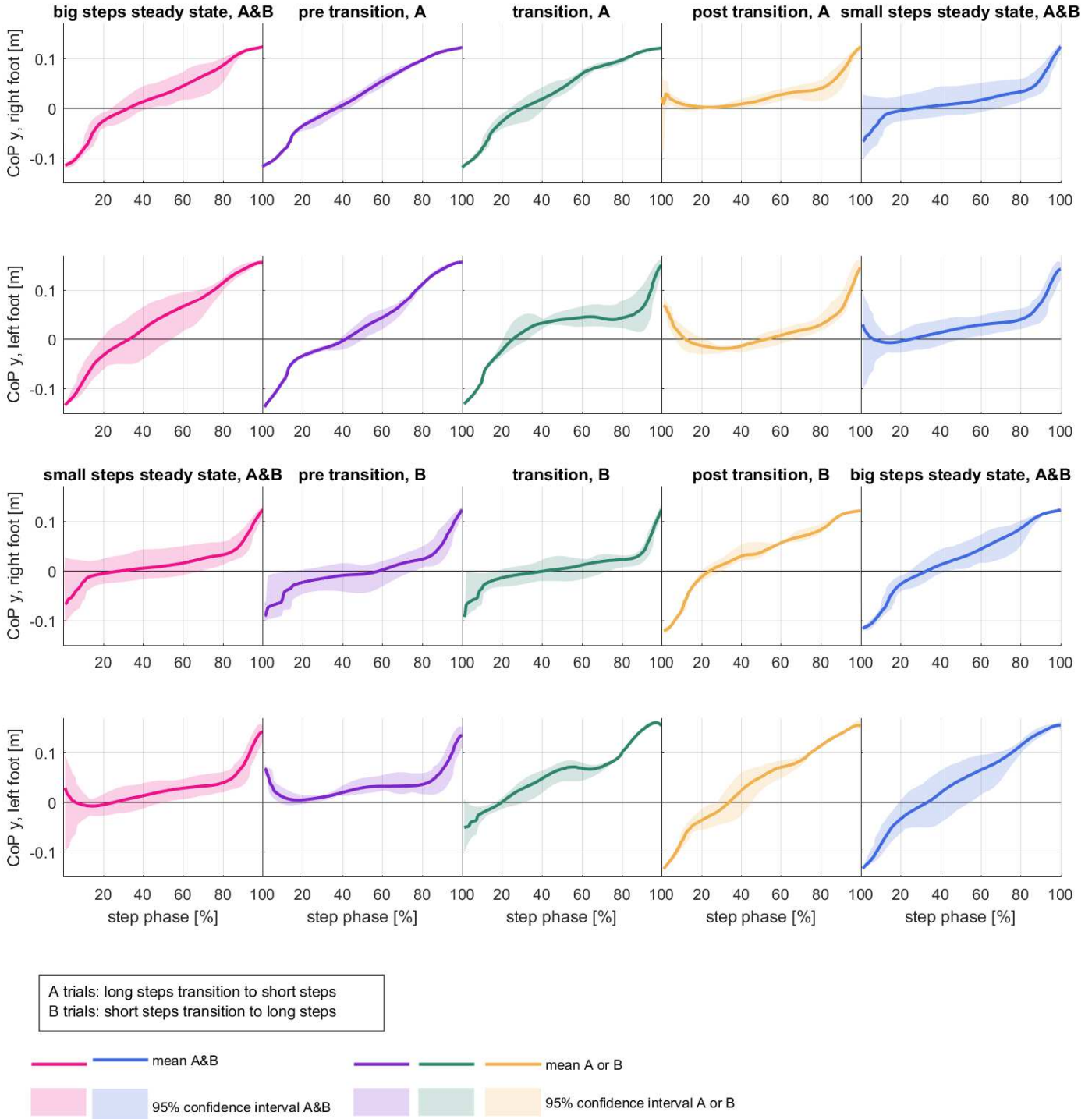


Figure B.6: CoPY mean and 95% confidence interval per step group across four trials for subject 1. Different colors refer to the five step groups. Top two rows from left to right: steady state long steps (A&B), pre transition (A), transition (A), post transition (A) and steady state short steps (A&B). Bottom two rows from left to right: steady state short steps (A&B), pre transition (B), transition (B), post transition (B) and steady state long steps (A&B). First and third row from the top show left foot data, second and fourth row from the top show right foot data. X-axes show the time, expressed as percentage of stance phase. Y-axes show force in Newton.

## **Appendix C**

### **Comparisons 5 and 7, subjects 2 and 3**

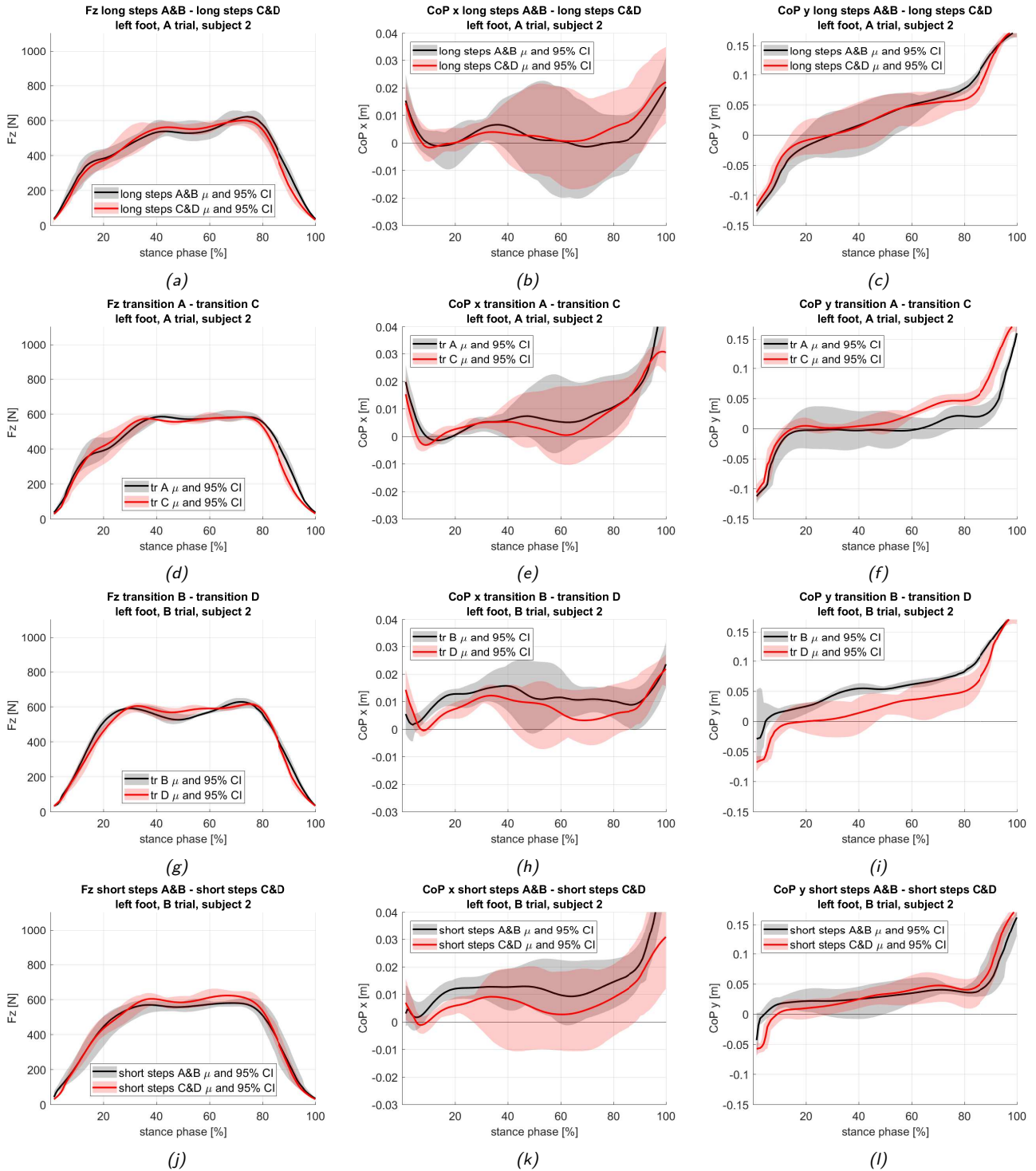


Figure C.1: The three parameters  $F_z$ ,  $CoP_x$  and  $CoP_y$ , comparisons 5, 6 and 7, subject 2, left foot. Black: A- and/or B-trials. Red: C- and/or D-trials. Top row: steady state long steps from A&B compared to steady state long steps from C&D. Second row: transition A compared to transition C. Third row: transition B compared to transition D. Bottom row: steady state short steps from A&B compared to steady state short steps from C&D. From left to right:  $F_z$ ,  $CoP_x$ ,  $CoP_y$ . Solid lines: mean values. Shaded areas: 95% CI.

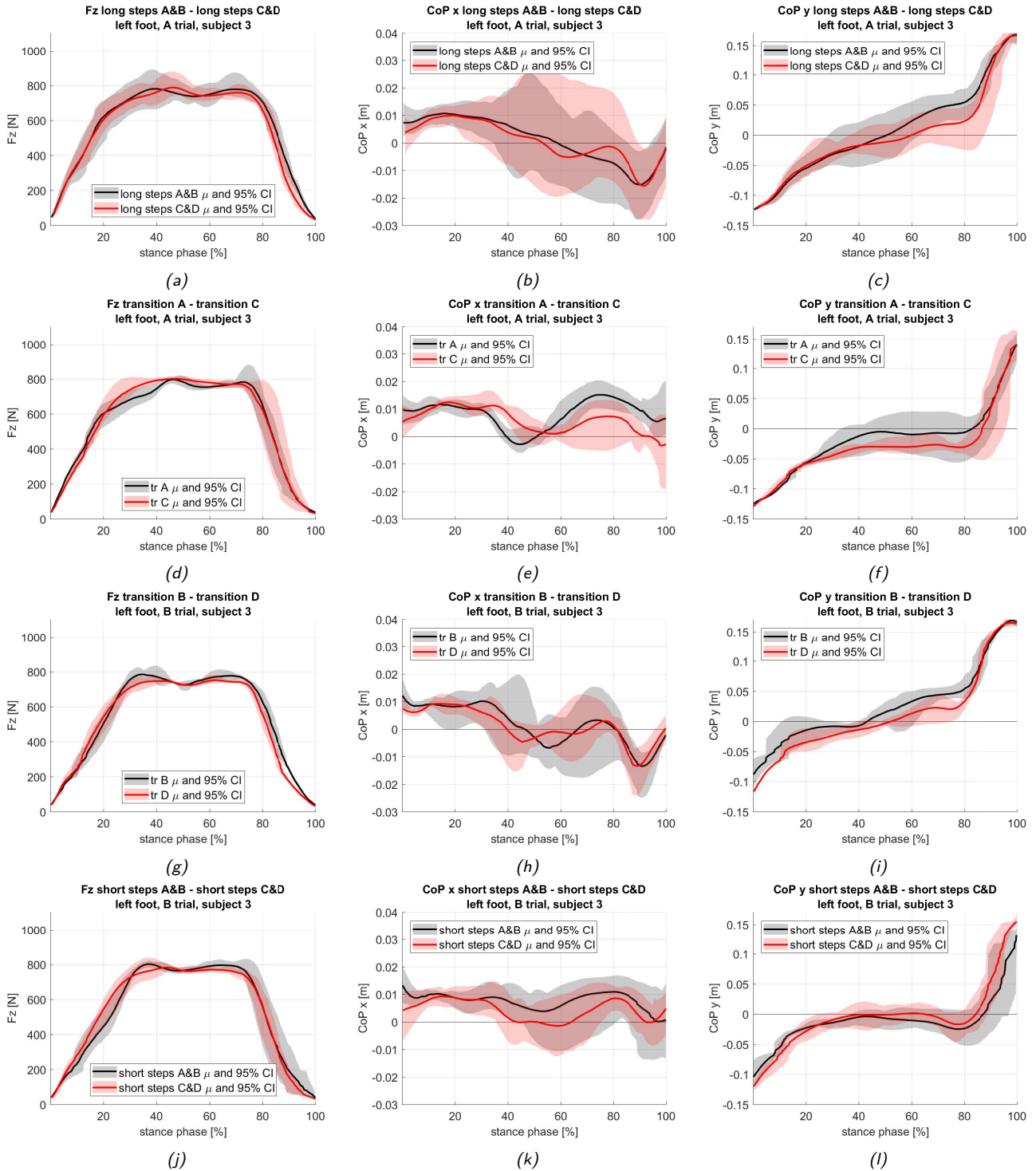


Figure C.2: The three parameters  $F_z$ ,  $CoP_x$  and  $CoP_y$ , comparisons 5,6 and 7, subject 3, left foot. Black: A- and/or B-trials. Red: C- and/or D-trials. Top row: steady state long steps from A&B compared to steady state long steps from C&D. Second row: transition A compared to transition C. Third row: transition B compared to transition D. Bottom row: steady state short steps from A&B compared to steady state short steps from C&D. From left to right:  $F_z$ ,  $CoP_x$ ,  $CoP_y$ . Solid lines: mean values. Shaded areas: 95% CI.

# References

- Acosta-Marquez, C., & Bradley, D. a. (2005). The analysis, design and implementation of a model of an exoskeleton to support mobility. *Proceedings of the 2005 IEEE 9th International Conference on Rehabilitation Robotics, 2005*, 99–102.
- Alvarez, D., Gonzalez, R. C., Lopez, A., & Alvarez, J. C. (2006). Comparison of step length estimators from wearable accelerometer devices. *Annual International Conference of the IEEE Engineering in Medicine and Biology - Proceedings*, 5964–5967.
- Arazpour, M., Chitsazan, A., Hutchins, S. W., Mousavi, M. E., Takamjani, E. E., Ghomshe, F. T., ... Bani, M. A. (2012). Evaluation of a novel powered gait orthosis for walking by a spinal cord injury patient. *Prosthetics and orthotics international*, 36(2), 239–46.
- Cheron, G., Duvinage, M., De Saedeleer, C., Castermans, T., Bengoetxea, A., Petieau, M., ... Ivanenko, Y. (2012). From spinal central pattern generators to cortical network: Integrated BCI for walking rehabilitation. *Neural Plasticity, 2012*.
- Chevalier, T. L., Hodgins, H., & Chockalingam, N. (2010). Plantar pressure measurements using an in-shoe system and a pressure platform: A comparison. *Gait and Posture*, 31(3), 397–399.
- Chiu, M.-c., Wu, H.-c., & Chang, L.-y. (2013). Gait speed and gender effects on center of pressure progression during normal walking. *Gait & Posture*, 37(1), 43–48. Retrieved from <http://dx.doi.org/10.1016/j.gaitpost.2012.05.030>
- Contreras-Vidal, J. L., & Grossman, R. G. (2013). NeuroRex: a clinical neural interface roadmap for EEG-based brain machine interfaces to a lower body robotic exoskeleton. In *Annual international conference of the IEEE engineering in medicine and biology society*. (Vol. 2013, pp. 1579–1582).
- Crowe, A., Schiereck, P., De Boer, R. W., & Keessen, W. (1995). Characterization of human gait by means of body center of mass oscillations derived from ground reaction forces. *IEEE Transactions on Biomedical Engineering*, 42(3), 293–303.
- Esquenazi, A., Talaty, M., Packel, A., & Saulino, M. (2012). The ReWalk Powered Exoskeleton to Restore Ambulatory Function to Individuals with Thoracic-Level Motor-Complete Spinal Cord Injury. *American Journal of Physical Medicine & Rehabilitation*, 91(11), 911–921.
- Fleischer, C., & Hommel, G. (2008). A Human–Exoskeleton Interface Utilizing Electromyography. *Robotics, IEEE Transactions on*, 24(4), 872–882.
- Fuchioka, S., Iwata, A., Higuchi, Y., Miyake, M., Kanda, S., & Nishiyama, T. (2015). The Forward Velocity of the Center of Pressure in the Midfoot is a Major Predictor of Gait Speed in Older Adults \*. *International Journal of Gerontology*, 9(2), 119–122. Retrieved from <http://dx.doi.org/10.1016/j.ijge.2015.05.010>
- Gancet, J., Ilzkovitz, M., Motard, E., Nevatia, Y., Letier, P., De Weerd, D., ... Thorsteinsson, F. (2012). MINDWALKER: Going one step further with assistive

- lower limbs exoskeleton for SCI condition subjects. *Proceedings of the IEEE RAS and EMBS International Conference on Biomedical Robotics and Biomechanics, 2010*(June), 1794–1800.
- Grundy, M., Tosh, P. a., McLeish, R. D., & Smidt, L. (1975). An investigation of the centres of pressure under the foot while walking. *The Journal of bone and joint surgery. British volume*, 57(1), 98–103.
- Hasegawa, Y., Jang, J., & Sankai, Y. (2009). Cooperative walk control of paraplegia patient and assistive system. , 4481–4486.
- Hasegawa, Y., & Nakayama, K. (2014). Finger-mounted walk controller of powered exoskeleton for paraplegic patient ' s walk. In *World automation congress* (pp. 1–6). TSI Press.
- Hasegawa, Y., & Ozawa, K. (2014). Pseudo-somatosensory Feedback about Joint's Angle Using Electrode Array. , 644–649.
- Hasegawa, Y., Sasaki, M., & Tsukahara, A. (2012). Pseudo-proprioceptive motion feedback by electric stimulation. *2012 International Symposium on Micro-NanoMechatronics and Human Science, MHS 2012*, 409–414.
- Hassan, M., Kadone, H., Suzuki, K., & Sankai, Y. (2014). Wearable gait measurement system with an instrumented cane for exoskeleton control. *Sensors*, 14(1), 1705–1722.
- Hayafune, N., Hayafune, Y., & Jacob, H. A. (1999). Pressure and force distribution characteristics under the normal foot during the push-off phase in gait. *Foot*, 9(2), 88–92.
- Hof, A. L., Gazendam, M. G. J., & Sinke, W. E. (2005). The condition for dynamic stability. *Journal of Biomechanics*, 38(1), 1–8.
- Jamshidi, N., Rostami, M., Najarian, S., Bagher Menhaj, M., Saadatnia, M., & Salami, F. (2010). Differences in center of pressure trajectory between normal and steppage gait. *Journal of Research in Medical Sciences*, 15(1), 33–40.
- Jang, E.-H., Cho, Y.-J., Chi, S.-Y., Lee, J.-Y., Kang, S. S., & Chun, B.-T. (2010). Recognition of walking intention using multiple bio/kinesthetic sensors for lower limb exoskeletons. In *Control automation and systems (iccas), 2010 international conference on* (pp. 1802–1805). IEEE.
- Johnson, D., Repperger, D., & Thompson, G. (1996). Development of a mobility assist for the paralyzed, amputee, and spastic patient. *Proceedings of the 1996 Fifteenth Southern Biomedical Engineering Conference*, 67–70.
- Kilicarslan, A., Prasad, S., Grossman, R. G., & Contreras-Vidal, J. L. (2013). High accuracy decoding of user intentions using EEG to control a lower-body exoskeleton. In *Annual international conference of the ieee engineering in medicine and biology society*. (Vol. 2013, pp. 5606–5609).
- Kolakowsky-Hayner, S. a. (2013). Safety and Feasibility of using the Ekso™ Bionic Exoskeleton to Aid Ambulation after Spinal Cord Injury. *Journal of Spine*.
- Lugade, V., & Kaufman, K. R. (2014). Center of Pressure Trajectory during Gait: A Comparison of Four Foot Positions. *Gait Posture*, 40(1), 252–254.
- Lugade, V., Lin, V., & Chou, L. S. (2011). Center of mass and base of support interaction during gait. *Gait and Posture*, 33(3), 406–411. Retrieved from <http://dx.doi.org/10.1016/j.gaitpost.2010.12.013>
- Martin-Felez, R., Mollineda, R. A., & Sanchez, J. S. (2011). Human recognition based on gait poses. In *Lecture notes in computer science (including subseries lecture notes in artificial intelligence and lecture notes in bioinformatics)* (Vol. 6669 LNCS, pp. 347–354).

- Maynard Jr., F. M., Bracken, M. B., Creasey, G., Jr, J. F. D., Donovan, W. H., Ducker, T. B., . . . Young, W. (1997). International Standards for Neurological and Functional Classification of Spinal Cord Injury. *Spinal Cord*, 35(5), 266–274.
- Quintero, H. A., Farris, R. J., & Goldfarb, M. (2012). A Method for the Autonomous Control of Lower Limb Exoskeletons for Persons With Paraplegia. *Journal of Medical Devices*, 6(4), 041003.
- Quintero, H. A., Farris, R. J., Hartigan, C., Clesson, I., & Goldfarb, M. (2011). A Powered Lower Limb Orthosis for Providing Legged Mobility in Paraplegic Individuals. *Topics in spinal cord injury rehabilitation*, 17(1), 25–33.
- Quintero, H. a., Farris, R. J., & Members, M. G. (2012). Control and Implementation of a Powered Lower Limb Orthosis to Aid Walking in Paraplegic Individuals.
- Raj, A. K., Neuhaus, P. D., Moucheboeuf, A. M., Noorden, J. H., & Lecoutre, D. V. (2011). Mina: A Sensorimotor Robotic Orthosis for Mobility Assistance. *Journal of Robotics*, 2011, 1–8.
- Sadowsky, C., Volshteyn, O., Schultz, L., & McDonald, J. W. (2002). Spinal cord injury. *Disability and rehabilitation*, 24(13), 680–687.
- Singh, A., Tetreault, L., Kalsi-Ryan, S., Nouri, A., & Fehlings, M. G. (2014). Global Prevalence and incidence of traumatic spinal cord injury. *Clinical Epidemiology*, 6, 309–331.
- Stokes, V. P., Andersson, C., & Forsberg, H. (1989). Rotational and translational movement features of the pelvis and thorax during adult human locomotion. *Journal of Biomechanics*, 22(1), 43–50.
- Strausser, K. A., & Kazerooni, H. (2010). *Development of a Human Machine Interface for a Wearable Exoskeleton for Users with Spinal Cord Injury* (Unpublished doctoral dissertation). UC Berkeley.
- Suzuki, K., Kawamura, Y., Hayashi, T., Sakurai, T., Hasegawa, Y., & Sankai, Y. (2005). Intention-based walking support for paraplegia patient. *Conference Proceedings - IEEE International Conference on Systems, Man and Cybernetics*, 3, 2707–2713.
- Torricelli, D., Gonzalez, J., Weckx, M., Jiménez-Fabián, R., Vanderborght, B., Sartori, M., . . . Von Twickel, A. (2016). Human-like compliant locomotion: state of the art of robotic implementations. *Bioinspiration and Biomimetics*, 11(5). Retrieved from <http://iopscience.iop.org/article/10.1088/1748-3190/11/5/051002/pdf>
- Tsukahara, A., Kawanishi, R., Hasegawa, Y., & Sankai, Y. (2010). Sit-to-Stand and Stand-to-Sit Transfer Support for Complete Paraplegic Patients with Robot Suit HAL. *Advanced Robotics*, 24(11), 1615–1638.
- Tucker, M. R., Olivier, J., Pagel, A., Bleuler, H., Bouri, M., Lambercy, O., . . . Gassert, R. (2015). Control strategies for active lower extremity prosthetics and orthotics: a review. *Journal of neuroengineering and rehabilitation*, 12, 1.
- Ugurly, B., Doppmann, C., Hamaya, M., Forni, P., & Teramae, T. (2016). Control : Experiments on a Bipedal Exoskeleton. *IEEE/ASME Transactions on Mechatronics*, 21(1), 79–87.
- Vallery, H., & Buss, M. (2006). Complementary limb motion estimation based on inter-joint coordination using principal components analysis. In *Computer aided control system design, 2006 IEEE international conference on control applications, 2006 IEEE international symposium on intelligent control, 2006 IEEE* (pp. 933–938). IEEE.
- Vallery, H., Van Asseldonk, E. H. F., Buss, M., & van der Kooij, H. (2009). Reference trajectory generation for rehabilitation robots: complementary limb motion estima-

- tion. *Neural Systems and Rehabilitation Engineering, IEEE Transactions on*, 17(1), 23–30.
- Verkerke, G. J., Hof, A. L., Zijlstra, W., Ament, W., & Rakhorst, G. (2005). Determining the centre of pressure during walking and running using an instrumented treadmill. *Journal of Biomechanics*, 38(9), 1881–1885.
- Winter, D. (1995). Human balance and posture control during standing and walking. *Gait & Posture*, 3(4), 193–214.
- World Health Organization Fact sheet no.384*. (2013). Retrieved 2016-03-01, from <http://www.who.int/mediacentre/factsheets/fs384/en/>
- Wyndaele, M., & Wyndaele, J.-J. (2006). Incidence, prevalence and epidemiology of spinal cord injury: what learns a worldwide literature survey? *Spinal Cord*, 44(9), 523–529.
- Yousefifard, M., Rahimi-Movaghar, V., Nasirinezhad, F., Baikpour, M., Safari, S., Saadat, S., ... Hosseini, M. (2016). Neural stem/progenitor cell transplantation for spinal cord injury treatment; A systematic review and meta-analysis. *Neuroscience*(February).
- Zijlstra, W., & a.L. Hof. (1997). Displacement of the pelvis during human walking: experimental data and model predictions. *Gait & Posture*, 6(3), 249–262.
- Zijlstra, W., & Hof, A. L. (2003). Assessment of spatio-temporal gait parameters from trunk accelerations during human walking. *Gait and Posture*, 18(2), 1–10.